MIDWESTERN CLIMATE RECORDS FROM TREE RING $\delta^{13}C$ AND $\delta^{18}O$ VALUES

A Dissertation presented to the Faculty of the Graduate School
University of Missouri

In Partial Fulfillment
Of the Requirements for the Degree

Doctor of Philosophy

---

by
SCOTT LEPLEY

Dr. Kenneth G. MacLeod, Dissertation Supervisor

JULY 2009

The undersigned, appointed by the Dean of the Graduate School, have examined the dissertation entitled

MIDWESTERN CLIMATE RECORDS FROM TREE RING $\delta^{13}C$ AND $\delta^{18}O$ VALUES

presented by Scott Lepley

A candidate for the degree of Doctor of Philosophy

And hereby certify that in their opinion it is worthy of acceptance.

_____

Professor Kenneth MacLeod

_____

Professor Richard Guyette

_____

Professor Cheryl Kelley

_____

Professor Mitchell Schulte

_____

Professor Karyn Rogers

……. Dedicated to my family.

Without your love, extreme patience and belief in my dreams,
none of this would have been possible!

ACKNOWLEDGEMENTS

I would like to first and foremost acknowledge my dissertation advisor Dr. Kenneth MacLeod. Ken has not only been my mentor, but my friend as well. I could not have asked for a better advisor to guide me through the long and demanding task of obtaining my doctorate degree. Dr. Rich Guyette, my outside committee member, has allowed me the use of his American Long Oak Chronology sample database, for without, this project would not be possible. Also, I would like to recognize my additional committee members Dr. Cheryl Kelley, Dr. Mitch Schulte and Dr. Karyn Rogers for their knowledge and valuable insight concerning my research along the way.

My research would not have been possible without the help from Dr. Michael Stambaugh and Erin McMurry from the Missouri Tree Ring Laboratory of the University of Missouri who provided me with the necessary tree segments to complete my stable isotope research. Additionally, I would like to thank the Department of Geosciences for everything they have provided me since I began at the University in 2002. Also, I would like to thank Dr. Alvaro Jimenez Berrocoso for his guidance and mentorship while he was here as a post-doc.

Finally, I would like to whole-heartedly thank my fiancé, Dr. Carolina Isaza Londoño, for being the most patient person on this planet. Without her at my side the entire way through this process, I do not think I could have made it both academically and mentally!

TABLE OF CONTENTS

LIST OF FIGURES

LIST OF TABLES

MIDWESTERN CLIMATE RECORDS FROM TREE RING $\delta^{13}C$ AND $\delta^{18}O$ VALUES

Scott W. Lepley

Dr. Kenneth G. MacLeod, Dissertation Advisor

ABSTRACT

Determining the scope and nature of Midwestern climate change is difficult because most North American instrumental meteorological records (e.g. temperature and precipitation) span a relatively short period and fail to explain the full range of climate variability. However, long continuous tree-ring chronologies may provide a dated archive of climate variability beyond instrumental records. By analyzing tree ring $\delta^{13}C$ and $\delta^{18}O$ of samples from the American Long Oak Chronology (ALOC) developed at the Missouri Tree Ring Laboratory, we were able to better constrain and understand climate dynamics of the central Midwest by examining paleoclimate beyond the instrumental record.

By exploiting previously determined comparisons of the similarity of ring width patterns (RWP) from an individual tree to the pooled pattern for all indexed trees of that age in the ALOC as a means to select trees for analysis, we maximized the efficiency of generating climatologically significant $\delta^{13}C$ records. In other words, whereas climatically significant information seems to be recorded in the $\delta^{13}C$ values of all trees studied, the signal to noise ratio is maximized by selecting tree segments whose individual RWP best match the average ring width index developed for the region. From 1931-2002, averaged $\delta^{13}C$ measurements of bulk latewood from

highly correlated RWP trees were significantly correlated with June-July-August (JJA) precipitation ($R = -0.49$, $p<0.0001$) and Palmer Drought Severity Index (PDSI) values ($R = -0.40$, $p<0.001$).

The correlations lead to the development of a model that predicts average summer (JJA) precipitation from $\delta^{13}C$ values and estimates the accuracy and uncertainty of predictions. Using the model, average summer precipitation per month was estimated back to 1500 AD. The reconstruction suggests that numerous past summer precipitation extremes have been greater in magnitude and duration than any 20th century event, including the 1993 Great Flood and the 1930s Dust Bowl period. These results suggest that precipitation extremes larger than have been seen in the past century are part of the 'natural' variability of the Midwest, regardless of any effects resulting from anthropogenic related climate changes.

In addition to the $\delta^{13}C$ work, a pilot study was conducted utilizing oxygen isotopes of cellulose from tree rings dated from 1975-2002. The pooled $\delta^{18}O$ values were significantly correlated to average summer PDSI and precipitation ($R = -0.80$, $p<0.000001$ and $R = -0.63$, $p<0.001$ respectively). In addition, even though $\delta^{18}O$ and $\delta^{13}C$ covary during this period, these results suggest that tree ring $\delta^{18}O$ values more closely track moisture variations than $\delta^{13}C$ values.

Results from this study demonstrate that tree ring $\delta^{13}C$ and $\delta^{18}O$ measurements can provide a detailed annual isotopic record of climate variability beyond instrumental records in the central Midwest and more importantly beyond human induced anthropogenic influences.

Chapter 1

INTRODUCTION

Understanding and predicting possible global climate changes in response to increases in atmospheric CO_2 concentrations from fossil fuel burning is an important rationale for paleoclimate studies. More specifically, as illustrated by the damage caused by Hurricane Katrina in 2005 and the intense public and scientific debate that followed concerning whether the increase in the amount and/or intensity of hurricanes over the last decade results from "natural" cycles or anthropogenic global warming (Mann et al., 2003; Emanuel, 2005), it is the regional manifestation of climate change rather than globally averaged climatic trends that most dramatically impact people, environments, and potentially policy decisions. Uncertainty concerning the manifestation of global climate variability at this resolution strengthens the need to quantify recent climate changes at locations where human activities are most vulnerable (Stahle and Cleaveland, 1992; Meko et al., 1995; Raffalli-Delerce et al., 2004; Cook et al., 2004; Masson-Delmotte et al., 2005; Reynolds-Henne et al., 2007). This uncertainty and motivation is echoed by the most recent report of the Intergovernmental Panel on Climate Change (2007), which claims regional scale climatic variations are not fully understood and efforts should be focused on the investigation of climatically high impact areas.

The Midwestern region of the US is susceptible to a wide array of climatic change, has been considerably understudied, has an economy influenced by climate, and is a central location for global agricultural resources (Stockton and Meko, 1983;

Woodhouse and Overpeck, 1998; Woodhouse and Brown, 2001; Schubert et al., 2004; Leavitt, 2007). However, climate is often generalized throughout the Midwestern region. Stockton and Meko (1983) indicate that most Midwestern climatic interpretations have invoked teleconnections (such as El Niño) between existing climatic interpretations from regions outside the Midwest with little observational control. Thus, resulting interpretations may often be too broad to be significant for any particular region of the Midwest.

Further, determining the scope and nature of any Midwestern climate change is difficult because most North American historical instrumental climate records span a relatively short period and fail to explain the full range of climate variability (Meko et al., 1995; Woodhouse and Overpeck, 1998). Additionally, most high-resolution records used in paleoclimate studies (e.g., ice cores, tropical corals, speleothems) are either unavailable in the Midwest region or lack the temporal resolution desired to understand, in detail, how climate has changed through time and how it might evolve in the immediate future (Woodhouse and Overpeck 1998; McCarroll and Loader, 2004; Reynolds-Henne et al., 2007). This study focuses on using isotopic analyses of tree rings from northwest Missouri to investigate climate on an annual time scale for a central region of the Midwest over the past five centuries to begin to address this shortcoming.

The Missouri Tree Ring Laboratory has developed the American Long Oak Chronology (ALOC) for the central Midwest through a decade of field collection and ring width study. This ongoing project has resulted in the only continuous millennial-scale tree ring chronology developed within the American Great Plains

(Guyette et al., 2004). Furthermore, this chronology has been independently dated through techniques such as density dating, ^{14}C dating, and cross dating techniques to ensure each ring is accurately dated (Fritts, 1976; Guyette and Stambaugh, 2003; Guyette et al., 2004). Access to this tree ring database allowed for the direct investigation of tree ring isotopic signals as a response to climate from a lengthy and unambiguous chronological framework.

1.1. General Background

The climate of northern Missouri is generally humid with strong continental seasonality (NCDC, 2004). Strong seasonality results from systematic annual variations in the patterns of interactions among Arctic, Pacific and Gulf of Mexico air masses. Summer maximum temperatures commonly reach 38°C and minimum winter temperatures can drop below -18°C. Average summer (June-August) temperatures (Figure 1.1) from northwest Missouri climate division 1 are 24.0°C (1931-2002) and within this period July is the hottest month (25.3°C) and the coolest month is June (22.6°C). Both the hottest (48°C) and coldest (-40°C) temperatures recorded in Missouri were in Warsaw, MO, in 1948 and 1902 respectively (NCDC, 2004). Mean annual precipitation for northwest Missouri is approximately 33.9 inches per year, which is less than Missouri's average (41.2 in). Regional average summer monthly precipitation is 4.3 in/month with June being the wettest (5.0 in) and August being the driest (3.9 in). Summer precipitation is generally higher in the northern region than in the southern region of Missouri as

heavier thundershowers are more common in the north. Interestingly, the world record for most precipitation in the shortest time span is from Holt, MO, where in 1947, 12.0 in of rain fell in 44 minutes (NCDC, 2004).

White oak trees used in this study represent excellent specimens for studying paleoclimate characteristics in this Midwestern region. Oak trees (living and subfossil) are abundant in Missouri, which has enabled the Missouri Tree Ring Laboratory to develop a long, continuous record to 912 A.D. and floating intervals of a century or more back to approximately 14,000 radiocarbon years (Guyette et al., 2004). Additionally, oaks exhibit well defined and well preserved growth rings that have two main bulkwood constituents (Figure 1.2); earlywood and latewood (Miller, 1999; Domec and Gartner, 2002). Earlywood has been shown to incorporate stored photosynthates from previous years that could add complexity to interpretation of the earlywood isotopic signal (Hill et al., 1995; McCarroll et al., 2003; McCarroll and Loader, 2004), whereas latewood is primarily composed of organic matter formed throughout the main growing season (June through August) of a particular year (Hill et al., 1995; Miller, 1999; Lebourgeois, 2000). Therefore, measurements on latewood can confidently be compared with meteorological records from summer months (Gindi et al., 2000; Loader et al., 2003; McCarroll and Loader, 2004). For this reason, this study only utilized latewood.

Isotope dendroclimatology is increasingly being used to infer and distinguish among multiple climatic variables such as precipitation, temperature and relative humidity that may or may not primarily influence the growth (recorded as ring width) of the tree (Cook, 1991; Leavitt and Long, 1991; Loader et al., 1995;

McCarroll and Loader, 2004). For example, strong correlations between carbon isotopes of *Pinus radiata* and the Palmer Drought Severity Index (PDSI – a meteorological drought index of moisture supply deviations within a region based on temperature, precipitation and local soil water content; positive numbers indicate wetter conditions while negative numbers indicate drier conditions) have been noted in the southwest US (Leavitt and Long 1988; Leavitt, 2002b). In the UK, many studies have shown that carbon isotopes in certain oaks are strongly correlated to temperature (Gagen et al., 2007; Loader et al., 2008). Oxygen isotopes from oak tree rings in France have shown strong relationships to summer precipitation (Raffalli-Delerce et al., 2004; Danis et al., 2006). Leavitt (2002a; 2007) has further demonstrated that significant carbon isotope relationships exist between PDSI and numerous trees in the Great Lakes region of the upper Midwest. While intriguing, this variability of correlations shows isotopic paleoclimate studies are not straightforward. It is important to determine which climatic variables most influence the $\delta^{13}C$ or $\delta^{18}O$ values in a specific region in order to properly investigate paleoclimate using tree ring isotopic measurements.

Being able to separate climate variables would be a major advance in exploiting the ALOC archive. Ring widths from the ALOC have been correlated to climate data information such as PDSI over the last century (1895-1980), and a linear model from the tree ring index explained a significant amount (42%, $p<0.0001$) of the changes in drought over the last century, and this relationship has been projected into the past to 912 AD (Guyette et al., 2004). However, the linear tree ring model does a relatively poor job of identifying wetter periods over the

same time interval and a hope for this study is that $\delta^{13}C$ or $\delta^{18}O$ might capture the wet ends of climate variability.

1.2. Experimental Design

This project is designed to address potential tree ring isotopic challenges, open the door for tree ring isotopic climate reconstructions in the central Midwest, and examine paleoclimate beyond the instrumental record. Even though agricultural, economic, and societal adversities are often affiliated with climate change in this region, a fundamental lack of knowledge concerning prehistoric climate fluctuations exists. As a result, the following chapters, beginning with chapter 2, investigate how climate change has varied in the central Midwest during the previous five centuries through the examination of stable carbon and oxygen isotopes in tree rings.

The second chapter addresses basic feasibility issues for $\delta^{13}C$ measurements on ALOC samples. Specifically, can white oak tree rings from the ALOC be sampled and precisely measured? The central questions addressed were; 1) do oak samples from the ALOC provide sufficient latewood material for isotopic analysis, 2) how well do within-tree and between-tree isotopic values compare and 3) are isotopic offsets systematic between trees? The results were encouraging enough to proceed.

Chapter 3 examines two $\delta^{13}C$ time series for the 20^{th} century with instrumental records of environmental conditions (most importantly summer temperature and precipitation). Of methodological interest in this chapter are the sample selection criteria used for carbon isotopic studies. By exploiting previously

determined ring width relationships between individual trees and the pooled pattern over this period, we are able to demonstrate that it is possible to select tree segments that maximize the efficiency of generating climatologically significant $\delta^{13}C$ records. That is, by sampling from tree segments whose growth patterns most closely correlate to average ring width patterns for the region (i.e., highly correlated samples), a statistically robust $\delta^{13}C$ record can be generated with as few as three samples per year. This refinement saves time, samples, and reduces the cost associated with generating isotopic time series.

The fourth chapter constructs a model to explain the relationship between precipitation and $\delta^{13}C$ values from 1931-2002 utilizing only highly correlated samples from chapter two. By using a split calibration assessment, a model was developed to predict average summer (June-August) precipitation from $\delta^{13}C$ values and estimate the accuracy and uncertainty of predictions. The assessment reveals the model has some reconstruction skill and can be used when estimating long prehistoric records of precipitation with ALOC samples. While $\delta^{13}C$ values alone represents a good predictor, future refinements may add $\delta^{18}O$ values and ring width patterns to further constrain the model.

Using the model developed in chapter 4, summer precipitation was estimated back to 1500 AD in chapter 5. The estimated precipitation record represents the first pre-instrumental tree ring isotope reconstruction of climate in the central Midwest. The record suggests that numerous past precipitation extremes have been greater in magnitude and duration than any 20th century event, including the 1993 Great Flood and the 1930 Dust Bowl period. This indicates that potentially greater

precipitation extremes could occur in the future. In addition, potential long-term correlations appear to exist with sunspot variations that may suggest a mechanism responsible for Midwest precipitation.

Chapter 6 explores the potential of utilizing $\delta^{18}O$ values as both an alternative and complementary proxy for reconstructing paleoclimate in the Midwest. This pilot study aimed to characterize both the use of a new method used in oxygen isotope studies and establish how climate influences (if at all) ALOC tree ring $\delta^{18}O$ values. A $\delta^{18}O$ time series was developed from alpha cellulose (not bulk wood) of three highly correlated segments during 1975-2002. Results show a significant correlation to both PDSI and precipitation on both yearly and decadal time scales that is greater than $\delta^{13}C$. Additionally, both $\delta^{18}O$ and $\delta^{13}C$ time series co-vary during this time period. Thus, by using only three segments and one sample preparation technique, pilot study observations reveal that tree ring cellulose $\delta^{18}O$ values provide significant evidence of moisture variation and should be explored in future research.

References

Cook, E.R., 1991. Tree rings as indicators of climate change and the potential response of forests to the greenhouse effect. *In*: Wyman, R.L. (ed.), Global Climate Change and Life on Earth. Routledge, Chapman and Hall, New York. pp. 56-64.

Cook, E.R., Woodhouse, C., Eakin, C.M., Meko, D.M. and Stahle, D.W., 2004. Long-term aridity changes in the western United States. *Science* **306**: 1015-1018.

Danis, P.A., Masson-Delmotte, V., Stievenard, M., Guillemin, M.T., Daux, V. Naveau, Ph., and von Grafenstein, U., 2006. Reconstruction of past precipitation d18O using tree-ring cellulose d18O and d13C: A calibration study near Lac d' Annecy, France. *Earth and Planetary Science Letters* **243**: 439-448.

Domec, J.-C., and Gartner, B.L., 2002. How do water transport and water storage differ in coniferous earlywood and latewood. *Journal of Experimental Botany* **53-379**: 2369-2379.

Emanuel, K.A., 2005. Increasing destructiveness of tropical cyclones over the past 30 years. *Nature* **436**: 686-688.

Fritts, H.C., 1976. Tree Rings and Climate. The Blackburn Press, New Jersey, 567 pp.

Gagen, M., McCarroll, D., Loader, N.J., Robertson, I., Jalkanen, R., and Anchukaitis, K.J., 2007. Exorcising the 'segment length curse': summer temperature reconstruction since AD 1640 using non-detrended stable carbon isotope ratios from pine trees in northern Finland. *The Holocene* **17-4**: 435-446.

Gagen, M., McCarroll, D., Robertson, I., Loader, N.J., and Jalkanen, R., 2008. Do tree ring $\delta^{13}C$ series from *Pinus sylvestris* in northern Fennoscandia contain long-term non-climatic trends? *Chemical Geology* **252**: 42-51.

Gindi, W., Brabner, M., and Wimmer, R., 2000. The influence of temperature on latewood lignin content in treeline Norway spruce compared with maximum density and ring width. *Trees* **14**: 409-414.

Guyette, R.P., and Stambaugh, M.C., 2003. The Age and Density of Ancient and Modern Oak Wood in Streams and Sediments. *IAWA Journal* **24-4**: 345-353.

Guyette, R.P., Stambaugh, M.C., and Dey, D.C., 2004. Ancient Oak Climate Proxies From the Agricultural Heartland. *EOS* **85-46**: 485.

Hill, S.A., Waterhouse, J.S., Field, E.M., Switsur, V.R., and Rees, T., 1995. Rapid recycling of triose phosphates in oak stem tissue. *Plant, Cell, Environment* **18**: 931-936.

Intergovernmental Panel on Climate Change (IPCC), 2007. Climate Change 2007: The Physical Science Basis. Fourth Assessment Report of the IPCC Summary for Policymakers, 18p.

Leavitt, S.W., 2002a. Prospects for reconstruction of seasonal environment from tree-ring $\delta^{13}C$: baseline findings from the Great Lakes area, USA. *Chemical Geology* **192**: 47-58.

Leavitt, S.W., 2002b. Spatial expression of ENSO, drought, and summer monsoon in seasonal $\delta^{13}C$ of ponderosa pine tree rings in southern Arizona and New Mexico. *Journal of Geophysical Research* **107**: D18, 4349, doi:10.1029/2001JD00131.

Leavitt, S.W., 2007. Regional expression of the 1988 U.S. Midwest drought in seasonal $\delta^{13}C$ of tree rings. *Journal of Geophysical Research* **112**: D06107, doi:10.1029/2006JD007081.

Leavitt, S.W., and Long, A., 1988. Stable carbon isotope chronologies from trees in the southwestern United States. *Global Biogeochemical Cycles* **2:**189-198.

Leavitt, S.W., and Long, A., 1991. Seasonal stable-carbon isotope variability in tree rings: possible paleoenvironmental signals. *Chemical Geology (Isotope Geoscience Section)* **87:** 59-70.

Lebourgeois, F., 2000. Climatic signals in earlywood, latewood and total ring width of Corsican pine from western France. *Annals of Forestry Science* **57**: 155-164.

Loader, N.J., Switsur, V.R., Field, E.M., and Carter, A.H.C., 1995. High resolution stable isotope analysis of tree rings: implications of microdendroclimatology for palaeoenvironmental research. *The Holocene.* **1-5**: 457-460.

Loader, N.J., Robertson, I., and McCarroll, D., 2003. Comparison of stable carbon isotope ratios in the whole wood, cellulose and lignin of oak trees-rings. *Palaeogeography, Palaeoclimatology, Palaeoecology* **196**: 395-407.

Loader, N.J., Santillo, P.M., Woodman-Ralph, J.P., Rolfe, J.E., Hall, M.A., Gageb, M., Robertson, I., Wilson, R., Froyd, C.A., and McCarroll, D., 2008. Multiple stable isotopes from oak trees in southwestern Scotland and the potential for stable isotope Dendroclimatology in maritime climatic regions. *Chemical Geology* **252**: 62-71.

Mann, M.E., Ammann, C.M., Bradley, R.S., Briffa, K., Crowley, T.J., Jones, P.D., Oppenheimer, M., Osborn, T.J., Overpeck, J.T., Rutherford, S., Trenberth, K.E., and Wigley, T.M.L., 2003. On past temperatures and anomalous late-20th century warmth. *EOS* **84-27**: 256-257.

Masson-Delmotte, V., Raffalli-Delerce, G., Danis, P.A., Yiou, P., Stievenard, M., Guibal, F., Mestre, O., Bernard, V., Goosse, H., Hoffmann, G., and Jouzel, J., 2005. Changes in European precipitation seasonality and in drought frequencies revealed by a four-century-long tree-ring isotopic record from Brittany, western France. *Climate Dynamics* **24**: 57-69.

McCarroll, D., and Loader N.J., 2004. Stable isotopes in tree rings. *Quaternary Science Reviews* **23**: 771–801.

McCarroll, D., Jalkanen, R., Hicks, S., Tuovinen, M., Gagen, M., Pawellek, F., Eckstein, D., Schmitt, U., Autio, J., and Heikkinen, O., 2003. Multiproxy dendroclimatology: a pilot study in northern Finland. *The Holocene* **13-6**: 831-841.

Meko, D.C., Stockton, W., and Boggess, W.R., 1995. The tree-ring record of severe sustained drought. *Water Resources Bulletin* **31**: 789-801.

Miller, R., 1999. Structure of Wood. *In*: Wood Handbook – Wood as an engineering material. Gen Tech. Rep. FPL-GTR-113. Madison, WI: USDA, Forest Service, Forest Products Laboratory, 463p.

National Climate Data Center (NCDC), 2004. Time bias corrected divisional temperature-precipitation-drought index. www.ncdc.noaa.gov/oa/climate/climatedata.html.

Raffalli-Delerce, G., Masson-Delmotte, V., Dupouey, J.L., Stievenard, M., Breda, N., and Moisselin, J.M., 2004. Reconstruction of summer droughts using tree-ring cellulose isotopes: a calibration study with living oaks from Brittany (western France). *Tellus* **56B**: 160-174.

Reynolds-Henne, C.E., Siegwolf, R.T.W., Treydte, K.S., Esper, J., Henne, S., and Saurer, M., 2007. Temporal stability of climate-isotope relationships in tree rings of oak and pine (Ticino, Switzerland). *Global Biogeochemical Cycles* **21**: GB4009, doi:10.1029/2007GB002945.

Schubert, S.D., Suarez, M.J., Pegion, P.J., Koster, R.D., and Bacmeister, J.T., 2004. Causes of Long-Term Drought in the U.S. Great Plains. *Journal of Climate* 17-3: 485-503.

Stahle, D.W., Cleaveland, M.K., 1992. Reconstruction and analysis of spring rainfall over the southeastern U.S. for the past 1000 years. *Bulletin of the American Meteorological Society* **73-12**: 1947-1961.

Stockton, C.W., and Meko, D.M., 1983. Drought Recurrence in the Great Plains as Reconstructed from Long-Term Tree-Ring Records. *Journal of Climate and Applied Meteorology* **22**: 17-29.

Woodhouse, C.A., and Overpeck, J.T. 1998. 2000 years of drought variability in the central United States, *Bulletin of the American Meteorological Society* **79-12**: 2693-2714.

Woodhouse, C.A., and Brown, P.M., 2001. Tree-ring evidence for Great Plains drought. *Tree-Ring Research* **57-1**: 89-103.

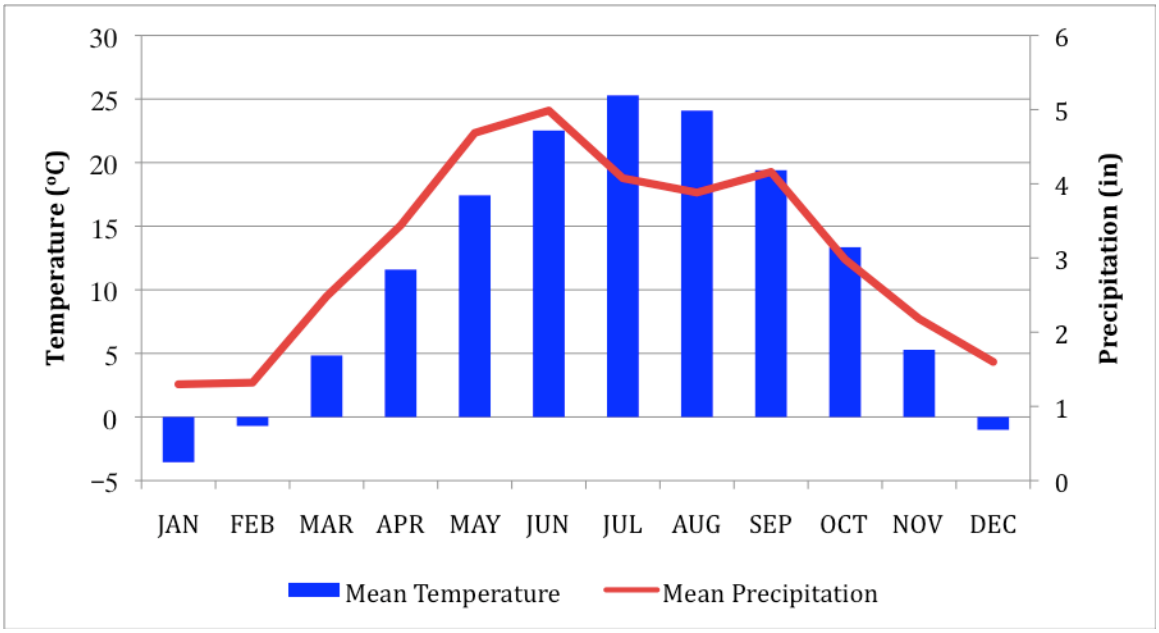

Figure 1.1: Monthly climate statistics for northwestern Missouri Climate Division 1. The graph shows average temperature (bars) and average precipitation (line) during each month from 1931-2002.

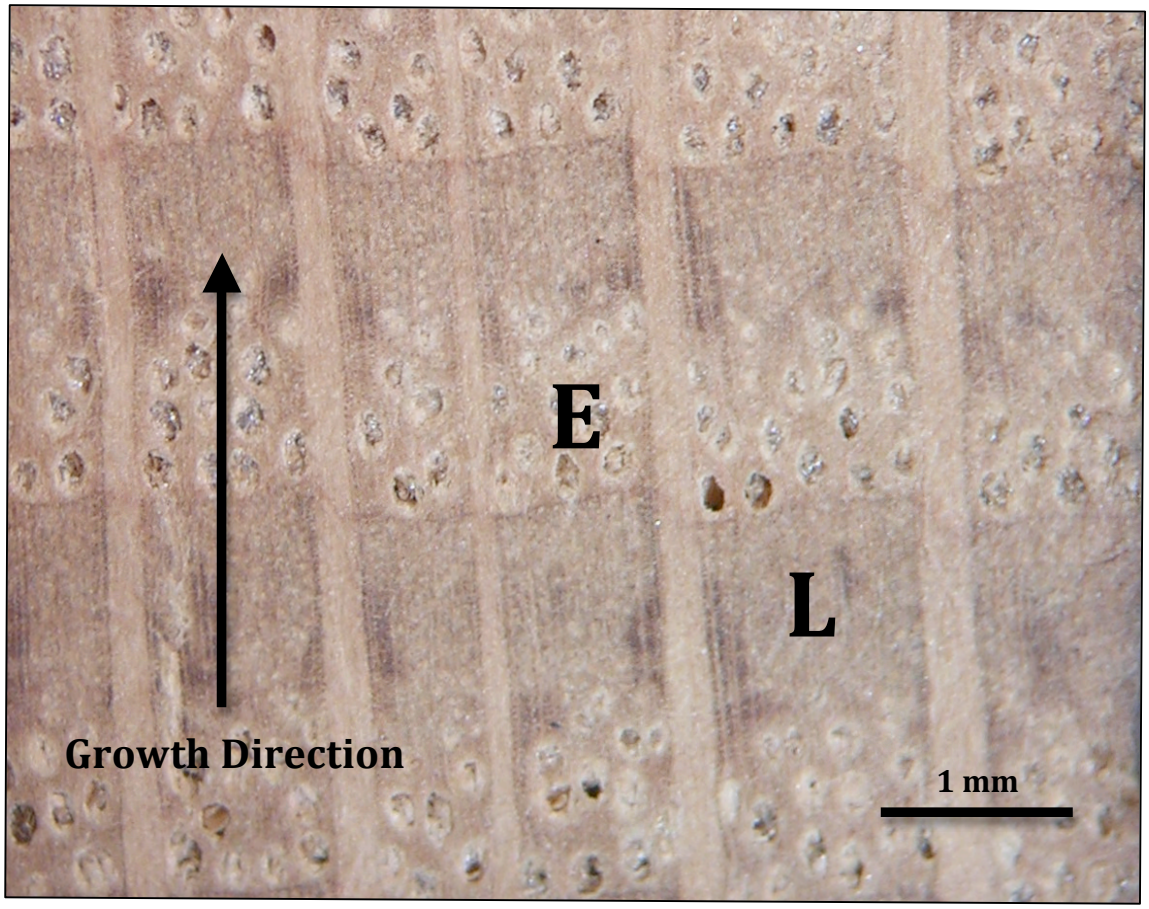

Figure 1.2: Large vessels are indicative of earlywood (E) whereas latewood (L) is denser. The vertical bands are structural rays within the tree and these are avoided during latewood extraction. Direction of growth is towards the top of the page. Latewood is extracted by 1) micro-drilling the adjacent earlywood, 2) inspecting and removing remaining earlywood, structural rays and shaving the exposed ring surfaces with a razor blade, and 3) removing the latewood material with a razor blade.

Chapter 2

A CARBON ISOTOPE METHODS FEASIBILITY STUDY

Summary

The American Long Oak Chronology (ALOC) is a regionally important historical archive constructed from samples of over 400 trees and increasing. It provides a sample base suitable to investigate yearly and potentially seasonal climatic fluctuations for much of the post-glacial interval and a continuous record of the last millennium prior to current instrumental records. A pilot study tested $\delta^{13}C$ variability of latewood within and among trees for multiple years. The goal of this study was to estimate the size of the potential signal (year to year differences) relative to potential noise (within and between tree differences) within the sample base. Results demonstrate that ALOC samples possess ample material (0.5 mg) to construct a time series with annual resolution, the within-tree carbon isotopic signals are comparable to machine error, and as few as three trees are adequate to capture average regional isotopic signals. By establishing basic methodological protocols and testing potential sources of variability, this study provides a foundation for subsequent work investigating how climate influences tree ring $\delta^{13}C$ values.

2.1. Introduction

Generating carbon isotopes from tree rings for paleoclimate studies has become well established and is increasingly efficient. Over the last few decades, the

advent of high-precision isotope ratio mass spectrometers and new sample preparation techniques allow high throughput of relatively small samples, which can reduce the cost and preparation time while increasing the isotopic signal to noise ratio (McCarroll and Loader, 2004). However, a fundamental working knowledge of a tree's isotopic response to climate or environmental change must be established to begin a detailed study. The focus of this chapter is to characterize the isotopic variability of ALOC trees by addressing several questions: 1) do ALOC samples contain sufficient wood of the right type to generate a carbon isotopic record with annual resolution, 2) for any given year are within-tree isotopic values reproducible, 3) how variable are values between trees, 4) are offsets systematic between trees, and 5) what is the minimum number of trees necessary to produce a statistically significant $\delta^{13}C$ time series?

2.2. Stable Carbon Isotope Background

Stable carbon isotopes are expressed in standard δ-notation form defined as:

$$\delta^{13}C = [(^{13}C/^{12}C_{\text{sample}})/(^{13}C/^{12}C_{\text{standard}}) - 1] * 1000$$

where $\delta^{13}C$ is expressed in parts per thousand (‰). The sample is the material being analyzed and the standard is a known isotopic reference (VPDB) (Faure, 1986).

Tree ring carbon isotopic ratios vary mainly from fractionation during photosynthesis modified by the rate of CO_2 exchange through leaf stomata. Stomata are pores in leaves that regulate gas exchange between the interior of the leaf and the atmosphere. They function largely to control moisture loss from the leaf, but

they also regulate CO_2 exchange (Farquhar et al., 1989; McCarroll and Loader 2004). $^{12}CO_2$ diffuses more rapidly than $^{13}CO_2$ and because internal pCO_2 is lower than atmospheric pCO_2, there is a relative depletion of $^{13}CO_2$ within leaves compared to the outside ambient air. The process results in fractionation due to diffusion of up to -4.4‰ depending on the concentration gradient (Farquhar and Sharkey, 1982; Farquhar et al., 1989; McCarroll and Loader, 2004). Fractionation further occurs during carbon fixation when internal CO_2 is utilized by the photosynthetic enzyme whereby trees preferentially use ^{12}C with respect to ^{13}C called 'net fractionation due to carboxylation' which has been estimated at about -27‰ (Farquhar and Sharkey, 1982; Farquhar et al., 1989; McCarroll and Loader, 2004). Because the fractionation causes an increase in the $\delta^{13}C$ value of CO_2 within the leaf, the fractionation expressed depends on the rate of carbon fixed relative to the rate at which CO_2 enters the leaf. This balance among the different processes determines the effective discrimination against ^{13}C during carbon fixation has been modeled as

$$\delta^{13}C_{plant} = \delta^{13}C_{air} - a - (b-a)(ci/ca)$$

where the constants *a* and *b* represent fractionation due to diffusion (≈ -4.4‰) and carboxylation (≈ -27‰) respectively, *ci* & *ca* are the intercellular and ambient CO_2 concentrations, and $\delta^{13}C_{air}$ is the $\delta^{13}C$ of atmospheric CO_2 (Farquhar et al., 1989).

As moisture stress likely affects $\delta^{13}C$ values (by influencing how open stomata are), variations in these isotopic values should provide a yearly record of water stress. During times of low water stress (low temperature and/or high precipitation) the stomata will tend to open and ci/ca will increase, resulting in

lower $\delta^{13}C$ isotopic values. In contrast, when water stress is high, the stoma begins to close, ci/ca decreases, and $\delta^{13}C$ values are higher. Importantly for my research, fixed carbon used in wood formation does not exchange between rings or with other parts of the tree during ring formation (McCarroll and Loader, 2004) and latewood is formed during summer months only. Thus, fluctuations in the final isotopic signatures of photosynthates (ranging from about -20‰ to -30‰) should be recorded through time with at least an annual resolution in latewood.

2.3. Materials and Methods

2.3.1. Sample Selection Strategy

White oak trees used in this study exhibit well-defined and well preserved growth rings. Each oak ring is easily distinguishable and has two main components; earlywood and latewood (Miller, 1999; Domec and Gartner, 2002). Earlywood is formed in as little as a few weeks during the spring, is distinguished by large vessels (see Figure 1.2), and has been shown to use stored photosynthates from previous years that could add complexity to interpretation of the earlywood isotopic signal (Hill et al., 1995; McCarroll et al., 2003; McCarroll and Loader, 2004). Latewood is primarily formed during the main growing season (June through August) of a particular year (Hill et al., 1995; Miller, 1999; Lebourgeois, 2000) from carbon fixed during that growing season and is denser than earlywood allowing measurement of very thin rings. Therefore, to the extent that environment controls $\delta^{13}C$ values, latewood $\delta^{13}C$ should track meteorological conditions (such as precipitation or temperature) during summer months (Antonova et al., 1997; Gindi et al., 2000;

Lebourgeois, 2000; Loader et al., 2003; McCarroll and Loader, 2004). Hence, this study only utilized latewood.

Segments originate from slices of subfossil tree wedges and cores of living trees that were collected in the field and prepared for ring width analyses at the Missouri Tree Ring Laboratory. For this study, three 20th century segments that had wide rings were drawn from the ALOC sample base. Also, from 1920 to 1923, triplicate samples of each ring were prepared for analysis. The samples analyzed were used to examine within- and between-tree carbon isotopic variations.

Latewood portions of each tree ring were removed using a razor blade. All visual components not of latewood material were carefully removed or avoided (i.e., earlywood, structural rays). This procedure minimizes potential contributions from carbon fixed at times other than the sampled year. Less than 2 mg of sample material were used for analyses and in most cases each individual ring could provide enough material for replicate analyses if needed. By conducting analytical measurements on yearly individual samples, the aim was to retain as much high-frequency variability as possible.

2.3.2. Analytical Procedure

Individual bulk samples were weighed, loaded into tin boats, and analyzed by continuous flow stable isotope mass spectrometry techniques (further details in Brenna et al., 1997; Ghosh and Brand, 2003; McCarrol and Loader, 2004). Prepared samples are loaded into a 50-port autosampler connected to a Carlo-Erba 1500 elemental analyzer (EA). Each sample is individually dropped into a combustion

reactor within the EA that is heated to 1020°C where flash combustion occurs with O_2 and produces gases such as CO_2, NO_x, H_2O and excess O_2. The gases are carried in a helium stream and enter a secondary reduction reactor where excess O_2 is retained and nitrogen oxides are reduced to N_2. Then the gasses pass first through a trap where water is removed and secondly through a gas chromatagraphic column to separate different compounds. The outflow (helium with entrained CO_2 and N_2 gas) pass through a Finnigan Conflo III device into a Finnigan DeltaPlusXL Isotope Ratio Mass Spectrometer (IRMS) where $\delta^{13}C$ values are determined for CO_2 based on comparison with a reference CO_2 gas of known isotopic composition. To monitor accuracy and precision, an average of five samples for every Acetanilide standard were used for each full run. In less than 12 hours, 50 analyses (samples plus standards) can be run with excellent analytical precision (<0.1‰, 1 standard deviation). Raw isotopic results are expressed as per mil deviations using delta notation (δ) relative to the VPDB standard.

2.4. Results and Discussion

Results (Table 2.1) address the first question posed, which while simple, is vital for the development of an isotopic time series. A broad survey of ALOC samples revealed that a majority of latewood ring widths were between 2 mm and 3 mm. Using current methods, we can generally expect to extract 1.0 mg of latewood from rings of this thickness, an amount that should be adequate to generate a signal well above machine detection limits. The removal of sufficient latewood material

demonstrates this calculation is correct. We can confidently generate reproducible $\delta^{13}C$ results from a small amount of latewood. Thus, the Missouri Tree Ring Lab contains adequate sample material for the development of a carbon isotopic time series.

The total range of isotopic results span from -24.3‰ to -27.1‰ whereas the span within a year for any tree is no more than 0.3‰. The standard deviation for 9 of 12 triplicate years was below 0.1 (the other three were below 0.15), which demonstrates good internal (within-ring) consistency comparable to machine error (Table 2.1). As a result, one sample per ring within a tree should be adequate to document that tree's carbon isotopic value.

Unfortunately, the variation among trees for any given year is high. The average $\delta^{13}C$ value of each tree segment ranges from -24.7‰ to -27.1‰ (Table. This might be expected because local factors can affect the raw isotopic value of one tree relative to another in a region. For example, during an abnormally wet summer, a community of trees should exhibit a similar, climate induced, decrease in $\delta^{13}C$ values. In spite of this, high local competition for water may leave some trees less access to the water supply and consequently show a more positive $\delta^{13}C$ value than the other trees while still exhibiting the negative trend.

There are many potential complicating site-specific or finer scaled factors (other than climate) that could potentially influence the final carbon isotope value in the Midwest (McCarroll and Loader, 2004). For instance, trees living above the forest canopy might capture more light but be exposed and more susceptible to water loss. Additionally, older trees within a forest may have deeper rooting depths

and, as such, have better access to a groundwater supply. Thus, it is possible that these processes (along with others) are responsible for influencing the variability among trees reported here.

For time series, this might not be important if interannual patterns are constant. The results shown in Table 2.2 indicate that interannual patterns are different in magnitude but not direction. Specifically, the total range of isotopic variation between oaks A, B, and C is 1.2‰, 1.9‰, and 1.2‰ respectively. In addition, high yearly standard deviations among tree segments as well as the difference between summer year segment averages illustrate that between-tree variations are apparent. These findings suggest that tree ring carbon isotopes are influenced by common regional factors as well as potential local changes described previously. Therefore, while $\delta^{13}C$ values are variable among trees, the offsets appear systematic and $\delta^{13}C$ values can be employed to investigate regional-scale climate changes.

To test further the relationship between $\delta^{13}C$ and climate variables, we qualitatively compared the Missouri climate division 1 instrumental PDSI record (NCDC, 2004) to our generated carbon isotope values during the 'Dust Bowl' period where, during much of the 1930s, a significant drought (both hotter and drier than average conditions) persisted for several years in the Midwest (Figure 2.1). Observed $\delta^{13}C$ trends show increased $\delta^{13}C$ values, as expected, during times of water stress (Farquhar et al., 1989). Furthermore, despite the many potential confounding factors, this correlation is apparent by utilizing the average of only three trees. The latter idea will be examined in further detail during chapter 3.

2.5. Conclusions

The tests from this initial study indicated the following: 1) available latewood samples from the ALOC contain sufficient (>1.0 mg) material to reliably characterize the carbon isotopic signal, 2) the within-tree carbon isotopic variation is small, with replicates from the same year showing reproducibility comparable to machine error, 3) absolute values for given years between trees are not very consistent, but year to year trends are consistent among trees, and 4) averaged isotopic values from three trees display expected excursions during a period of known extreme weather. These results empirically demonstrate the feasibility using a $\delta^{13}C$ record from oak trees to investigate climate change and provide a framework for sampling protocols in subsequent analyses.

References

Antonova, G.E., and Stasova, V.V., 1997. Effects of environmental factors on wood formation in larch (*Larix sibirica* Lbd.) stems. *Trees* **11**: 462-468.

Brenna, J.T., Corso, T.N., Tobias, H.J., and Caimi, R.J., 1997. High-precision continuous-flow isotope ratio mass spectrometry. *Mass Spectrometry Reviews* **16**: 227-258.

Domec, J.-C., and Gartner, B.L., 2002. How do water transport and water storage differ in coniferous earlywood and latewood. *Journal of Experimental Botany* **53-379**: 2369-2379.

Farquhar, G.D., and Sharkey, T.D., 1982. Stomatal Conductance and Photsynthesis. *Annual Review of Plant Physiology* **33**: 317-346.

Farquhar, G.D., Ehleringer, J.R., and Hubick, K.T., 1989. Carbon Isotope Discrimination and Photosynthesis. *Annual Review of Plant Physiology and Plant Molecular Biology* **40**: 503-537.

Faure, G., 1986. *Principles of Isotope Geology*. John Wiley and Sons, New York, pp 589.

Gindi, W., Brabner, M., and Wimmer, R., 2000. The influence of temperature on latewood lignin content in treeline Norway spruce compared with maximum density and ring width. *Trees* **14**: 409-414.

Ghosh, P., and Brand, W., 2003. Stable Isotope ratio mass spectrometry in global climate change research. *International Journal of Mass Spectrometry* **228**: 1-33.

Hill, S.A., Waterhouse, J.S., Field, E.M., Switsur, V.R., and Rees, T., 1995. Rapid recycling of triose phosphates in oak stem tissue. *Plant, Cell, Environment* **18**: 931-936.

Lebourgeois, F., 2000. Climatic signals in earlywood, latewood and total ring width of Corsican pine from western France. *Annals of Forestry Science* **57**: 155-164.

McCarroll D., and Loader N.J., 2004. Stable isotopes in tree rings. *Quaternary Science Reviews* **23**: 771–801.

McCarroll, D., Jalkanen, R., Hicks, S., Tuovinen, M., Gagen, M., Pawellek, F., Eckstein, D., Schmitt, U., Autio, J., and Heikkinen, O., 2003. Multiproxy dendroclimatology: a pilot study in northern Finland. *The Holocene* **13-6**: 831-841.

Miller, R., 1999. Structure of Wood. *In*: Wood Handbook – Wood as an engineering material. Gen Tech. Rep. FPL-GTR-113. Madison, WI: USDA, Forest Service, Forest Products Laboratory, 463p.

National Climate Data Center (NCDC), 2004. Time bias corrected divisional temperature-precipitation-drought index. www.ncdc.noaa.gov/oa/climate/climatedata.html.

YEAR	OAK A-1	OAK A-2	OAK A-3	Average	STDEV
1923	-26.4	-26.4	-26.7	-26.5	0.14
1922	-25.8	-26.0	-26.0	-25.9	0.08
1921	-26.2	-26.4	-26.5	-26.4	0.15
1920	-25.6	-25.5	-25.6	-25.5	0.05
Average	**-26.0**	**-26.1**	**-26.2**	**-26.1**	**0.11**

YEAR	OAK B-1	OAK B-2	OAK B-3	Average	STDEV
1923	-27.1	-27.1	-27.1	-27.1	0.01
1922	-26.0	-26.0	-25.9	-26.0	0.07
1921	-26.8	-26.7	-26.8	-26.8	0.07
1920	-25.9	-26.0	-25.9	-25.9	0.04
Average	**-26.5**	**-26.5**	**-26.5**	**-26.5**	**0.05**

YEAR	OAK C-1	OAK C-2	OAK C-3	Average	STDEV
1923	-24.8	-24.7	-24.7	-24.7	0.04
1922	-24.4	-24.3	-24.3	-24.3	0.04
1921	-25.0	-25.1	-25.3	-25.1	0.14
1920	-25.0	-25.0	-24.9	-25.0	0.05
Average	**-24.8**	**-24.8**	**-24.8**	**-24.8**	**0.07**

Table 2.1: Raw carbon isotope (in ‰) results from triplicate analyses of segments Oak A, Oak B, and Oak C. The standard deviation among samples is represented in the column denoted STDEV. The average, standard deviation and range is computed for each year using all three isotopic samples generated from each oak.

	OAK A	OAK B	OAK C	OVERALL	
Summer Year	**Average**	**Average**	**Average**	**Average**	**Standard Deviation**
1923	-26.5	-27.1	-24.7	-26.1	1.25
1922	-25.9	-26.0	-24.3	-25.4	0.95
1921	-26.4	-26.8	-25.1	-26.1	0.86
1920	-25.5	-25.9	-25.0	-25.5	0.48

	OAK A	OAK B	OAK C	OVERALL	
Summer Year	**Yearly Change**	**Yearly Change**	**Yearly Change**	**Average**	**Standard Deviation**
1922-1923	-0.6	-1.1	-0.4	-0.7	0.38
1921-1922	0.4	0.8	0.8	0.7	0.21
1920-1921	-0.8	-0.8	-0.1	-0.6	0.40

Table 2.2: The top table shows average raw carbon isotope (in ‰) results from triplicate analyses summarized by tree segment. The bottom table illustrates the isotopic change between summer years of each oak segment. While the magnitudes (values) of isotopic yearly changes are different, the direction of isotopic change is systematic.

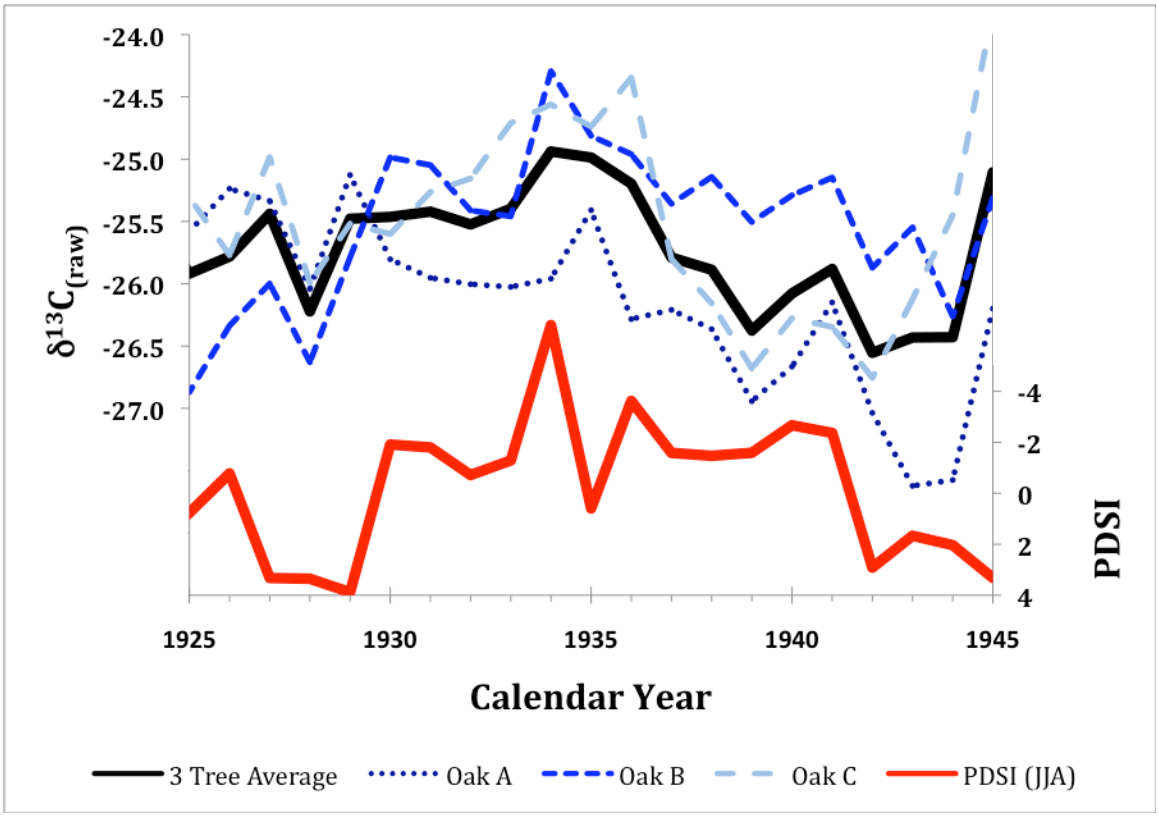

Figure 2.1: Carbon isotopic results from 1925-1945 of all individual oaks and the three-tree average of all oaks graphically compared against June-August PDSI. Averaging three trees appears to more fully capture the overall trends depicted from instrumental PDSI records.

Chapter 3

AN INNOVATIVE SAMPLING STRATEGY TO INCREASE THE RESOLUTION OF CLIMATICALLY LINKED $\delta^{13}C$ ISOTOPE CHANGES FROM TREE RINGS.

Abstract

By exploiting previously determined comparisons of the similarity of ring width patterns (RWP) from an individual tree to the pooled pattern for all indexed trees of that age in the American Long Oak Chronology as a means to select trees for analysis, we can maximize the efficiency of generating climatologically significant $\delta^{13}C$ records within temperate climate regions. From 1931-2002, the period with reliable instrumental data for the study region, averaged $\delta^{13}C$ measurements of bulk latewood is significantly correlated with June-July-August precipitation and PDSI values for entire data set. Further, the correlation is better for an average of three trees with relatively high correlation ($R = -0.49$, $p<0.0001$ and $R = -0.40$, $p<0.001$ for precipitation and PDSI, respectively) between their RWP and the regional ring width index than it is for an average of three trees with a relatively low correlation ($R = -0.32$, $p<0.01$ and $R = -0.40$, $p<0.001$ for precipitation and PDSI, respectively). In other words, whereas climatically significant information seems to be recorded in the $\delta^{13}C$ values of all trees studied, the signal to noise ratio is maximized by selecting tree segments whose individual RWP best match the average ring width index developed for the region. Since the ring width similarity metric is available for all indexed trees back to 912 A.D., this selection criterion can be used to maximize data quality and efficiency when generating millennial scale isotopic records.

3.1. Introduction

Current climate change is the subject of intense scientific, public and political debate. These discussions center upon whether the rising global average temperatures are the result of natural climatic cycles or feedbacks from global anthropogenic input into the climate system (Mann et al., 2003; Emanuel, 2005; IPCC, 2007). Notably, 13 of the 14 globally hottest years have been recorded since 1995 (IPCC, 2007; NASA, 2009). Unraveling detailed connections and, equally important, estimating potential economic and societal consequences of global warming or other climatic events require examining regional scale data. In particular, there is an urgent need to quantify recent climatic changes in regions where human activities are most vulnerable (Stahle and Cleaveland, 1992; Meko et al., 1995; Raffalli-Delerce et al., 2004; Cook et al., 2004; Masson-Delmotte et al., 2005; Reynolds-Henne et al., 2007).

The midwest of the United States is an agricultural center of the world, with an economy intimately tied to crop growth and, thus, climate. This region (unlike other North American regions) exhibits a strong continental seasonality (NCDC, 2004) and, as a result, has also experienced some of the most extreme climatic events over the 20th century including the Dust Bowl Drought and the 1993 Flood (Stockton and Meko, 1983; Schubert et al., 2004a and 2004b; Perry, 2006; White et al., 2008; Dirmeyer and Kinter, 2009; Stahle et al., 2009). Hence, the midwest is ideal to study how regional manifestations of global climate change may influence this area in the near future.

Unfortunately, high-resolution climate records prior to instrumental data are lacking in this region of the US (Meko et al., 1995; Woodhouse and Overpeck, 1998). A potential archive of climate variability beyond instrumental records may lie with long continuous tree-ring chronologies (Fritts, 1976; Guyette et al., 2004, McCarroll and Loader 2004). By utilizing tree ring stable carbon isotopes from white oak in northern Missouri, we may be able to better constrain and understand climate dynamics of the central Midwest.

This project is possible due to the existence of the American Long Oak Chronology (ALOC) project developed at the University of Missouri Tree Ring Laboratory. The ALOC record is the only northern hemisphere continuous millennial-scale (912-2004 AD) tree ring chronology within the American Great Plains (Guyette et al., 2004). It is, thus, a unique archive that permits the direct construction of a $\delta^{13}C$ tree ring time series to investigate the climatic history of America's agricultural heartland. To test empirically whether $\delta^{13}C$ in oaks provide an accurate and accessible record of climatic variability, we have generated tree ring $\delta^{13}C$ time series at a yearly resolution and compared them to instrumental records of temperature, precipitation and PDSI from 1931 to 2002 (Appendix 3).

Relatively high regional moisture conditions have been documented as an important confounding variable to consider prior to interpreting tree ring $\delta^{13}C$ time series (Leavitt and Long, 1984; Loader et al., 1997; Robertson et al, 1997; Loader et al., 2003; McCarroll and Loader, 2004; Verheyden et al., 2005; Leavitt, 2008). Numerous studies have demonstrated that where water stress is a dominant factor

(like the American Southwest), the carbon isotope records closely track climate (see section 3.2.2. for further information) and robust records can be generated with generally 4-6 samples per year (Leavitt and Long, 1988; Gagen et al., 2004; McCarroll and Loader, 2004). However, within humid regions, like the Midwest US where severe water stress is not a leading concern, $\delta^{13}C$ records in general do not demonstrate strong relationships to climate variables. Because the $\delta^{13}C$ signal tends to exhibit more variability (likely due to lack of a single dominant variable), one solution to capture a high-quality climate record might be to increase the number of samples per year with the hope of removing the local variations within the signal and more accurately capture regional climate change (Saurer et al., 1995; Robertson et al., 1997; McCarroll and Pawlick, 2001; Gagen et al., 2004). Unfortunately, this solution is not always practical because of the associated increase in analytical time and costs (assuming sample availability). Another potential solution is to improve the selection criteria for samples used to infer regional climate change. This paper investigates an innovative sampling approach to achieve this end.

Specifically, the goal of this paper is to investigate the feasibility of generating a meaningful carbon isotopic time series from oak trees within the central Midwest by addressing important questions such as 1) which trees should be selected for isotopic analysis, 2) which samples correlate best with what climate variables and 3) how many trees are required to develop a carbon isotope time series from ALOC samples?

3.2. Scientific Background

3.2.1. The American Long Oak Chronology Development

Living trees and sub-fossil samples of white oak were collected in north-central Missouri (Figure 3.1). The topography of the surrounding area is mainly low-lying plains with gently sloping hills. Valleys contain floodplains up to two miles wide (Pauls, 1990). Subsurface materials are primarily glacial tills and agriculturally modified soils. Sub-fossil trees are primarily found partially submerged within or eroding out of the banks of small rivers (Guyette and Stambaugh, 2003) which meander freely across their floodplains burying, exposing, and reburying trees on sub millennial time scales.

The Missouri Tree Ring Laboratory has been developing the ALOC project for the central Midwest with archived samples and data representing over a decade of field collection and ring width study. The resulting chronology is developed from widely abundant white oak trees (*Quercus bicolor, Quercus macrocarpa*), which have several excellent characteristics for studying paleoclimate. Their abundance has enabled the Missouri Tree Ring Laboratory to develop a long, continuous record extending back to 912 AD. Additional floating century-scale chronologies go back to approximately 14,000 radiocarbon years (Guyette et al., 2004). Furthermore, this chronology has been independently dated through techniques such as density dating, ^{14}C dating, and cross dating techniques to confirm age assignments and correlations between trees (Fritts, 1976; Guyette and Stambaugh, 2003; Guyette et al., 2004). Important for this study, the RWP of all individual segments have been compared to the pattern of pooled, normalized ring widths for the ALOC and

expressed as a correlation coefficient (varies from R = 0.0 to 1.0). The more closely the RWP of an individual tree-segment corresponds to the average pooled patterns, the higher the correlation coefficient.

Segments originate from slices of subfossil tree wedges and cores of living white oak trees that were collected in the field and prepared for ring width analyses at the Missouri Tree Ring Laboratory. Trees used in this study exhibit well-defined and well preserved growth rings. Each oak ring is easily distinguishable and has two main components; earlywood and latewood (Miller, 1999; Domec and Gartner, 2002). Earlywood is formed in as little as a few weeks during the spring, is distinguished by large vessels (see Figure 1.2), and has been shown to use stored photsynthates from previous years that could add complexity to interpretation of the earlywood isotopic signal (Hill et al., 1995; McCarroll et al., 2003; McCarroll and Loader, 2004). Latewood is primarily formed during the main growing season (June through August) of a particular year (Hill et al., 1995; Miller, 1999; Lebourgeois, 2000) from carbon fixed during that growing season and is denser than earlywood allowing measurement of very thin rings. Therefore, to the extent environment controls $\delta^{13}C$ values, latewood $\delta^{13}C$ should track meteorological conditions (such as precipitation or temperature) during summer months (Antonova et al., 1997; Gindi et al., 2000; Lebourgeois, 2000; Loader et al., 2003; McCarroll and Loader, 2004). Hence, this study only utilized latewood.

3.2.2. Stable Carbon Isotopes

Stable carbon isotopes are expressed in standard δ-notation form defined as:

$$\delta^{13}C = [(^{13}C/^{12}C_{\text{sample}})/(^{13}C/^{12}C_{\text{standard}}) - 1] * 1000$$

where $\delta^{13}C$ is expressed in parts per thousand (‰). The sample is the material being analyzed and the standard is a known isotopic reference (VPDB) (Faure, 1986).

Tree ring carbon isotopic ratios vary mainly from fractionation during photosynthesis modified by the rate of CO_2 exchange through leaf stomata. Stomata are pores in leaves that regulate gas exchange between the interior of the leaf and the atmosphere. They function largely to control moisture loss from the leaf, but they also regulate CO_2 exchange (Farquhar et al., 1989; McCarroll and Loader 2004). $^{12}CO_2$ diffuses more rapidly than $^{13}CO_2$, and, because internal pCO_2 is lower than atmospheric pCO_2, there is a relative depletion of $^{13}CO_2$ within leaves compared to the outside ambient air. The process results in fractionation due to diffusion of up to -4.4‰ depending on the concentration gradient (Farquhar and Sharkey, 1982; Farquhar et al., 1989; McCarroll and Loader, 2004). Fractionation further occurs during carbon fixation when internal CO_2 is utilized by the photosynthetic enzyme whereby trees preferentially use ^{12}C with respect to ^{13}C called 'net fractionation due to carboxylation' which has been estimated at about -27‰ (Farquhar and Sharkey, 1982; Farquhar et al., 1989; McCarroll and Loader, 2004). Because the fractionation causes an increase in the $\delta^{13}C$ value of CO_2 within the leaf, the fractionation expressed depends on the rate of carbon fixed relative to the rate at which CO_2

enters the leaf. This balance determines the effective discrimination against ^{13}C during carbon fixation and has been modeled as

$$\delta^{13}C_{plant} = \delta^{13}C_{air} - a - (b\text{-}a)(ci/ca)$$

where the constants *a* and *b* represent fractionation due to diffusion (≈ -4.4‰) and carboxylation (≈ -27‰) respectively, *ci* & *ca* are the intercellular and ambient CO_2 concentrations, and $\delta^{13}C_{air}$ is the $\delta^{13}C$ of atmospheric CO_2 (Farquhar et al., 1989).

As moisture stress likely affects $\delta^{13}C$ values (by influencing how open stomata are), variations in these isotopic values should provide a yearly record of water stress. During times of low water stress (low temperature and/or high precipitation) the stomata will tend to open and ci/ca will increase, resulting in lower $\delta^{13}C$ isotopic values. In contrast, when water stress is high, the stoma begins to close, ci/ca decreases, and $\delta^{13}C$ values are higher. Importantly for my research, fixed carbon used in wood formation does not exchange between rings or with other parts of the tree during ring formation (McCarroll and Loader, 2004) and latewood is formed during summer months only. So, fluctuations in the final isotopic signatures of photsynthates (ranging from -20‰ to -30‰) should be recorded through time with at least an annual resolution in latewood.

3.2.3. Northern Missouri Climate

The climate of northern Missouri is generally humid with strong continental seasonality (NCDC, 2004). Average summer (June-August) temperatures (see Figure 1.1) from northwest Missouri climate division 1 are 24.0°C (1931-2002)

where June, July, and August have average temperatures of 22.6°C, 25.3°C and 24.1°C respectively. Mean annual precipitation for northwest Missouri is approximately 33.9 inches per year, which is less than Missouri's average (41.2 in). Regional average summer monthly precipitation is 4.3 in where June, July, and August have average precipitation amounts of 5.0 in, 4.1 in, and 3.9 in. Summer precipitation is generally higher in the northern region than in the southern region of Missouri as heavier thundershowers are more common in the north.

3.3. Methods

3.3.1. Sample Selection

To test for potential isotopic differences in ALOC samples and examine relationships with regional climate and RWP, this study defined two data sets over the 20th century using developed RWP. Being that all individual trees have previously been compared to the pattern of pooled, normalized ring-widths, the previously described criteria was used for the creation of our data sets as: 1) segments whose RWP have a high correlation to the pooled, normalized RWP ($R \geq 0.60$) are data set '*HC*' and 2) segments whose RWP have a low correlation to the pooled, normalized RWP ($R \leq 0.40$) are data set '*LC*'. Additionally, to test how increasing the sample size improves the isotopic signal, segments that were combined from the first two data sets to approximate sample selection without consideration of RWP will be designated hereafter as data set '*RS*'. For both HC and LC, there are three samples per year, although six trees were used to generate the

HC as well as LC data set. The reason for this difference is that too few individual trees have correlation patterns than span the entire interval of interest. To account for these complications and anticipating further work in the pre-instrumental period where switching between trees will be needed, only the portion of segments (a minimum of 25 years) that conform to the defined correlation values for each data set were used (Table 3.1).

3.3.2. Sample Preparation and Analysis

Latewood portions of each tree ring were sampled using a razor blade. All visual components not of latewood material were carefully removed or avoided (i.e. earlywood, structural rays). This procedure minimizes potential contributions from carbon fixed during times other than the sampled year. Approximately 2 mg of sample material were used for analyses and in most cases each individual ring could provide enough material for replicate analyses if needed. By conducting analytical measurements on individual yearly samples, we aimed to retain as much high-frequency variability as possible.

Individual bulk samples were weighed, loaded into tin boats, and analyzed by continuous flow stable isotope mass spectrometry techniques (further details in Brenna *et al.*, 1997; Ghosh and Brand, 2003; McCarroll and Loader, 2004). Prepared samples are loaded into a 50-port autosampler connected to a Carlo-Erba 1500 elemental analyzer (EA). Each sample is individually dropped into a combustion reactor within the EA that is heated to 1020ºC where flash combustion with O_2 occurs and produces gases such as CO_2, N_2, NO_x, H_2O and excess O_2. The gases are

carried in a helium stream and enter a secondary reduction reactor where excess O_2 is retained and nitrogen oxides are reduced to N_2. Then the gases pass first through a filter where water is removed and second through a gas chromatographic column to separate different compounds. The outflow (helium with entrained CO_2 and N_2 gas) pass through a Finnigan Conflo III device into a Finnigan DeltaPlusXL Isotope Ratio Mass Spectrometer (IRMS) where $\delta^{13}C$ values are calculated for CO_2 based on comparison with a reference CO_2 gas of known isotopic composition. To monitor accuracy and precision, an average of five samples for every Acetanilide standard were used for each full run. In less than 12 hours, 50 analyses (samples plus standards) can be run with excellent analytical precision (<0.1‰, 1σ standard deviation). Raw isotopic results are expressed as per mil deviations using delta notation (δ) relative to the VPDB standard.

3.3.3. Data Evaluation

The raw isotope data were corrected for the 'industrial effect' (Saurer et al., 1997; McCarroll and Loader 2004; Raffalli-Delerce et al., 2004; Gagen et al., 2004, 2006, 2007, 2008; Loader et al., 2008; McCarroll et al., 2009). This correction removes the effect of declining atmospheric $\delta^{13}C$ values due to addition of CO_2 with low $\delta^{13}C$ values as a result of fossil fuel burning since 1850 (start of industrialization). These trends can be mathematically removed using the modified equation from McCarroll et al. (2009):

$$\delta^{13}C_{cor} = \delta^{13}C_{raw} - (\delta^{13}C_{atm} + 6.4)$$

where $\delta^{13}C_{cor}$ is the corrected value after removal of the 'industrial effect', $\delta^{13}C_{raw}$ is the individual plant isotopic value generated from isotopic analyses, and $\delta^{13}C_{atm}$ is the measured isotopic atmospheric value taken from McCarroll and Loader (2004). These corrected values are then recalculated (normalized) as the difference from the average value for the segment.

This normalization is needed because average $\delta^{13}C$ differences between trees are high relative to interannual variability (chapter 2). However, this potentially introduces at least three complications. First, because the average for each segment is set to zero, estimated climate variability is dampened. For example, if 20 of 25 years during a given segment were drier than average, normalization underestimates the effect of this aridity in the pooled results. Second, such a bias could create an artificial change at the boundary of segments (if the previous or subsequent segment did not have similar average conditions). Third, trends longer than the longest segment length could potentially be invisible to this analysis. Uneven segment lengths and using only HC trees (which have lower between tree differences than LC trees) may reduce the contributions of the first and second concerns, but the third remains problematic.

Finally the normalized data were averaged for each data type (i.e., HC and LC trees) as well as the total data set. The resulting isotopic time series were compared statistically to multidecadal temperature, precipitation and PDSI from averaged monthly records of nearby regional climate stations within northwest Missouri Climate Division 1 from 1931-2002 (NCDC, 2004). Prior to 1931, relatively few stations record climate data.

3.4. Results

Overall raw carbon isotope values ranged from -23.3‰ to -29.9‰ with a mean of -26.2‰. The total range of values for HC (-28.5‰ to -23.8‰) was approximately two-thirds as large the range of values for LC (-23.3‰ to -29.9‰). The mean values for the HC, LC and RS were -25.8‰, -26.7‰ and -26.2‰ respectively. All raw $\delta^{13}C$ data are presented in Appendix 1. The differences between corrected and raw $\delta^{13}C$ values are shown in Figure 3.2.

The carbon isotopic time series generated were characterized by a decline in $\delta^{13}C$ values, especially following 1950 with a more dramatic decrease in LC compared to HC (Table 3.2). As expected the correction for anthropogenic inputs removed much of this decline (Figure 3.2).

A linear regression between normalized HC and LC data show a significant relationship ($R = 0.38$, $p<0.001$) during the climate data period of 1931-2002 (Figure 3.3). However, while these data sets are correlated, the LC record shows higher variability in both pattern and magnitude of $\delta^{13}C$ values than the HC record.

In addition to correlating with each other, both HC and LC $\delta^{13}C$ trends are statistically correlated with the average summer (JJA) precipitation per month (HC: $R = -0.49$, $p<0.00005$; LC: $R = -0.32$, $p<0.01$) and PDSI (HC: $R = -0.40$, $p<0.001$; LC: $R = -0.40$, $p<0.001$) though poorly correlated with temperature (HC: $R = 0.27$, $p<0.05$; LC: $R = 0.24$, $p<0.05$). Precipitation and temperature exhibit correlations to $\delta^{13}C$ mainly during JJA whereas PDSI correlates significantly (at $p<0.1$), yet moderately to $\delta^{13}C$ values in most months during and before the growing the season (Figure 3.4).

When all data from chapter 2 are incorporated into data set RS, correlations do not improve.

3.5. Discussion

3.5.1. Data Set Evaluations

Despite concerns that Missouri's humid summer climate might reduce the influence of water stress on the growth of white oaks in the region, limiting the utility of $\delta^{13}C$ as a paleoclimate proxy, all $\delta^{13}C$ values are consistently correlated with summer precipitation per month. However, HC $\delta^{13}C$ values demonstrate the strongest overall relationship while LC demonstrates the lowest.

The differences between HC and LC correlations could be the result of the relative importance of local vs. regional variables that influence tree ring $\delta^{13}C$ values. Because all trees exhibit a significant correlation to precipitation and PDSI, tree ring $\delta^{13}C$ values are at least in part influenced by regional moisture variations. However, the noise associated with the isotopic signals of HC and LC is most likely the result of local environmental factors. For instance, trees emergent from the forest canopy might capture more light but be more exposed and, thus, more susceptible to water loss than trees with leaves largely within or below the canopy. Additionally, older trees within a forest may have deeper rooting depths and, as a result, have better access to a groundwater supply (McCarroll and Loader, 2004). Thus, it is possible that these examples of local processes (along with others) are responsible for influencing the variability among tree ring isotopic results reported here that, in turn, lead to the correlation differences between HC and LC seen in

Figure 3.3. By discriminating among samples based on RWP, we selected trees whose growth patterns most closely reflect regional, not local, forcing patterns. It is important to note that this selection criterion includes no prior knowledge of $\delta^{13}C$ values.

Because the HC record seems to exhibit a higher quality regional climate record than the LC record, the remaining discussions here and chapters in the dissertation will make use of only HC segments. The rationale for using only HC-type segments is that they provide the most robust $\delta^{13}C$ signal. Therefore, reconstruction of climate beyond instrumental records using as few as three samples per year can be achieved.

3.5.2. Climatic Evaluations

$\delta^{13}C$ values are correlated best to summer (JJA) climate variables whereas conditions during other times of the year show little association to $\delta^{13}C$ values (Figure 3.4). Additionally, when yearly (September of previous year to August of current year) climate averages are compared to $\delta^{13}C$ values, the degree of correlation is less than with the JJA relationships. Also, while all climate variables are significantly correlated to $\delta^{13}C$ during JJA, temperature is considerably less correlated ($p<0.05$) relative to that of precipitation and PDSI ($p\leq0.001$ respectively). Although p values cannot be directly compared, qualitatively it seems that summer moisture is the most important variable for predicting $\delta^{13}C$ values in the instrumental climate data set.

In addition, when compared to instrumental precipitation, the $\delta^{13}C$ patterns from 1931-2002 seem to recognize wetter periods more clearly than drier periods (Figure 3.5). As an example, the wettest 20th century summer (1993) clearly stands out in the $\delta^{13}C$ record whereas the driest summer (1936) does not correspond to a clear peak in tree ring $\delta^{13}C$ values. Conversely, the ALOC ring width index has previously demonstrated a significant correlation to drier periods associated with PDSI (i.e. droughts). In addition, there is no correlation between RWP and $\delta^{13}C$ values. Therefore, these observations hint that together, $\delta^{13}C$ values and RWP records may allow for a reconstruction of a more complete climate record than either can alone.

Interestingly, there is an apparent improvement in the correlation between summer precipitation and $\delta^{13}C$ if precipitation totals from the previous two summers are also included in the moisture metric. By generating a weighted precipitation (WP) scale of:

$$WP = JJA_t + (JJA_{t-1})(0.5) + (JJA_{t-2})(0.25)$$

where JJA_t is the average June-August precipitation for a given year t, the correlation increases to $R = -0.63$, $p<0.000000005$ (from $R = -0.49$, $p<0.00005$) (Figure 3.6). The WP is relatively insensitive to altering weighting factors. The WP used here (present year + 50% of previous year (t-1) + 25% of two years (t-2) prior to the present) generates correlations that are very close to the empirically estimated maximum. In other words, when adding additional years beyond t-2 or attempting to incorporate other months, resultant correlations decline or only improve marginally. These interesting correlations suggest that summer precipitation from

up to two years past may have some relationship to a current growing season's carbon isotopic value. We cannot explain this apparent "memory" in the system and it may be a coincidence. However, it appears to be robust and future studies may aim to constrain the possible physiological mechanism (e.g., the number of buds set in the previous growing season effects the current years leaf area and the next years twig density) behind this relationship.

3.5.3 Summary of Normalization Strengths and Weaknesses

This chapter has demonstrated that the use of HC-type samples is important in order to improve the signal to noise ratio when generating tree ring $\delta^{13}C$ values. In addition, because of the need to switch among trees, normalization is needed. However, these solutions were not without their own artifacts (Table 3.3). For example, the potential to study longer-term climate variability is limited by the shortest segment length of 25 years in this study. In addition, by selecting individual segments based on a certain criteria (i.e., HC or LC), we may not be sampling a representative population and therefore introduce a bias into the data. Also, a drawback of using HC-type samples is that while the ALOC has a large sample base of which to choose segments from, the lack of segments that exhibit high correlation values may prove an obstacle in obtaining the minimum of three samples per year.

3.6. Conclusions

Two separate white oak data seta sets (HC-high correlation and LC-low correlation) were generated based upon the correlations of individual segment ring widths to the pattern of pooled normalized widths in the region in order to test for isotopic differences. Results indicate that both data sets show significant ($p<0.001$) correlations to summer (June-August) precipitation and PDSI while being poorly, yet still significantly, correlated ($p<0.05$) to summer temperature. HC samples showed the overall best correlation to precipitation ($R = -0.49$, $p<0.00001$). However, considerable differences in both the pattern and magnitude of $\delta^{13}C$ values occur between HC and LC. Local processes are likely responsible for influencing the variability among tree ring isotopic results reported here that, in turn, lead to the correlation differences between HC and LC. As a result, selecting the best samples (HC) prior to isotopic analyses was shown to reduce the noise associated with tree ring $\delta^{13}C$ signals and produce more robust climatic correlations. Utilizing the selection method reveals that an isotopic investigation to investigate climate change beyond instrumental records is reasonable through the use of tree ring $\delta^{13}C$ in Midwest white oaks.

References

Antonova, G.E., and Stasova, V.V., 1997. Effects of environmental factors on wood formation in larch (*Larix sibirica* Lbd.) stems. *Trees* **11**: 462-468.

Brenna, J.T., Corso, T.N., Tobias, H.J., and Caimi, R.J., 1997. High-precision continuous-flow isotope ratio mass spectrometry. *Mass Spectrometry Reviews* **16**: 227-258.

Cook, E.R., Woodhouse, C., Eakin, C.M., Meko, D.M. and Stahle, D.W., 2004. Long-term aridity changes in the western United States. *Science* **306**: 1015-1018.

Dirmeyer, P.A., and Kinter III, J.L., 2009. The "Maya Express": Floods in the U.S. Midwest. *EOS* **90-12**: 101-102.

Domec, J.-C., and Gartner, B.L., 2002. How do water transport and water storage differ in coniferous earlywood and latewood. *Journal of Experimental Botany* **53-379**: 2369-2379.

Emanuel, K. A., 2005. Increasing destructiveness of tropical cyclones over the past 30 years. *Nature* **436**: 686-688.

Farquhar, G.D., and Sharkey, T.D., 1982. Stomatal Conductance and Photsynthesis. *Annual Review of Plant Physiology* **33**: 317-346.

Farquhar, G.D., Ehleringer, J.R., and Hubick, K.T., 1989. Carbon Isotope Discrimination and Photosynthesis. *Annual Review of Plant Physiology and Plant Molecular Biology* **40**: 503-537.

Faure, G., 1986. *Principles of Isotope Geology*. John Wiley and Sons, New York, pp 589.

Fritts, H.C., 1976. Tree Rings and Climate. The Blackburn Press, New Jersey, 567 pp.

Gagen, M., McCarroll, D., and Edouard, J-L., 2004. Latewood width, maximum density and stable carbon isotope ratios of pine as paleoclimate indicators in a dry, subalpine environment. *Arctic, Antarctic and Alpine Research* **36**: 166-171.

Gagen, M., McCarroll, D., and Edouard, J.-L., 2006. Combining ring width, density and stable carbon isotope proxies to enhance the climate signal in tree-rings: an example from the southern French Alps. *Climatic Change* **78**: 363-379.

Gagen, M., McCarroll, D., Loader, N.J., Robertson, I., Jalkanen, R., and Anchukaitis, K.J., 2007. Exorcising the 'segment length curse': summer temperature

reconstruction since AD 1640 using non-detrended stable carbon isotope ratios from pine trees in northern Finland. *The Holocene* **17-4**: 435-446.

Gagen, M., McCarroll, D., Robertson, I., Loader, N.J., and Jalkanen, R., 2008. Do tree ring $\delta^{13}C$ series from *Pinus sylvestris* in northern Fennoscandia contain long-term non-climatic trends? *Chemical Geology* **252**: 42-51.

Gindi, W., Brabner, M., and Wimmer, R., 2000. The influence of temperature on latewood lignin content in treeline Norway spruce compared with maximum density and ring width. *Trees* **14**: 409-414.

Ghosh, P., and Brand, W., 2003. Stable Isotope ratio mass spectrometry in global climate change research. *International Journal of Mass Spectrometry* **228**: 1-33.

Guyette, R.P., and Stambaugh, M.C., 2003. The Age and Density of Ancient and Modern Oak Wood in Streams and Sediments. *IAWA Journal* **24-4**: 345-353.

Guyette, R.P., Stambaugh, M.C., and Dey, D.C., 2004. Ancient Oak Climate Proxies From the Agricultural Heartland. *EOS* **85-46**: 485.

Hill, S.A., Waterhouse, J.S., Field, E.M., Switsur, V.R., and Rees, T., 1995. Rapid recycling of triose phosphates in oak stem tissue. *Plant, Cell, Environment* **18**: 931-936.

Intergovernmental Panel on Climate Change (IPCC), 2007. Climate Change 2007: The Physical Science Basis. Fourth Assessment Report of the IPCC Summary for Policymakers, 18p.

Leavitt, S.W., 2008. Tree-ring isotopic pooling without regard to mass: No difference from averaging $\delta^{13}C$ values of each tree. *Chemical Geology* **252**: 52-55.

Leavitt, S.W., and Long, A., 1984. Sampling strategy for stable carbon isotope analysis of tree rings in pine. *Nature* **311**: 145-147.

Leavitt, S.W., and Long, A., 1988. Stable carbon isotope chronologies from trees in the southwestern United States. *Global Biogeochemical Cycles* **2:**189-198.

Lebourgeois, F., 2000. Climatic signals in earlywood, latewood and total ring width of Corsican pine from western France. *Annals of Forestry Science* **57**: 155-164.

Loader, N.J., Robertson, I., Barker, A.C., Switsur, V.R., and Waterhouse, J.S., 1997. An improved technique for the batch processing of small wholewood samples to α-cellulose. *Chemical Geology* **136**: 313-317.

Loader, N.J., Robertson, I., and McCarroll, D., 2003. Comparison of stable carbon isotope ratios in the whole wood, cellulose and lignin of oak trees-rings. *Palaeogeography, Palaeoclimatology, Palaeoecology* **196**: 395-407.

Loader, N.J., Santillo, P.M., Woodman-Ralph, J.P., Rolfe, J.E., Hall, M.A., Gageb, M., Robertson, I., Wilson, R., Froyd, C.A., and McCarroll, D., 2008. Multiple stable isotopes from oak trees in southwestern Scotland and the potential for stable isotope Dendroclimatology in maritime climatic regions. *Chemical Geology* **252**: 62-71.

Mann, M.E., Ammann, C.M., Bradley, R.S., Briffa, K., Crowley, T.J., Jones, P.D., Oppenheimer, M., Osborn, T.J., Overpeck, J.T., Rutherford, S., Trenberth, K.E., and Wigley, T.M.L., 2003. On past temperatures and anomalous late-20th century warmth. *EOS* **84-27**: 256-257.

Masson-Delmotte, V., Raffalli-Delerce, G., Danis, P.A., Yiou, P., Stievenard, M., Guibal, F., Mestre, O., Bernard, V., Goosse, H., Hoffmann, G., and Jouzel, J., 2005. Changes in European precipitation seasonality and in drought frequencies revealed by a four-century-long tree-ring isotopic record from Brittany, western France. *Climate Dynamics* **24**: 57-69.

McCarroll D., and Loader N. J., 2004. Stable isotopes in tree rings. *Quaternary Science Reviews* **23**: 771–801.

McCarroll, D., and Pawlick, F., 2001. Stable Carbon isotope ratios of *Pinus sylvestris* from northern Finland and the potential for extracting a climate signal from long Fennoscandian chronologies. *The Holocene* **11**: 675-684.

McCarroll, D., Jalkanen, R., Hicks, S., Tuovinen, M., Gagen, M., Pawellek, F., Eckstein, D., Schmitt, U., Autio, J., and Heikkinen, O., 2003. Multiproxy dendroclimatology: a pilot study in northern Finland. *The Holocene* **13-6**: 831-841.

McCarroll, D.J., Gagen, M.H., Loader, N.J., Robertson, I., Anchukaitis, K.J., Los, S., Young, G.,H.F., Jalkanen, R., Kirchhefer, A., and Waterhouse, J.S., 2009. Correction of tree ring stable carbon isotope chronologies for changes in the carbon dioxide content of the atmosphere. *Geochimica et Cosmochimica Acta* **73**: 1539-1547.

Meko, D.C., Stockton, W., and Boggess, W.R., 1995. The tree-ring record of severe sustained drought. *Water Resources Bulletin* **31**: 789-801.

Miller, R., 1999. Structure of Wood. *In*: Wood Handbook – Wood as an engineering material. Gen Tech. Rep. FPL-GTR-113. Madison, WI: USDA, Forest Service, Forest Products Laboratory, 463p.

Missouri Tree Ring Laboratory, 2006. Map of study location provided by Dr. Mike Stambaugh.

National Aeronautics and Space Administration (NASA), 2009. GISS Surface Temperature Analysis. http://data.giss.nasa.gov/gistemp/graphs.

National Climate Data Center (NCDC), 2004. Time bias corrected divisional temperature-precipitation-drought index. http://www.ncdc.noaa.gov/oa/climate/climatedata.html.

Pauls, W., 1990. Soil Survey of Grundy County, Missouri. USDA: Soil Conservation Service, 127 p.

Perry, C.A., 2006. Midwestern streamflow, precipitation, and atmospheric vorticity influenced by Pacific sea-surface temperatures and total solar-irradiance variations. *International Journal of Climatology* **26-2**: 207-218.

Raffalli-Delerce, G., Masson-Delmotte, V., Dupouey, J.L., Stievenard, M., Breda, N., and Moisselin, J.M., 2004. Reconstruction of summer droughts using tree-ring cellulose isotopes: a calibration study with living oaks from Brittany (western France). *Tellus* **56B**: 160-174.

Reynolds-Henne, C.E., Siegwolf, R.T.W., Treydte, K.S., Esper, J., Henne, S., and Saurer, M., 2007. Temporal stability of climate-isotope relationships in tree rings of oak and pine (Ticino, Switzerland). *Global Biogeochemical Cycles* **21**: GB4009, doi:10.1029/2007GB002945.

Robertson, I., Switsur, V.R., Carter, A.H.C., Barker, A.C., Waterhouse, J.S., Briffa, K.R. and Jones, P.D., 1997. Signal strength and climate relationships in the $^{13}C/^{12}C$ ratios of tree ring cellulose from oak in east England. *Journal of Geophysical Research* **102-D16**: 19507-19516.

Saurer, M., Siegenthaler, H., and Schweingruber, F., 1995. The climate-carbon isotope relationship in tree rings and the significance of site conditions. *Tellus* **47B**: 320-330.

Saurer, M., Borella, S., Schweingruber, F., Siegwolf, R., 1997. Stable carbon isotopes in tree rings of beech: climatic versus site-related influences. *Trees* **11**: 291-297.

Schubert, S.D., Suarez, M.J., Pegion, P.J., Koster, R.D., and Bacmeister, J.T., 2004a. On the Cause of the 1930s Dust Bowl. *Science* **303**: 1855-1859.

Schubert, S.D., Suarez, M.J., Pegion, P.J., Koster, R.D., and Bacmeister, J.T., 2004b. Causes of Long-Term Drought in the U.S. Great Plains. *Journal of Climate* **17-3**: 485-503.

Stahle, D.W., Cleaveland, M.K., 1992. Reconstruction and analysis of spring rainfall over the southeastern U.S. for the past 1000 years. *Bulletin of the American Meteorological Society* **73-12**: 1947-1961.

Stahle, D.W., Cook, E.R., Villanueva, J., Diaz, F.K., Burnette, D.J., Griffin, R.D., Acuña Soto, R., Seager, R., and Heim Jr., R.R., 2009. Early 21st-Century Drought in Mexico. *EOS* **90-11**: 89-90.

Stambaugh, M.C., Guyette, R.P., 2009. Progress in constructing a long oak chronology from the central United States. Tree Ring Research 65-2: 147-156.

Stockton, C.W., and Meko, D.M., 1983. Drought Recurrence in the Great Plains as Reconstructed from Long-Term Tree-Ring Records. *Journal of Climate and Applied Meteorology* **22**: 17-29.

Verheyden, A., Roggeman, M., Bouillon, S., Elskens, M., Beeckman, H., and Koedam, N., 2005. Comparison between $\delta^{13}C$ of α-cellulose and bulk wood in the mangrove tree *Rhizophore mucronata*: Implications for dendrochemistry. *Chemical Geology* **219**: 275-282.

White, W.B., Gershunov, A., and Annis, J., 2008. Climatic Influences on Midwest Drought during the Twentieth Century. *Journal of Climate* **21-3**: 517-531.

Woodhouse, C.A., and Overpeck, J.T., 1998. 2000 years of drought variability in the central United States. *Bulletin of the American Meteorological Society* **79-12**: 2693-2714.

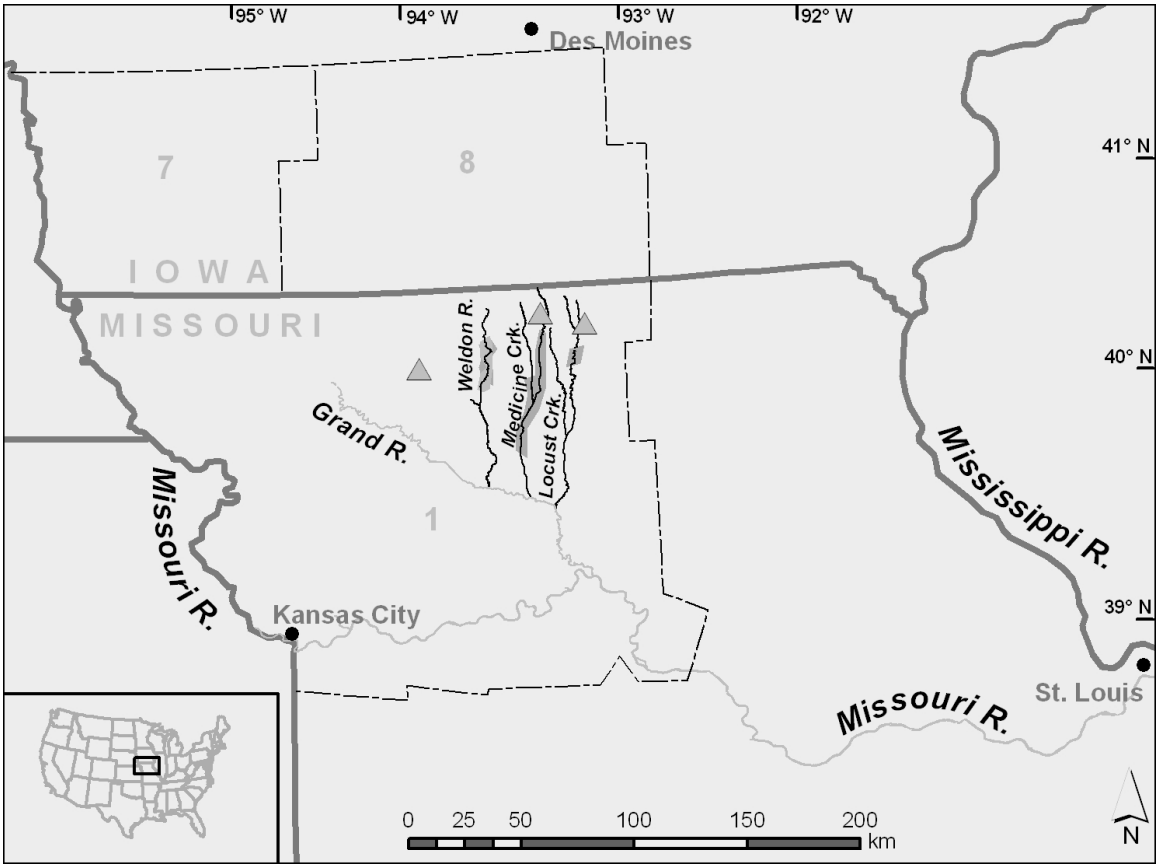

Figure 3.1: The regional location map (modified from Stambaugh and Guyette, 2009) shows the sampling location for many of the American Long Oak Chronology trees. Triangles denote sites where many samples used in this study were collected. Also, the dashed lines represent climate divisions from the National Climate Division Center of the National Oceanic and Atmospheric Administration. Climate data (temperature, precipitation and PDSI) from meteorological stations within climate division 1 of northwest Missouri (dashed border) were used to determine to how tree ring $\delta^{13}C$ relates with climate.

Oak	Set	R	Oak Type	Location
B	*HC*	>0.6	Swamp White Oak	Platte River
F	*HC*	>0.7	Swamp White Oak	Little Medicine Creek
G	*HC*	>0.7	Swamp White Oak	Little Medicine Creek
H	*HC*	>0.7	Bur Oak	Little Medicine Creek
K	*HC*	>0.7	Swamp White Oak	Little Medicine Creek
L	*HC*	>0.7	Swamp White Oak	Little Medicine Creek
AA	*LC*	<0.4	Swamp White Oak	Medicine Creek
BB	*LC*	<0.4	Swamp White Oak	Crooked Creek
CC	*LC*	<0.4	Swamp White Oak	Locust Creek
DD	*LC*	<0.4	Swamp White Oak	Crooked Creek
EE	*LC*	<0.4	Swamp White Oak	Locust Creek
FF	*LC*	<0.4	Swamp White Oak	Crooked Creek

Table 3.1: Segment information for samples used to in both HC and LC data sets for this study. All segments lengths used for evaluation of RWP correlation were ≥ 25-year intervals starting at 1925, 1950, and 1975.

Data	Type	1925-2004	1950-2004	1975-2004
HC	***RAW***	-0.016	-0.023	-0.043
	CORR	0.001	0.004	-0.014
LC	***RAW***	-0.002	-0.033	-0.069
	CORR	0.017	-0.007	-0.040
RC	***RAW***	-0.009	-0.028	-0.056
	CORR	0.009	-0.002	-0.027

Table 3.2: The values represent raw and corrected (CORR) isotopic slopes of best-fit lines (in ‰/yr) through each time period. As the data are analyzed closer to the present, the best-fit lines exhibit an increased negative slope for all data sets. The corrected data remove much of the existing negative slopes in the data suggesting the correction procedure was fairly successful in removing anthropogenic effects seen in the raw carbon isotopic data.

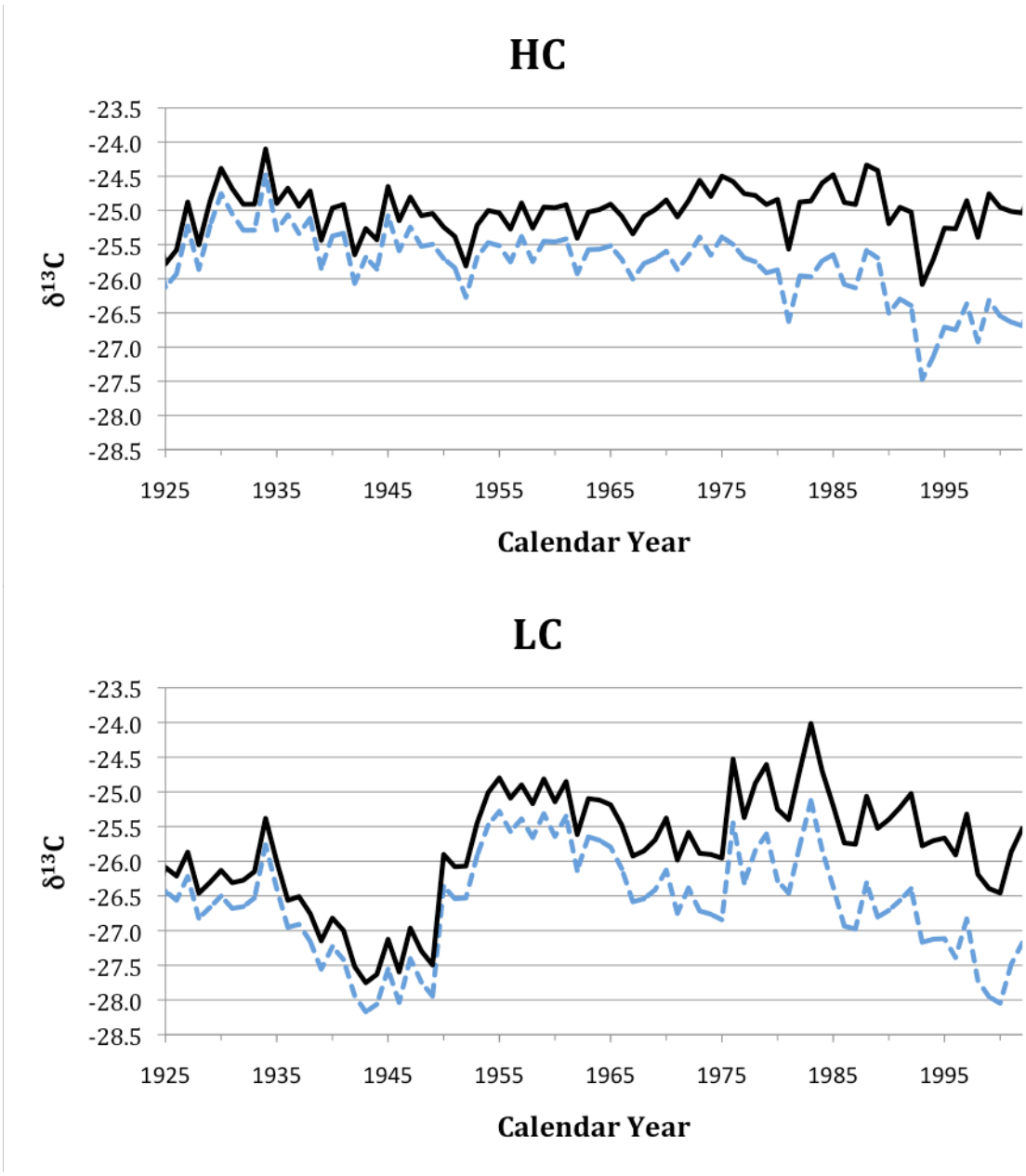

Figure 3.2: Raw and corrected (for industrial effect) $\delta^{13}C$ plots of HC and LC data sets from 1925-2002. The darker solid line on both plots is the corrected time series. The standard deviation around the average of HC (0.95) is lower than that of LC (1.14).

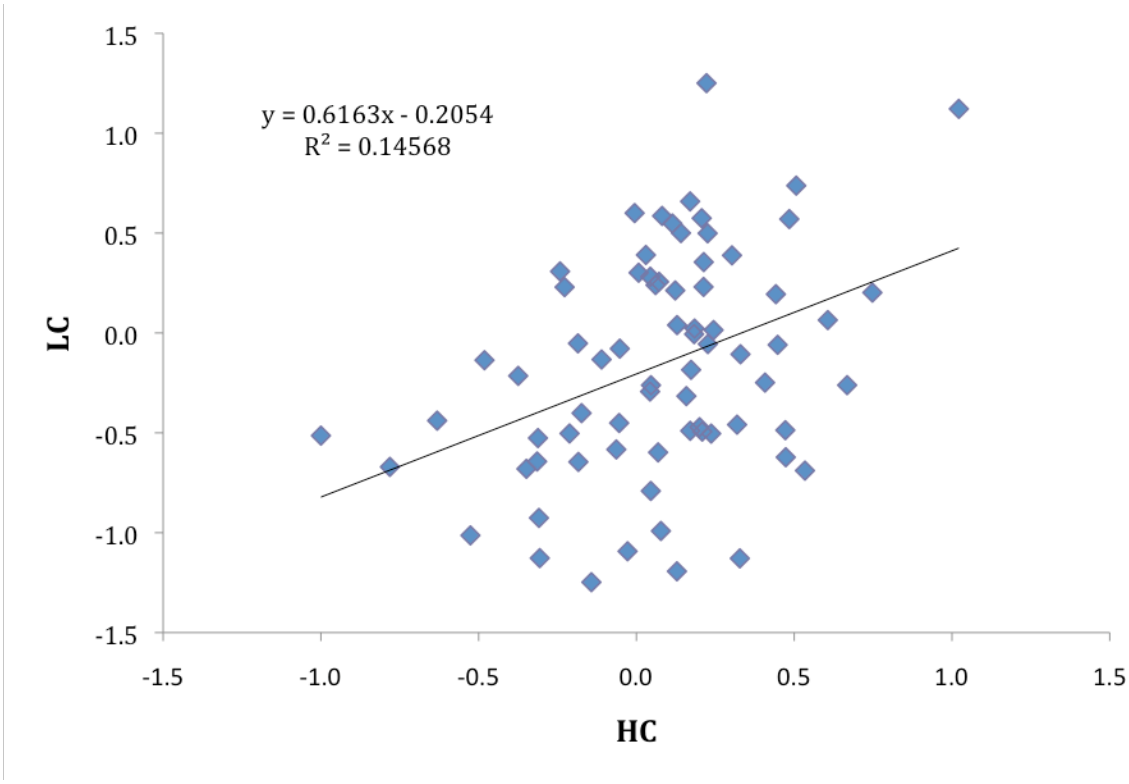

Figure 3.3: Scatter plot of HC vs. LC normalized $\delta^{13}C$ values from 1931-2002. While weak, a significant correlation still exists ($R^2 = 0.15$, $R = 0.38$, $p<0.001$) between the data sets.

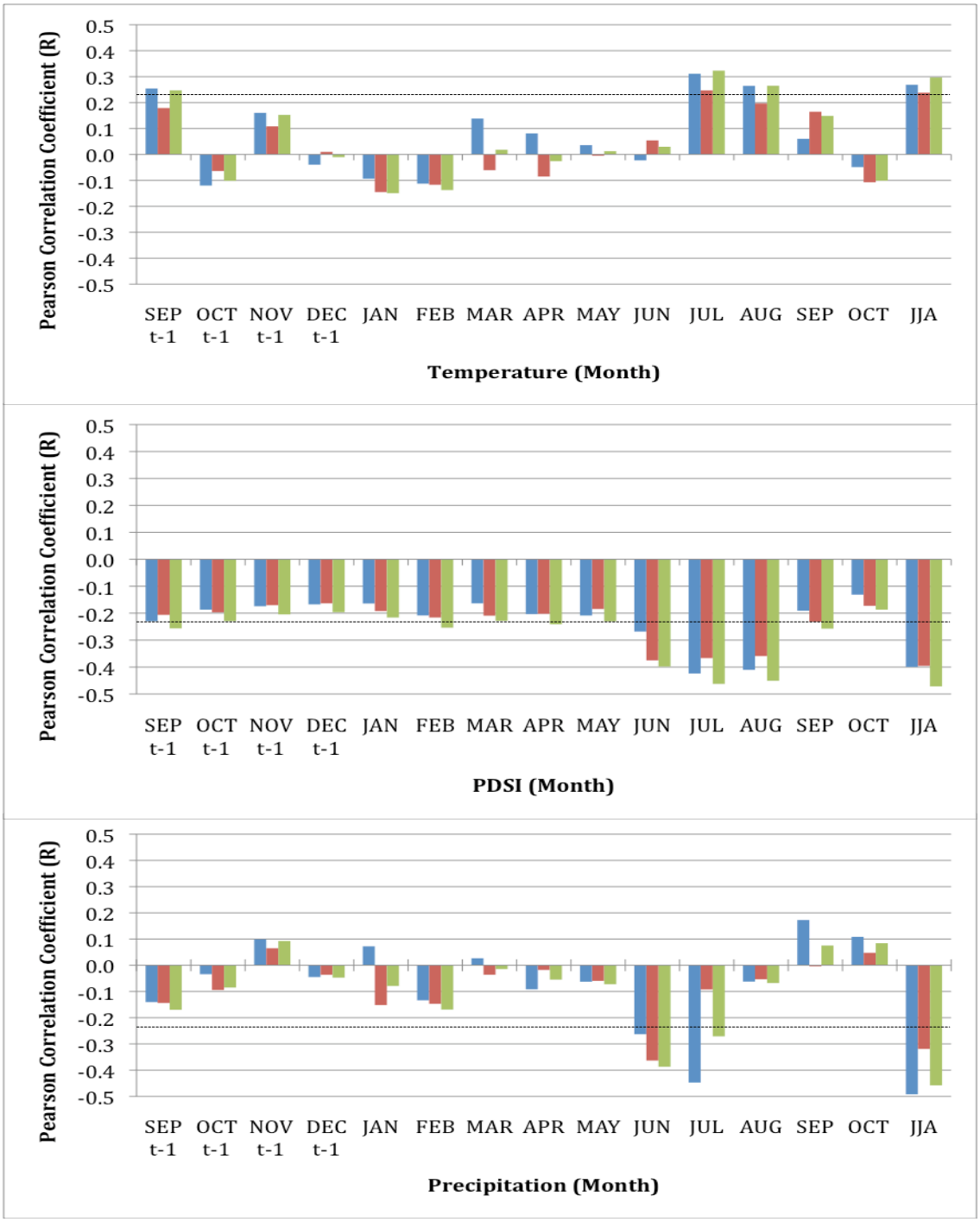

Figure 3.4: Composite correlation diagrams from 1931-2002 illustrating Pearson correlations (R) between normalized $\delta^{13}C$ values and temperature (top graph), PDSI (middle graph) and precipitation (lower graph). These diagrams are presented with all three data sets HC (left), LC (middle), and RC (right) during a given month. Only correlations greater than 0.23 are significant at the 95% confidence level (dashed line on diagrams). Climatic months previous to the current year are denoted by *t-1*.

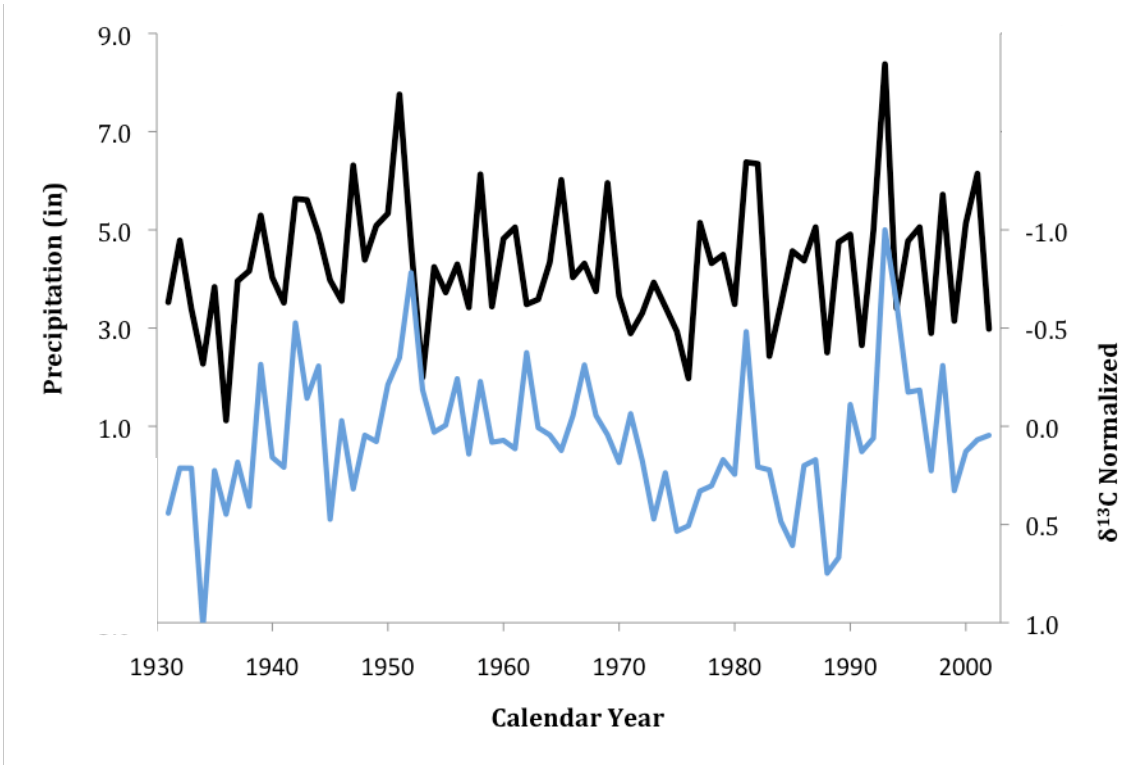

Figure 3.5: Instrumental average summer (JJA) precipitation (in) per month (top-dark line) plotted against normalized $\delta^{13}C$ values (light line).

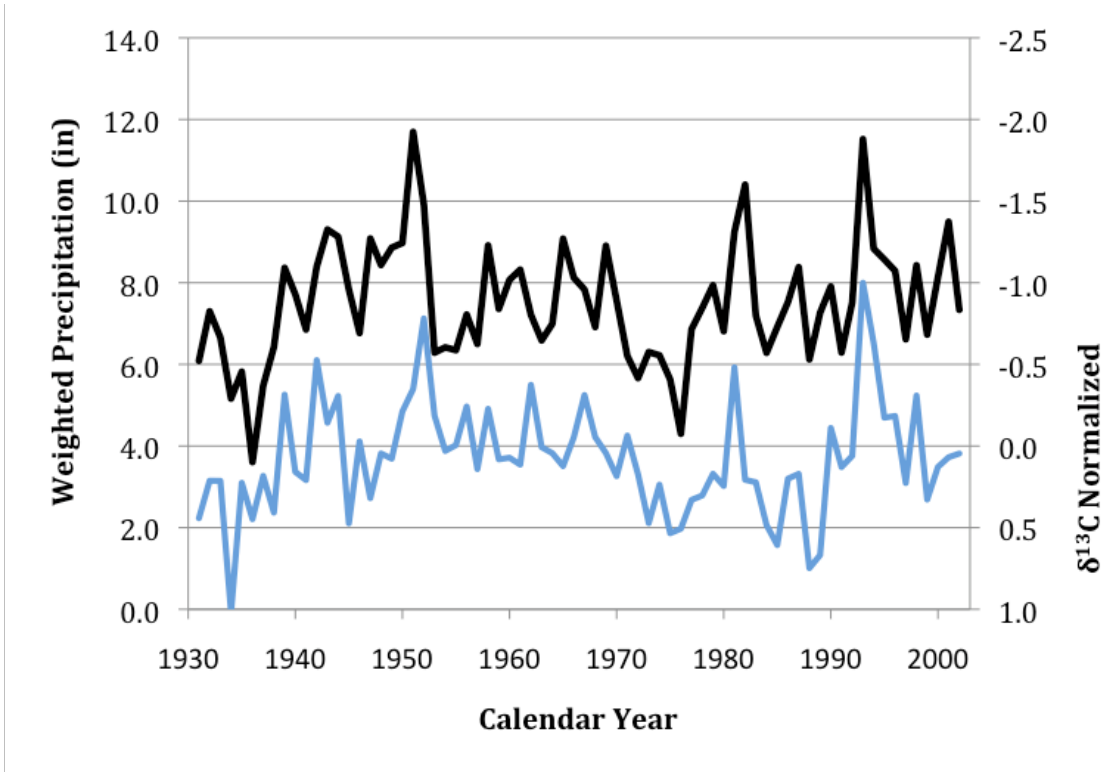

Figure 3.6: Weighted instrumental average summer (JJA) precipitation (in) per month (top-dark line) plotted against normalized $\delta^{13}C$ values (light line).

	HC segments	LC segments	RS segments	Raw Data	Normalized Data
Reduced cost	+	-	--	X	X
Short-term variance	+	+	+	+	+
Long-term variance	-	-	-	-	+
Between-tree variance	+	-	X	+	-
Population vs. sample	-	-	-	+	-
Samples available	-	-	+	X	X

Table 3.3: Summary of the strengths and weaknesses of sample selection techniques (HC, LC, and RS) used in this study. A plus (+) indicates the method has supplemental or favorable benefit, a minus (-) indicates unfavorable benefit, a double minus (--) indicates very unfavorable benefit, and an X indicates not applicable.

Chapter 4

PREDICTING SUMMER PRECIPITATION FROM TREE RING $\delta^{13}C$ VARIATIONS

Abstract

Twentieth century tree ring carbon isotopic data and instrumental weather records were used to develop the first Midwestern $\delta^{13}C$ model to reconstruct past precipitation variability. The initial model, derived from linear regression correlations, explains 24% of the variance in observed summer (June-August) precipitation from 1931-2002. Additionally, a split calibration and verification testing scheme confirms the model has modest predictive skill as the reduction of error (RE) and coefficient of efficiency (CE) tests both are positive. Reconstructed values appear to under-predict the total range of variability in observed precipitation. However, wet extremes are more noticeably captured than dry extremes. As a result, it is likely that $\delta^{13}C$ data will be useful in identifying extreme wet periods in the time before instrumental data. Additionally, an 11-year moving average calculated for both reconstructed and instrumental average summer precipitation values shows the model may capture decadal-scale trends in precipitation that are also seen in instrumental average summer precipitation.

4.1. Introduction

Ongoing global climate change discussions emphasize the importance of understanding past climatic variability in order to understand what we may expect

in the future (IPCC, 2007). Of particular importance are regions where human activities are most vulnerable to climate change, such as the midwestern US (Stahle and Cleaveland, 1992; Meko et al., 1995; Raffalli-Delerce et al., 2004; Cook et al., 2004; Masson-Delmotte et al., 2005; Reynolds-Henne et al., 2007). The midwestern US has experienced frequent severe drought and flooding in the last century, including the 1930s Dust Bowl era and the 1951 and 1993 Great Floods. If the frequency or magnitude of these events varies with regional climate, the Midwest may be particularly vulnerable to anthropogenic climate change. The Dust Bowl was a decade of excessively hot and dry weather throughout the midcontinent, leading to crop failures and compounding hardships of the Great Depression (Woodhouse and Brown, 2001). The Great Floods inundated homes and crops over much of the Missouri and Mississippi, basins producing widespread economic problems, resulting in the relocation of entire towns, especially after the 1993 flood (FEMA, 2009). Given the worldwide importance of agricultural and economic activities in the US midwest, understanding past precipitation variability would aid in preparing for potential future events (Cook et al., 1999), especially if the last century is a poor guide for what to expect in the next.

Understanding climate variability has relied heavily on 20th century instrumental meteorological records. However, instrumental records represent a relatively short time interval in any given region and may sample only a fraction of natural climate variability. Thus, they are insufficient to completely assess long-term climate change (Meko et al 1995; Cook and Evans, 2000; Woodhouse, 2003). This shortcoming is especially acute in the midwestern US, where climate records

have relatively poor spatial and temporal coverage that do not extend to times before the 1900s and have coverage that is quite sparse as recently as the 1930s (NCDC, 2004). Consequently, finding long-term climate records are essential to examine low frequency (decadal scale) climate variability in order to investigate how potential large scale forcing mechanisms may interact with local climate regimes (Cayan et al, 1998; Woodhouse 2003).

The American Long Oak Chronology (ALOC) provides an archive of prehistoric climate variability on a yearly scale. High-resolution $\delta^{13}C$ time series generated from ALOC tree rings provide a chemical means to reconstruct climate variability beyond instrumental records. Chapter 3 examined sampling schemes and developed a 20th century carbon isotope record from the ALOC. Most importantly, this isotope record demonstrates a significant correlation with regional precipitation ($R = -0.49$, $p<0.0001$). In this chapter, that same carbon isotopic record is used to develop an isotopic model for the 20th century to reconstruct Midwest precipitation that will be used for the pre-instrumental record.

4.2. Methods

4.2.1. Sample Selection

The Missouri Tree Ring Laboratory has been developing the ALOC project for the central Midwest (see Figure 3.1) with archived samples and data representing over a decade of field collection and ring width study. The resulting chronology is developed from white oak trees, which have several excellent characteristics for studying paleoclimate. They are abundant, which has enabled the Missouri Tree

Ring Laboratory to develop a long, continuous record extending back to 912 AD. Additional floating century-scale chronologies go back to approximately 14,000 radiocarbon years (Guyette et al., 2004). Furthermore, this chronology has been independently dated through techniques such as density dating, ^{14}C dating, and cross dating techniques to confirm age assignments and correlations between trees (Fritts, 1976; Guyette and Stambaugh, 2003; Guyette et al., 2004). Important for this study, the ring width patterns (RWP) of all individual segments are compared to the pattern of pooled, normalized ring widths for the ALOC and expressed as a correlation coefficient (R). The more closely the RWP of a span of years in an individual corresponds to the average pooled patterns, the higher the correlation coefficient. In this chapter, only results from the 'high correlation' data set (HC) in chapter 3 were used to develop a model to reconstruct summer precipitation in the Midwest.

4.2.2. Sample Preparation and Analysis

Latewood portions of each tree ring were sampled using a razor blade. All visual components not of latewood material were carefully removed or avoided (i.e. earlywood, structural rays). This procedure minimizes potential contributions from carbon fixed during times other than the sampled year. Approximately 2 mg of sample material were used for analyses, and, in most cases each individual ring could provide enough material for replicate analyses if needed. By conducting analytical measurements on individual yearly samples, we aimed to retain as much high-frequency variability as possible.

Individual bulk samples were weighed, loaded into tin boats, and analyzed by continuous flow stable isotope mass spectrometry techniques (further details in Brenna *et al.*, 1997; Ghosh and Brand, 2003; McCarroll and Loader, 2004). Prepared samples are loaded into a 50-port autosampler connected to a Carlo-Erba 1500 elemental analyzer (EA). Each sample is individually dropped into a combustion reactor within the EA that is heated to 1020ºC where flash combustion occurs and produces gases such as CO_2, N_2, NO_x, H_2O and excess O_2. The gases are carried in a helium stream and enter a secondary reduction reactor where excess O_2 is retained and nitrogen oxides are reduced to N_2. Then the gases pass first through a filter where water is removed and second through a gas chromatagraphic column to separate different molecules. The outflow (helium with entrained CO_2 and N_2 gas) pass through a Finnigan Conflo III device into a Finnigan DeltaPlusXL Isotope Ratio Mass Spectrometer (IRMS) where $\delta^{13}C$ values are calculated for CO_2 based on comparison with a reference CO_2 gas of known isotopic composition. To monitor accuracy and precision, an average of five samples for every standard were used for each full run. In less than 12 hours, 50 analyses (samples plus standards) can be run with excellent analytical precision (<0.1‰, 1σ). Raw isotopic results are expressed as per mil deviations using delta notation (δ) relative to the VPDB standard.

4.2.3. Data Evaluation of HC Segments

The HC $\delta^{13}C$ time series was corrected for the 'industrial effect' (Saurer et al., 1997; McCarroll and Loader 2004; Raffalli-Delerce et al., 2004; Gagen et al., 2004,

2005, 2007, 2008; Loader et al., 2008; McCarroll et al., 2009) through removal of the effect of declining atmospheric values due to addition of CO_2 with low $\delta^{13}C$ values as a result of fossil fuel burning since 1850 (start of industrialization). These corrected values are then recalculated as the difference from the average value for the segment from the sample collected (normalized) to remove potential edge effects of segments when switching between trees in order to emphasize a tree's relative isotopic change (broad response to climate) on a yearly scale regardless of the absolute raw values.

Finally, the resulting isotopic time series were compared statistically to multidecadal temperature, precipitation and PDSI from averaged monthly records of nearby regional climate stations within northwest Missouri Climate Division 1 from 1931-2002 (NCDC, 2004). Prior to 1931, relatively few stations record climate data. The results led to the conclusion that $\delta^{13}C$ values are significantly influenced by summer precipitation (Figure 4.1).

4.2.4. Model Development

A calibration analysis was used to assess the climatic reconstruction potential of carbon isotopes from white oak trees in northern Missouri. A split sample calibration and verification scheme was used to examine the ability of HC tree ring carbon isotopes with annual resolution to predict regional summer precipitation (Meko and Graybill, 1995; Woodhouse, 2003). The data set was split into two equal groups where the first group encompasses 1931-1966 and the second group is 1967-2002. A linear regression analysis (Test 1) from the first

group yielded a calibration equation that was applied to the $\delta^{13}C$ values of the second group. The resulting predictions for precipitation were compared to measured values for verification. Then, a linear regression analysis (Test 2) from the second group yields a second calculation that was applied using the first group for secondary verification. A final linear regression (Test 3) was run on the entire 1931-2002 period and compared to the results of the first two tests for comparison of R, R^2, significance (p) and Standard Error (SE) values to assess the predictive ability of the $\delta^{13}C$ linear regression model (Meko and Graybill, 1995; Woodhouse, 2003).

Three additional verification statistics were calculated to assess the predictive ability of the regression equations used. The reduction of error (RE) and coefficient of efficiency (CE) tests examine the ability of the model to estimate precipitation compared to the calibration mean (measure of shared variance between the observed and predicted series). The average RE in the verification period is:

$$RE = 1.0 - \left[\frac{\sum (x_i - \hat{x}_i)^2}{\sum (x_i - \bar{x}_c)^2} \right]$$

where x_i and $\hat{x}_i$ are the observed and predicted data in year *i* of the verification period and $\bar{x}_c$ is the mean of the actual data from the calibration period. Values range from -∞ to +1 and only values greater than zero indicate that the model predictions have reconstruction ability and match observed values better than

expected by chance (Lorenz, 1956; Fritts, 1976; Cook, et al., 1999; Woodhouse 2003). The average CE in the verification period is:

$$CE = 1.0 - \left[\frac{\sum (x_i - \hat{x}_i)^2}{\sum (x_i - \bar{x}_v)^2} \right]$$

where x_i and $\hat{x}_i$ are the observed and predicted data in year *i* of the verification period and $\bar{x}_v$ is the mean of the actual data in the verification period. Values range from -∞ to +1 and only values greater than zero indicate that the model predictions have reconstruction ability and match observed values better than expected by chance (Lorenz, 1956; Fritts, 1976; Cook, et al., 1999; Woodhouse 2003). Finally, the Sign Test (ST) determines the agreements-disagreements in sign of departure from the mean in the observed and reconstructed series to broadly show the ability of the model to track interannual variability in precipitation. In general, when the ST has more agreements than disagreements, this indicates the model has some skill in predicting summer precipitation.

4.3. Results

Using only HC segments (as defined in chapter 3), the results of the split sample calibration analysis indicate the full reconstruction model exhibits the ability to predict precipitation beyond instrumental records (Table 4.1). Regression analyses from Test 1 and Test 2 yield similar results ($R=0.45$, $R^2=0.20$ and $R=0.53$, $R^2=0.28$ respectively). Each test is significant at $p<0.01$. RE and CE tests are positive for both tests (Test 1: RE = 0.27, CE = 0.27, Test 2: RE = 0.19, CE = 0.19),

which demonstrates that the model has the ability to reconstruct precipitation. Sign tests 1 and 2 were significant ($p<0.05$) with more agreements than disagreements (23/13 and 21/15 respectively). The final full period regression model yielded similar results as both Tests 1 and 2 ($R=0.49$, $R^2=0.24$, $p<0.001$), where average summer precipitation units per month = $-1.8667(\delta^{13}C) + 4.4381$. This equation is from the full period regression that was used to develop the model.

4.4. Discussion

The carbon isotopic model explains 24% ($R^2 = 0.24$) of the variance in observed instrumental precipitation from 1931-2002, where estimated average summer (JJA) precipitation shows a range of 3.77 in per month (Figure 4.2). The model also estimates an error of 0.75 inches of summer precipitation per month based on the average standard deviation among normalized segment $\delta^{13}C$ values (0.4). The wettest and driest estimated average summer precipitation is during 1993 and 1934 (6.30 in and 2.53 in respectively). These extreme years from reconstructed precipitation correspond to the Great Flood of 1993 and a dry year during the 1930s Dust Bowl that have been frequently mentioned in previous chapters. Also, despite a greater observed instrumental range of average summer precipitation per month from 1931-2002 (1.1 to 8.4 in), the wettest average summer precipitation year from instrumental records is still 1993 and the driest instrumental summer is during the Dust Bowl period. This correspondence strengthens the confidence in the model's ability to predict extreme summer precipitation events beyond instrumental records.

To simulate decadal scale variability, an 11-year moving average was calculated for both average summer instrumental and predicted precipitation series, and these smoothed records show similar periods of high and low precipitation. For example, predicted average summer precipitation indicates prolonged dry periods of less precipitation during the 1930s, 1970s and 1980s, whereas the instrumental precipitation record also shows extensive dry periods during the 1930s and 1970s as well (Figure 4.3). In addition, the predicted precipitation series indicates prolonged wet periods of increased average summer precipitation from the 1940s through to the 1960s as well as the 1990s, which is also generally comparable with the instrumental precipitation record. Consequently, reconstructed average summer precipitation from tree ring $\delta^{13}C$ values appears to maintain decadal-scale trends in precipitation occurring in northern Missouri.

4.5. Conclusions

The first carbon isotopic based model developed in humid regions of the central US provides the ability to reconstruct average summer precipitation beyond instrumental records. A split-calibration analysis scheme was used to test the model, along with RE, CE and sign tests, which indicated significant predictive skill. The reconstruction explains 24% of the variance in observed precipitation and is capable of identifying extreme precipitation years reasonably well. Calculating 11-year moving averages also reveals comparable multidecadal scale patterns between both observed and predicted average summer precipitation records. Thus, the isotopic model exhibits reconstruction potential for generating long continuous $\delta^{13}C$

records beyond instrumental records to examine variations in Midwest precipitation.

References

Brenna, J.T., Corso, T.N., Tobias, H.J., and Caimi, R.J., 1997. High-precision continuous-flow isotope ratio mass spectrometry. *Mass Spectrometry Reviews* **16**: 227-258.

Cook, E.R., and Evans, M., 2000. Improving estimates of drought variability and extremes from centuries-long tree-ring chronologies: A PAGES/CLIVAR example. CLIVAR *Exchanges*. **5-1**, *PAGES* Newsletter, **8-1**, International CLIVAR Project Office, Southampton, United Kingdom, 10-12.

Cook, E.R., Briffa, K.R., and Jones, P.D., 1994. Spatial regression methods in dendroclimatology: A review and comparison of two techniques. *International Journal of Climatology* **14**: 379-402.

Cook, E.R., Meko, D.M., Stahle, D.W., and Cleaveland, M.K., 1999. Drought reconstructions for the continental United States. *Journal of Climate* **12**: 1145-1162.

Cook, E.R., Woodhouse, C., Eakin, C.M., Meko, D.M. and Stahle, D.W., 2004. Long-term aridity changes in the western United States. *Science* **306**: 1015-1018.

Federal Emergency and Management Agency (FEMA), 2009. The 1993 Great Midwest Floods: Voices 10 Years Later. http://www.fema.gov/library/viewRecord.do?id=1789.

Fritts, H.C., 1976. Tree Rings and Climate. The Blackburn Press, New Jersey, 567 pp.

Gagen, M., McCarroll, D., and Edouard, J-L., 2004. Latewood width, maximum density and stable carbon isotope ratios of pine as paleoclimate indicators in a dry, subalpine environment. *Arctic, Antarctic and Alpine Research* **36**: 166-171.

Gagen, M., McCarroll, D., and Edouard, J.-L., 2006. Combining ring width, density and stable carbon isotope proxies to enhance the climate signal in tree-rings: an example from the southern French Alps. *Climatic Change* **78**: 363-379.

Gagen, M., McCarroll, D., Loader, N.J., Robertson, I., Jalkanen, R., and Anchukaitis, K.J., 2007. Exorcising the 'segment length curse': summer temperature reconstruction since AD 1640 using non-detrended stable carbon isotope ratios from pine trees in northern Finland. *The Holocene* **17-4**: 435-446.

Gagen, M., McCarroll, D., Robertson, I., Loader, N.J., and Jalkanen, R., 2008. Do tree ring $\delta^{13}C$ series from *Pinus sylvestris* in northern Fennoscandia contain long-term non-climatic trends? *Chemical Geology* **252**: 42-51.

Ghosh, P., and Brand, W., 2003. Stable Isotope ratio mass spectrometry in global climate change research. *International Journal of Mass Spectrometry* **228**: 1-33.

Guyette, R.P., and Stambaugh, M.C., 2003. The Age and Density of Ancient and Modern Oak Wood in Streams and Sediments. *IAWA Journal* **24-4**: 345-353.

Guyette, R.P., Stambaugh, M.C., and Dey, D.C., 2004. Ancient Oak Climate Proxies From the Agricultural Heartland. *EOS* **85-46**: 485.

Intergovernmental Panel on Climate Change (IPCC), 2007. Climate Change 2007: The Physical Science Basis. Fourth Assessment Report of the IPCC Summary for Policymakers, 18p.

Leavitt, S.W., and Long, A., 1984. Sampling strategy for stable carbon isotope analysis of tree rings in pine. *Nature* **311**: 145-147.

Loader, N.J., Santillo, P.M., Woodman-Ralph, J.P., Rolfe, J.E., Hall, M.A., Gageb, M., Robertson, I., Wilson, R., Froyd, C.A., and McCarroll, D., 2008. Multiple stable isotopes from oak trees in southwestern Scotland and the potential for stable isotope Dendroclimatology in maritime climatic regions. *Chemical Geology* **252**: 62-71.

Lorenz, E.N., 1956. Empirical orthogonal functions and statistical weather prediction. Statistical Forecasting Scientific Representative 1, Department of Meteorology, Massachusetts Institute of Technology, Cambridge, MA, 57 pp.

Masson-Delmotte, V., Raffalli-Delerce, G., Danis, P.A., Yiou, P., Stievenard, M., Guibal, F., Mestre, O., Bernard, V., Goosse, H., Hoffmann, G., and Jouzel, J., 2005. Changes in European precipitation seasonality and in drought frequencies revealed by a four-century-long tree-ring isotopic record from Brittany, western France. *Climate Dynamics* **24**: 57-69.

McCarroll, D., and Loader N.J., 2004. Stable isotopes in tree rings. *Quaternary Science Reviews* **23**: 771–801.

McCarroll, D.J., Gagen, M.H., Loader, N.J., Robertson, I., Anchukaitis, K.J., Los, S., Young, G.,H.F., Jalkanen, R., Kirchhefer, A., and Waterhouse, J.S., 2009. Correction of tree ring stable carbon isotope chronologies for changes in the carbon dioxide content of the atmosphere. *Geochimica et Cosmochimica Acta* **73**: 1539-1547.

Meko, D.M., and Graybill, D.A., 1995. Tree-ring reconstruction of Upper Gila River discharge. *Water Resources Bulletin* **31-4**: 605-616.

Meko, D.C., Stockton, W., and Boggess, W.R., 1995. The tree-ring record of severe sustained drought. *Water Resources Bulletin* **31**: 789-801.

National Climate Data Center (NDCD), 2004. Time bias corrected divisional temperature-precipitation-drought index. www.ncdc.noaa.gov/oa/climate/climatedata.html.

Raffalli-Delerce, G., Masson-Delmotte, V., Dupouey, J.L., Stievenard, M., Breda, N., and Moisselin, J.M., 2004. Reconstruction of summer droughts using tree-ring cellulose isotopes: a calibration study with living oaks from Brittany (western France). *Tellus* **56B**: 160-174.

Reynolds-Henne, C.E., Siegwolf, R.T.W., Treydte, K.S., Esper, J., Henne, S., and Saurer, M., 2007. Temporal stability of climate-isotope relationships in tree rings of oak and pine (Ticino, Switzerland). *Global Biogeochemical Cycles* **21**: GB4009, doi:10.1029/2007GB002945.

Saurer, M., Borella, S., Schweingruber, F., and Siegwolf, R., 1997. Stable carbon isotopes in tree rings of beech: climatic versus site-related influences. *Trees* **11**: 291-297.

Stahle, D.W., and Cleaveland, M.K., 1992. Reconstruction and analysis of spring rainfall over the southeastern U.S. for the past 1000 years. *Bulletin of the American Meteorological Society* **73-12**: 1947-1961.

Woodhouse, C.A., 2003. A 431-Yr Reconstruction of Western Colorado Snowpack from Tree Rings. *Journal of Climate* **16**: 1551-1561.

Woodhouse, C.A., and Brown, P.M., 2001. Tree-ring evidence for Great Plains drought. *Tree-Ring Research* **57-1**: 89-103.

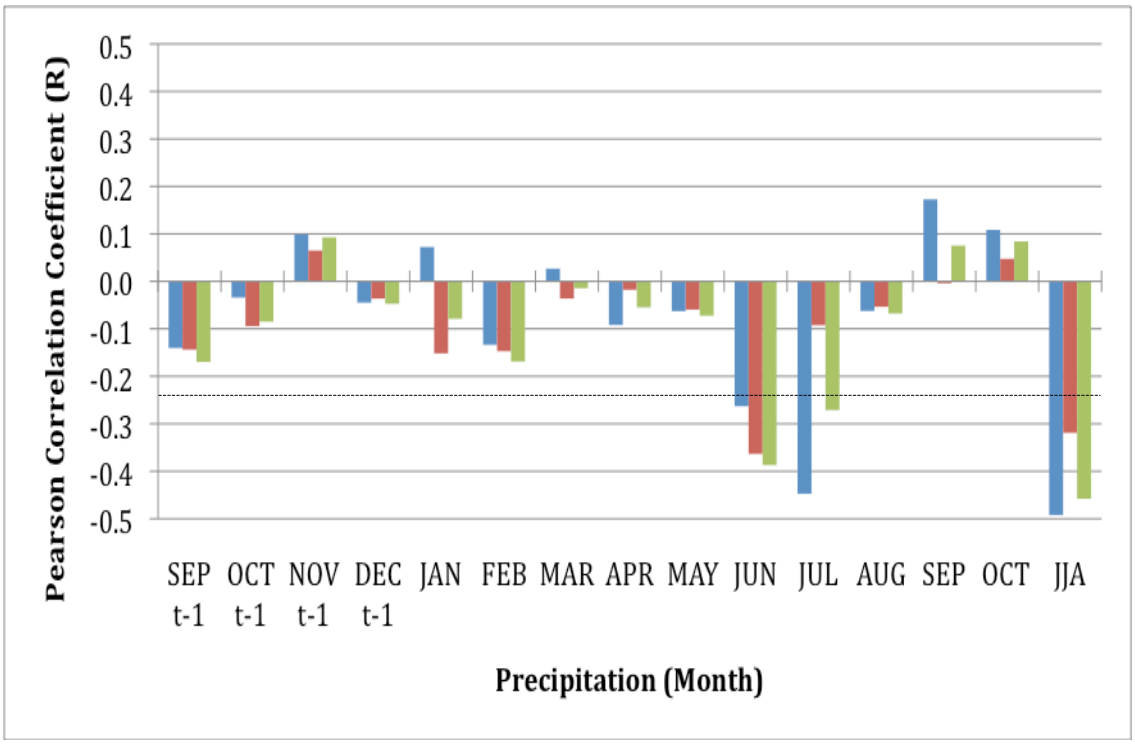

Figure 4.1: Composite correlation diagram illustrating Pearson correlations (R) between normalized $\delta^{13}C$ values and precipitation. These diagrams are presented with all three data sets HC (blue-first), LC (red), and RC (green). Only correlations less than -0.23 are significant at the 95% confidence level. These results led to the correlation that invokes $\delta^{13}C$ values are significantly influenced by summer precipitation.

Test 1		
	Calibration 1931-1966	Verification 1967-2002
R	0.45	0.53
R^2	0.20	0.28
p	<0.01	<0.001
RE		0.27
CE		0.27
ST		23/13

Test 2		
	Calibration 1967-2002	Verification 1931-1966
R	0.53	0.45
R^2	0.28	0.20
p	<0.001	<0.01
RE		0.18
CE		0.18
ST		21/15

Test 3	
R	0.49
R^2	0.24
p	<0.001

Table 4.1: Stepwise regression results from each test. The tests are: R = correlation coefficient; R^2 = explained variance; RE = reduction of error; CE = coefficient of efficiency; ST = sign test. Results demonstrate the predictive ability of the model derived from Test 3.

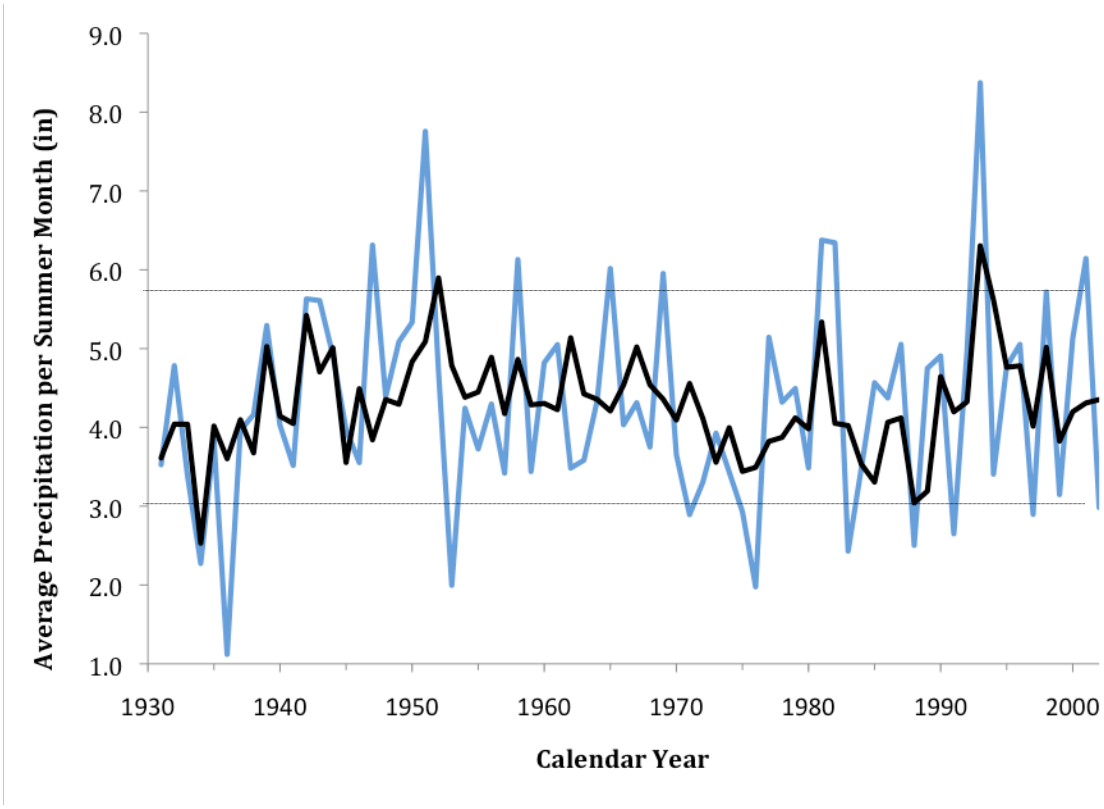

Figure 4.2: Average JJA instrumental average precipitation per summer month (light line) vs. reconstructed (dark line) precipitation series. Dotted lines are deviations of 1σ standard deviation (1.3 in) from the mean of observed values.

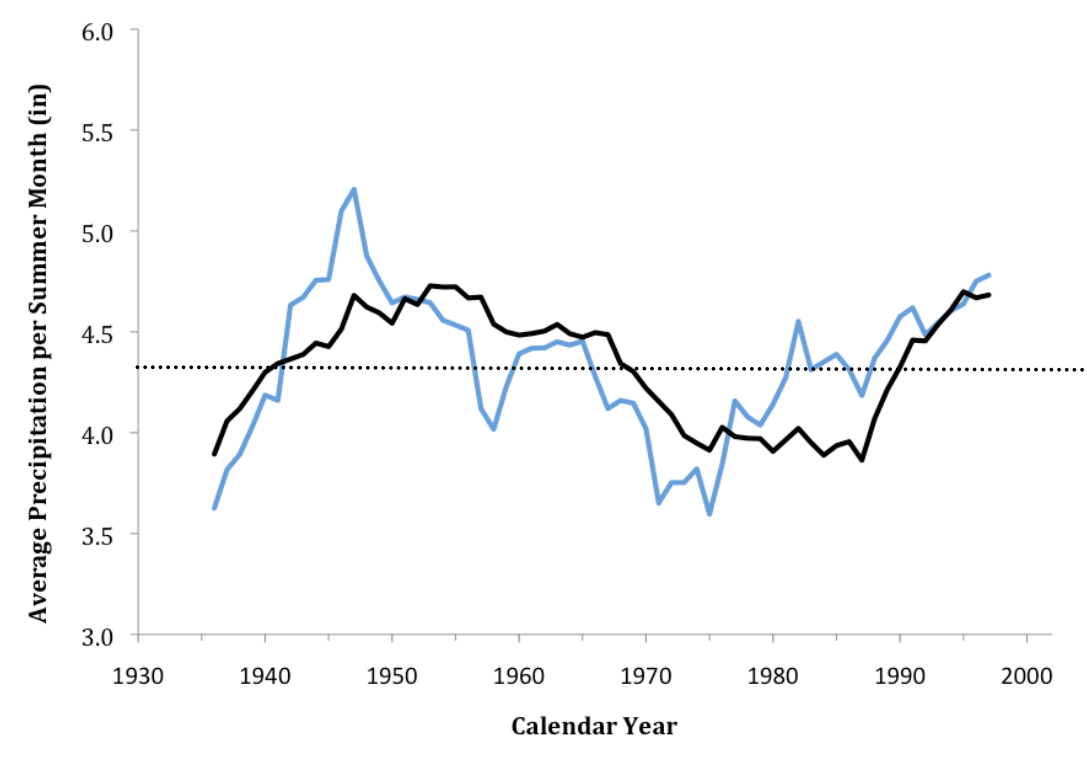

Figure 4.3: 11-year moving averages calculated from observed (lighter line) and reconstructed (darker line) average summer precipitation values that show similar multidecadal-scale trends. The dotted line is the average precipitation per summer month during this interval.

Chapter 5

A RECONSTRUCTED PRECIPITATION RECORD FROM 1500-2002

Abstract

Carbon isotopic values were generated from HC tree segments with an annual resolution back to 1500 AD following procedures developed in chapters 2 and 3. Reconstructed precipitation (predicted using the chapter 4 model) from tree ring $\delta^{13}C$ values suggests that 20th century drought and flooding extremes in the Midwest (e.g. the 1930s Dust Bowl and the 1993 Great Flood respectively) are relatively modest compared to events of past centuries. For example, 14 of the 15 wettest events and 8 of the 9 driest events, as estimated from oak $\delta^{13}C$ values, occurred prior to the Industrial Age (1850-present). Precipitation estimates also suggest that decadal and century scale patterns of precipitation were more pronounced prior to the 20th century. Whereas the driest decade from the 20th century was predicted to be during the 1930s Dust Bowl period (confirmed by instrumental data), five decades prior to the Industrial Age were estimated to be drier. In addition, eight decades prior to 1900 were projected to be considerably wetter than any recent decade. These results suggest that the potential exists for greater precipitation extremes to occur in the future than were experienced in the past 100 years.

5.1. Introduction

Current global climate modeling studies suggest that significant global changes in precipitation are likely to occur over the next century (IPCC, 2007). These changes are expected to intensify pressure on already stressed water resources in many regions resulting from population growth and urbanization. In addition, the expected increase in the frequency and magnitude of widespread flooding and drought will negatively impact water availability, health, agriculture, and energy production (McCabe et al., 2004; IPCC, 2007). By studying precipitation changes in regions where high socioeconomic impacts from climate change exists, a more reasonable evaluation of potential climate related hazards is possible.

Given the Midwest's economic connection to climate through agricultural activities in the region, regional climate studies are important. Examination of climate change within the Midwest has relied heavily on instrumental weather records from the 20th century. Unfortunately, the specific regional impacts from climate change are not well understood because there is a significant lack of pre-instrumental annual climate records available before the 20th century (Meko et al., 1995; Woodhouse and Overpeck, 1998). By extending climate proxy records beyond instrumental records, a more extensive assessment of climate variability is possible.

The American Long Oak Chronology (ALOC) can be employed as a proxy to assess prehistoric climate continuously back to 912 AD. High-resolution $\delta^{13}C$ time series generated from ALOC tree rings provide a chemical means to reconstruct precipitation variability beyond instrumental records (chapters 3 and 4). The

carbon isotope record presented in chapter 3 demonstrated a significant correlation between $\delta^{13}C$ and regional precipitation ($R = -0.49$, $p<0.001$) and was used in chapter 4 to develop a model to describe past precipitation variability. This chapter uses the results from those chapters and a new 503 year-long $\delta^{13}C$ record to generate a reconstructed precipitation record back to 1500 AD from the central Midwest. Reconstructed precipitation was used to 1) identify annual extreme events, 2) examine persistent long-term events, and 3) explore potential connections to astronomical influences.

5.2. Methods

5.2.1. Sample Selection

Tree ring $\delta^{13}C$ records were generated from tree segments using methods outlined in chapters one through three. Ring width patterns (RWP) of all individual segments are compared to the pattern of pooled, normalized ring widths for the ALOC and expressed as a correlation coefficient (R). The more closely the RWP of an individual segment corresponds to the average pooled patterns, the higher the correlation coefficient. Only high correlation (HC) samples were used in chapter three to develop a $\delta^{13}C$ model to explain past precipitation variability. This chapter uses only similar HC-type samples to generate annual $\delta^{13}C$ values back to 1500 AD.

5.2.2. Sample Preparation and Analysis

Latewood portions of each tree ring were sampled using a razor blade. All visual components not of latewood material were carefully removed or avoided (i.e.

earlywood, structural rays). This procedure minimizes potential contributions from carbon fixed during times other than the sampled year. Approximately 2 mg of material was used for analyses and in most cases each individual ring could provide enough material for replicate analyses if needed. By measuring individual years, we aimed to retain as much high-frequency variability as possible.

The samples were weighed, loaded into tin boats, and analyzed by continuous flow stable isotope mass spectrometry techniques (further details in Brenna *et al.*, 1997; Ghosh and Brand, 2003; McCarrol and Loader, 2004). Prepared samples are loaded into a 50-port autosampler connected to a Carlo-Erba 1500 elemental analyzer (EA). Each sample is dropped into a combustion tube heated to 1020ºC where sample combustion occurs and CO_2 gas is produced. The gas passes through a Finnigan Conflo III device into a Finnigan DeltaPlusXL Isotope Ratio Mass Spectrometer (IRMS) where $\delta^{13}C$ values are calculated based on comparison with a reference CO_2 gas of known isotopic composition flowing through the system. In addition, an average of five standards for every sample were used for each full run to assess precision and correct for machine drift. In less than 12 hours, 50 analyses (samples plus standards) can be run with excellent analytical precision (±0.1‰, 1σ standard deviation). Results are expressed as per mil deviations using delta notation (δ) relative to the VPDB standard.

5.2.3. Data Evaluation

The HC $\delta^{13}C$ time series was corrected for the 'industrial effect' (Saurer et al., 1997; McCarroll and Loader 2004; Raffalli-Delerce et al., 2004; Gagen et al., 2004, 2005, 2007, 2008; Loader et al., 2008; McCarroll et al., 2009) through removal of the effect of declining atmospheric values due to addition of CO_2 with low $\delta^{13}C$ values as a result of fossil fuel burning since 1850 (start of industrialization). These corrected values are then recalculated as the difference from the average value for the segment from the sample collected (normalized) to remove potential artifacts introduced when switching between trees with different average values. This approach emphasizes isotopic change from year to year. A final annual isotopic value is determined using the pooled average of three samples per year. A complete list of $\delta^{13}C$ raw data (total samples used and annual values generated from 1500-2002) is available in Appendix 1.

This normalization is needed because average $\delta^{13}C$ differences between trees are high relative to interannual variability (chapter 2). However, this potentially introduces at least three complications. First, because the average for each segment is set to zero, estimated climate variability is dampened. For example, if 20 of 25 years during a given segment were drier than average, normalization underestimates the effect of this aridity in the pooled results. Second, such a bias could create an artificial change at the boundary of segments (if the previous or subsequent segment did not have similar average conditions). Third, trends longer than the longest segment length could potentially be invisible to this analysis. The

differences between normalized and raw $\delta^{13}C$ values are shown in Figure 5.1 (values are presented in Appendix 4).

Uneven segment lengths and using only HC trees (which have lower between tree differences than LC trees) may reduce the contributions of the first and second concerns. Further, to qualitatively assess segment affects, segment lengths are shown in Figure 5.2. Also, the model, including estimated uncertainty, was based on instrumental era data collected and reduced with parallel techniques to the pre-instrumental era interval. Finally, $\delta^{18}O$ trends will be a target of future work, and, because they do not seem to suffer from large between tree differences, these concerns might be addressed empirically by subsequent studies (chapter 6).

5.2.4. Model Development

Normalized isotopic time series were statistically compared to multidecadal temperature, precipitation and PDSI from averaged monthly records of nearby regional climate stations within northwest Missouri Climate Division 1 from 1931-2002 (NCDC, 2004). The results led to the conclusion that $\delta^{13}C$ values are significantly influenced by summer precipitation (chapter 3). Chapter 4 developed a model to predict past precipitation changes from tree ring $\delta^{13}C$ values utilizing only HC segments. A split sample calibration and verification scheme was used to illustrate the ability of tree ring carbon isotopes to predict regional summer precipitation (Meko and Graybill, 1995; Cook et al., 1999; Woodhouse, 2003). Three additional verification statistics (reduction of error, coefficient of efficiency, and the sign test) were calculated to assess the predictive ability of the model used.

5.3. Results

The normalized carbon isotope time series from 1500-2002 reveal considerable isotopic variation with a range of ~2.6‰ (Figure 5.2). The maximum normalized isotopic value is 1.21‰ during 1807 and the minimum normalized isotopic value is -1.37‰ during 1683. The 17th century shows effectively the entire isotopic range (2.50‰) where values during the 18th century vary only by 1.53‰ (Figure 5.3).

Reconstructed average summer (JJA) precipitation values from 1500-2002 show considerable variability ranging from 6.99 in to 2.18 in per summer month (Figure 5.4). Average precipitation per summer month from 1500-2002 is 4.5 in with the 17th century averaging the highest amount of average summer precipitation (5.0 in) per month and the 18th century averaging the lowest amount of average summer rainfall (4.0 in) per month. The summer estimated to be driest was in 1807 with an average of 2.2 in per month and the wettest summer estimated was 1683 (during the peak of the Little Ice Age) with an average of 7.0 in of rainfall per month.

5.4. Discussion

5.4.1. Precipitation Variability and Extremes

While the reconstruction represents a moderate estimate of past precipitation amounts in the central Midwest (as stated in chapter 4), the results suggest large variations in precipitation during the previous five centuries. Reconstructed average summer (June-August) precipitation shows considerable

annual variability of 4.8 in per month from 1500-2002. During the Industrial Age (post-1850), the wettest and driest average summers were 1993 and 1934 (6.30 in and 2.53 in per summer month respectively) with a difference of 3.77 in (Figure 5.4). Not surprisingly, these extreme summers are the Great Flood of 1993 and a year from the 1930s Dust Bowl that have been frequently mentioned in previous chapters. Yet, by examining the remaining precipitation record (1500-1850; commonly known as the Little Ice Age), greater estimated average summer monthly precipitation extremes of 6.99 in (1683) and 2.18 in (1807) are suggested. In fact, the $\delta^{13}C$ record predicts that the twelve wettest and the three driest summers are all prior to 1850 (Table 5.1). Hence, it seems the 20th century may be a relatively moderate interval relative to summer precipitation extremes over the past 500 years.

Decadal scale precipitation variability is also demonstrated in the reconstructed record. The average estimated summer precipitation during each decade indicates that since the beginning of the Industrial Age, the three wettest decades were the 1880s, 1890s, and 1900s (average summer precipitation of 5.38, 5.24, and 5.11 in per month respectively). In addition, the three driest decades estimated were the 1850s, 1930s, and 1980s (average summer precipitation of 3.61, 3.77, and 3.87 in per month respectively).

As with estimated year to year precipitation estimates, more predicted extreme decades exist during the Little Ice Age than during the Industrial Age (Figure 5.5). The three decades with wettest summer months are estimated to be the 1650s, 1680s and 1690s (average summer precipitation of 5.63, 6.50, and 5.57

in per month respectively) and the three driest decades are estimated to be the 1640s, 1760s, and 1800s (average summer precipitation of 3.47, 3.65, and 3.30 in per month respectively). Interestingly, the recent 1930s Dust Bowl drought period, that was devastating both agriculturally and economically, is not even estimated to be a top three drought decade during the last 503 years. When 10-year averages are calculated at different points between decades instead of within them (i.e., changing the binning), the general trends remain the same even though some details change. This result suggests that the Midwest is prone to decadal scale precipitation episodes of greater magnitude than seen over the most recent 100 years, and future prolonged periods of extreme drought or flooding are possible. Because the wettest and driest extreme years and decades are estimated to have occurred prior to 1850, during a time when the central Midwest was not as populated or agriculturally significant, these events had little known consequences. If these events become more likely in the future, the disasters from the 1930s Dust Bowl and the 1993 Great Flood will only be a foreshadowing of the degree to which climate variability in the Midwest can affect people and economics.

Extreme precipitation events are defined here as summers that deviate from the overall estimated average by more than 2σ, which enable an assessment of extreme precipitation distribution (Figure 5.6). During the last five centuries, there have been an estimated 16 extreme wet years and 9 extreme dry years that deviate more than 2σ (1.66 in). The most striking observation is the amount and clustering of extreme wet summers that occur during the 17th century. Additionally, all but

one of the 2σ wet episodes from the late 1600s appears to be larger than the 1993 Great Flood. The transition from the 17th to the 18th century appears to mark a substantial shift from a persistently wet to a persistently dry regime in which no extreme wet episodes occurred for 120 years. As a result, even though the Midwest during the 20th century has been exposed to numerous precipitation extremes, the reconstruction suggests the most extreme years and periods occurred prior to the Industrial Age.

Chapter 4 previously determined the associated standard deviation of normalized $\delta^{13}C$ values (±0.4), which led to a corresponding uncertainty of ±0.75 inches of summer precipitation per month derived from the model. Even with this uncertainty, we can recognize extreme events. However, at this time, the uncertainty is too high to conclusively suggest that extreme events in the past estimated to be larger than those of the 20th century are without a doubt more extreme. For example, the 1993 Great Flood was estimated to be 0.7 inches drier than the wettest estimated summer during the last 500 years (1683) and because the uncertainty is above this difference there is the potential that 1993 was a wetter summer than 1683. However, an important observation is that 1993 is not exceptional within the estimated record. Despite the error, there seem to be numerous clusters of extreme years during the last 500 years that suggest the carbon isotopic record does reasonably well documenting extreme periods.

5.4.2. Sunspots and Precipitation

During the last ~400 years, a general correlation exists between observed average yearly sunspots (NGDC, 2009) and estimated average summer precipitation per month, where a decrease in sunspots correlates to an increase in precipitation on a multidecadal scale (Figure 5.7). This correlation is most notable during the Maunder Minimum period (approximately 1650-1700) when few to no sunspots were observed (Rind et al., 2004; Yoshimori et al., 2005; Miyahara et al., 2006; Yoshimori et al., 2006) and estimated average summer precipitation per month was considerably above average compared to the last 500 years. Also, the early 1800s exhibit a similar, yet less drastic, increase in estimated average summer precipitation during a period of prolonged sunspot minima known as the Dalton Minimum (Wagner and Zorita, 2005). Recent studies by Verschuren et al. (2000) and Zhao et al. (2004) have also suggested a similar relationship of decreased solar activity closely related to increased precipitation from northeastern China and western Africa respectively. In addition, a study by Starkel (2002) connected extreme flooding in central Europe with periods of declined solar activity during the Holocene.

To test this relationship further, we calculate 11-year moving averages through both the observed sunspot and estimated average summer monthly precipitation records and compare them using Pearson correlations (Zhao et al., 2004; D'Aleo and Taylor). An 11-year moving average is used to reduce the influence of the 11-year solar cycle from observed sunspots and capture long-term trends. During the Maunder Minimum (from 1650-1715), sunspots are significantly

correlated (Figure 5.8) with estimated average summer monthly precipitation ($R = -0.75$, $p<10^{-12}$). Interestingly, if we examine the 20th century, sunspot numbers during the interval from 1900-1949 significantly correlate (Figure 5.9) with estimated average summer monthly precipitation, whereas post-1950, it does not ($R = -0.58$, $p<0.00001$ and $R = -0.07$, $p>0.6$ respectively). While these correlations do not imply causation, these initial results suggest there is a connection between decreased sunspots and increased estimated precipitation, but this relationship may have broken down over the past 50 years.

5.4.3. Broader Implications and Considerations

Other proxy data on pre-instrumental climate are sparse, but suggest Holocene climate variability is greater than that seen during the instrumental period. Speleothem evidence from Missouri and Iowa suggests that century to millennial-scale periods of aridity and elevated temperatures (up to 3°C above modern) have occurred in this region during the Holocene (Dorale et al., 1992; Denniston et al., 2007). Millennial-scale flooding patterns observed from speleothems in southern Missouri have suggested that 1) flooding is in part influenced by El Niño cyclicity and 2) if the cyclicity continues, increased flooding could occur in the next few centuries (Lepley, 2004). In addition, pollen and ostracode records from Illinois have shown that century-scale climate changes (e.g., temperature and moisture) have occurred prior to the Holocene period when compared to the instrumental period (e.g., Curry, 2000). Historical accounts also indicate that in 1785, 1844 and 1951, Missouri has exhibited floods equivalent to or

larger than the 1993 Great Flood (NOAA, 2009). However, all of these are distinctly lacking in temporal resolution and there are difficulties in calibrating the pre-instrumental estimates to modern measured values. For this reason, tree rings arguably represent the best available archive to understand pre-instrumental climate change on an annual scale.

Normalized and bulk latewood $\delta^{13}C$ values show few convincing teleconnections with changes in distant sea surface temperature (SST) in various regions at this time. Teleconnections are naturally occurring relationships between distant phenomena and, in this case, we are interested in recurring and persistent, large-scale pattern of pressure and circulation anomalies that spans vast geographical areas and can be influenced by SST changes (CPC, 2009). Such changes could affect Midwest weather patterns. Each of the following phenomena were explored as potential features influencing summer precipitation in the Midwest: El Niño (Niño1+2, Niño 3.4, Niño4, Niño3), Southern Oscillation Index (SOI), Pacific Decadal Oscillation (PDO), Pacific North American Oscillation (PNA), Icelandic Sea Level Pressures systems (ASLP), Atlantic Multidecadal Oscillation (AMO), North American Oscillation (NAO) and the Caribbean SST changes. Those that significantly correlated ($n=52$, $p<0.05$) from 1950-2002 to normalized $\delta^{13}C$ values were the NAO averaged values of May-July ($R = 0.37$) and Caribbean SSTs during August ($R = 0.37$). The correlations suggest that a relationship with summer moisture from tropical latitudes may influence summer precipitation in the central Midwest. This also generally agrees with modern moisture patterns where moisture is drawn from

warm tropical North Atlantic and northern Caribbean Seas and then sent northward through the Gulf of Mexico into the interior plains of the Midwest (Lydolph, 1985).

When multiple proxies exhibit similar dominant forcing influences, the correlation may improve by combining them in order to remove potential noise within each signal (Gagen et al., 2006; Loader et al., 2008). To explore this potential benefit, both carbon isotopes and the American Long Oak Chronology ring width index (RWI) were normalized to values between 0 and 1 and weighted by their respective percent of variance to obtain a weighted estimate (Gagen et al., 2006). For example, when compared to precipitation from 1931-2002, the $\delta^{13}C$ explained variance (R^2) is 0.24 and the RWI explained variance (R^2) is 0.15. Therefore, the respective weighted percent variance when combined is 61.5% for $\delta^{18}O$ and 38.5% for $\delta^{13}C$. Because higher $\delta^{13}C$ and narrower rings are associated with drought and vice versa, annual values for each normalized isotope can be calculated using the equation

$$\textit{Weighted Isotope Estimate} = (\delta^{13}C_t * 0.615) - (RWI_t * 0.385)$$

where *t* is the specific year of interest. The results show the weighted correlation increases with precipitation to $R = -0.55$ and $p<0.01$. Future studies may use multiple linear regressions as another potential method for determining the weighted isotope estimate.

5.5. Conclusions

Compared to the 20th century, reconstructed Midwest precipitation from tree ring $\delta^{13}C$ values during the last five centuries reveals similar magnitude but longer

duration extreme events. In particular, the top three extreme wet and dry events of the last five centuries do not occur during the 20th century. Decadal to century-scale precipitation means also indicate that the driest and wettest periods occur prior to the 20th century. These results suggest that precipitation extremes (both drought and floods) larger than have been seen in the past century (including the 1993 Great Flood and 1930s Dust Bowl period), are part of the 'natural' variability of the Midwest, regardless of any effects from anthropogenic related climate changes. Additionally, initial evidence suggests the precipitation record is associated with sunspot cycles on multidecadal time scales. A decrease in long-term sunspot activity shows evidence for a general increase in precipitation.

References

Brenna, J.T., Corso, T.N., Tobias, H.J., and Caimi, R.J., 1997. High-precision continuous-flow isotope ratio mass spectrometry. *Mass Spectrometry Reviews* **16**: 227-258.

Cook, E.R., Meko, D.M., Stahle, D.W., and Cleaveland, M.K., 1999. Drought reconstructions for the continental United States. *Journal of Climate* **12**: 1145-1162.

Climate Prediction Center (CPC), 2009. National Oceanic and Atmospheric Administration. http://www.cpc.noaa.gov/data/teledoc/teleintro.shtml

Curry, B.B., and Baker, R.G., 2000. Palaeohydrology, vegetation, and climate since the late Illinois Episode (~130ka) in south-central Illinois. *Palaeogeography, Palaeoclimatology, Palaeoecology* **155**: 59-81.

D'Aleo, J., and Taylor, G., 2007. Temperatures in the United States, Greenland and the Arctic, Relationship to Ocean and Solar Cycles. International Climate and Environmental Change Assessment Project. http://icecap.us/index.php/go/climate-library

Denniston, R.F., DuPree, M., Dorale, J.A., Asmerom, Y., Polyak, V.J., and Carpenter, S.J., 2007. Episodes of late Holocene aridity recorded by stalagmites from Devil's Ice Box Cave, central Missouri, USA. *Quaternary Research* **68**: 45-52.

Dorale, J.A., Gonzalez, L.A., Reagan, M.K., Pickett, D.A., Murrell, M.T., and Baker, R.G., 1992. A High-Resolution Record of Holocene Climate Change in Speleothem Calcite from Cold Water Cave, Northeast Iowa. *Science* **258**: 1626-1630.

Gagen, M., McCarroll, D., and Edouard, J.-L., 2004. Latewood width, maximum density and stable carbon isotope ratios of pine as paleoclimate indicators in a dry, subalpine environment. *Arctic, Antarctic and Alpine Research* **36**: 166-171.

Gagen, M., McCarroll, D., and Edouard, J.-L., 2006. Combining ring width, density and stable carbon isotope proxies to enhance the climate signal in tree-rings: an example from the southern French Alps. *Climatic Change* **78**: 363-379.

Gagen, M., McCarroll, D., Loader, N.J., Robertson, I., Jalkanen, R., and Anchukaitis, K.J., 2007. Exorcising the 'segment length curse': summer temperature reconstruction since AD 1640 using non-detrended stable carbon isotope ratios from pine trees in northern Finland. *The Holocene* **17-4**: 435-446.

Gagen, M., McCarroll, D., Robertson, I., Loader, N.J., and Jalkanen, R., 2008. Do tree ring $\delta^{13}C$ series from *Pinus sylvestris* in northern Fennoscandia contain long-term non-climatic trends? *Chemical Geology* **252**: 42-51.

Ghosh, P., and Brand, W., 2003. Stable Isotope ratio mass spectrometry in global climate change research. *International Journal of Mass Spectrometry* **228**: 1-33.

Intergovernmental Panel on Climate Change (IPCC), 2007. Climate Change 2007: The Physical Science Basis. Fourth Assessment Report of the IPCC Summary for Policymakers, 18p.

Lepley, S.W., 2004. A High-Resolution Record of Holocene El-Niño Cyclicity from Crevice Cave, Missouri. MS Thesis. University of Missouri. 46 pp.

Loader, N.J., Santillo, P.M., Woodman-Ralph, J.P., Rolfe, J.E., Hall, M.A., Gageb, M., Robertson, I., Wilson, R., Froyd, C.A., and McCarroll, D., 2008. Multiple stable isotopes from oak trees in southwestern Scotland and the potential for stable isotope Dendroclimatology in maritime climatic regions. *Chemical Geology* **252**: 62-71.

Lydolph, P.E., 1985. *The Climate of the Earth*. Rowman & Littlefield, 386 pp.

McCabe, G.J., Palecki, M.A., and Betancourt, J.L., 2004. Pacific and Atlantic Ocean influences on multidecadal drought frequency in the United States. *Procedings of the National Academy of Sciences* **101-12**: 4136-4141.

McCarroll D., and Loader N. J., 2004. Stable isotopes in tree rings. *Quaternary Science Reviews* **23**: 771–801.

McCarroll, D.J., Gagen, M.H., Loader, N.J., Robertson, I., Anchukaitis, K.J., Los, S., Young, G.,H.F., Jalkanen, R., Kirchhefer, A., and Waterhouse, J.S., 2009. Correction of tree ring stable carbon isotope chronologies for changes in the carbon dioxide content of the atmosphere. *Geochimica et Cosmochimica Acta* **73**: 1539-1547.

Meko, D.M., and Graybill, D.A., 1995. Tree-ring reconstruction of Upper Gila River discharge. *Water Resources Bulletin* **31-4**: 605-616.

Meko, D.C., Stockton, W., and Boggess, W.R., 1995. The tree-ring record of severe sustained drought. *Water Resources Bulletin* **31**: 789-801.

Miyahara, H., Sokoloff, D., and Usoskin, I.L., 2006. The solar cycle at the Maunder Minimum epoch. In: *Advances in Geosciences, Volume 2: Solar Terrestrial (ST)*. Wing-Huen (ed.), World Scientific, Singapore, pp 1-20.

National Climate Data Center (NCDC), 2004. Time bias corrected divisional temperature-precipitation-drought index. www.ncdc.noaa.gov/oa/climate/climatedata.html.

National Geophysical Data Center (NGDC), 2009. Group Sunspot Numbers 1610-1995 (Doug Hoyt re-evaluation). http://www.ngdc.noaa.gov/stp/SOLAR/ftpsunspotnumber.html#hoyt.

National Oceanic and Atmospheric Association (NOAA), 2009. Historic flood events in the Missouri river basin. http://www.crh.noaa.gov/mbrfc/?n=flood

Raffalli-Delerce, G., Masson-Delmotte, V., Dupouey, J.L., Stievenard, M., Breda, N., and Moisselin, J.M., 2004. Reconstruction of summer droughts using tree-ring cellulose isotopes: a calibration study with living oaks from Brittany (western France). *Tellus* **56B**: 160-174.

Rind, D., Shindell, D., Perlwitz, J., and Lerner, J., 2004. The Relative Importance of Solar and Anthropogenic Forcing of Climate Change between the Maunder Minimum and the Present. *Journal of Climate* **17**: 906-929.

Saurer, M., Borella, S., Schweingruber, F., Siegwolf, R., 1997. Stable carbon isotopes in tree rings of beech: climatic versus site-related influences. *Trees* **11**: 291-297.

Starkel, L., 2002. Change in the frequency of extreme events as the indicator of climatic change in the Holocene (in fluvial systems). *Quaternary International* **9**: 25-32.

Vershuren, D., Laird, K.R., and Cumming, B.F., 2000. Rainfall and drought in equatorial East Africa during the past 1100 years. *Nature* **403**: 410-414.

Wagner, S., and Zorita, E., 2005. The influence of volcanic, solar and CO_2 forcing on the temperatures in the Dalton Minimum (1790-1830): a model study. *Climate Dynamics* **25**: 205-218.

Woodhouse, C.A., 2003. A 431-Yr Reconstruction of Western Colorado Snowpack from Tree Rings. *Journal of Climate* **16**: 1551-1561.

Woodhouse, C.A., and Overpeck, J.T., 1998. 2000 years of drought variability in the central United States. *Bulletin of the American Meteorological Society* **79-12**: 2693-2714.

Yoshimori, M., Stocker, T.F., Raible, C.C, and Renold, M., 2005. Externally Forced and Internal Variability in Ensemble Climate Simulations of the Maunder Minimum. *Journal of Climate* **18**: 4253-4270.

Yoshimori, M., Raible, C.C, Stocker, T.F., Renold, M., 2006. On the interpretation of low-latitude hydrological proxy records based on Maunder Minimum AOGCM simulations. *Climate Dynamics* **27**: 493-513.

Zhao, J., Han, Y.-B. and Li, Z.-A., 2004. The Effect of Solar Activity on the Annual Precipitation in the Beijing Area. *Chinese Journal of Astronomy and Astrophysics* **4-2**: 189-197.

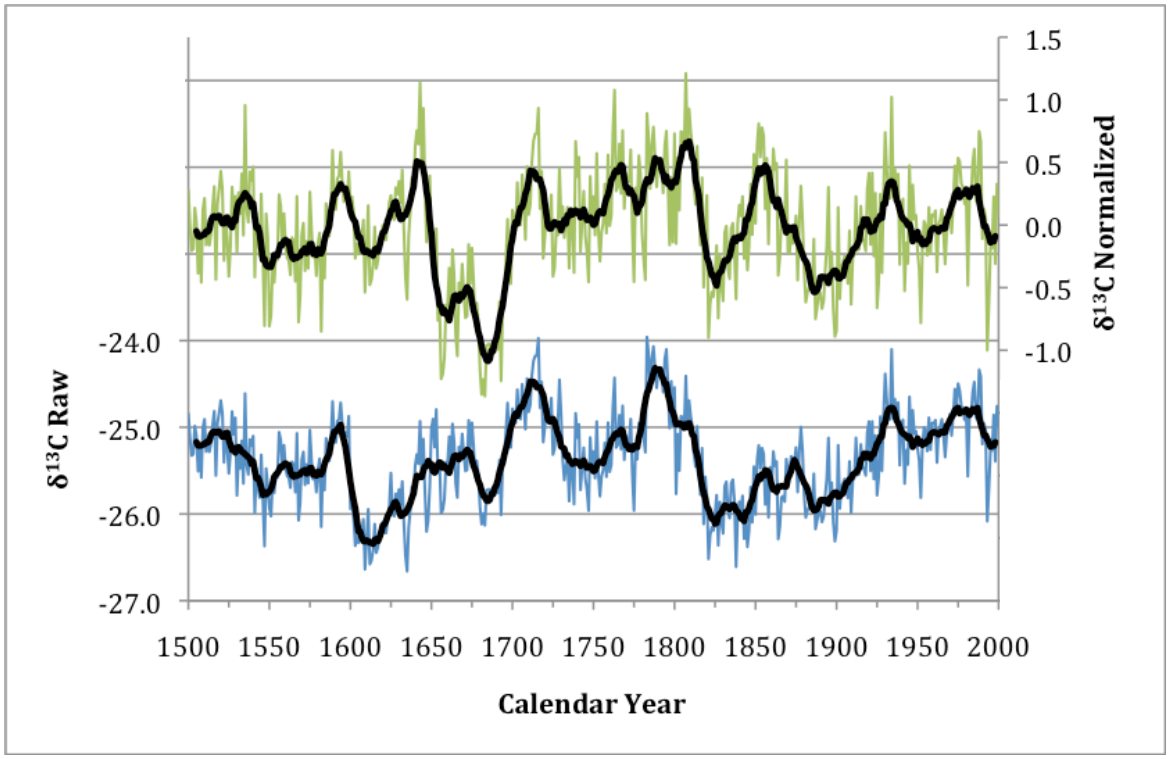

Figure 5.1: Normalized and raw carbon isotope time series from 1500-2002 AD. The darker line within the data is a 11-year moving average to show broader long-term trends.

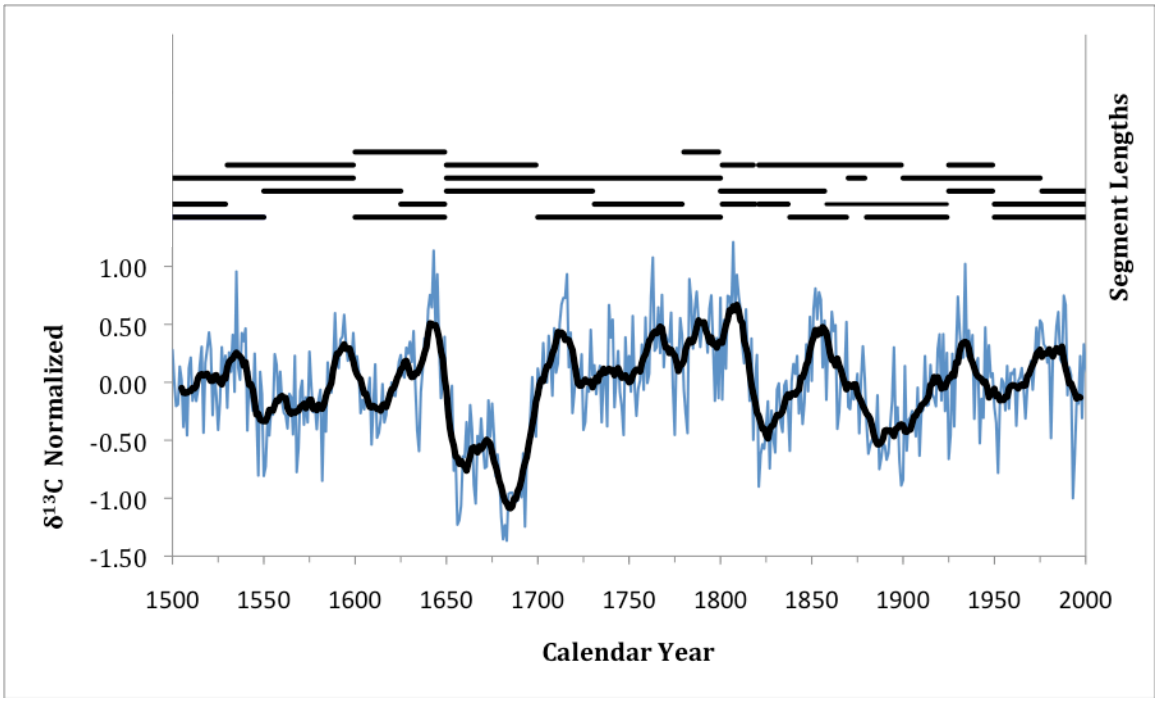

Figure 5.2: Normalized carbon isotope time series from 1500-2002 AD. The darker line within the data is a 11-year moving average to show broader long-term trends. All segments are shown above the carbon isotope time series.

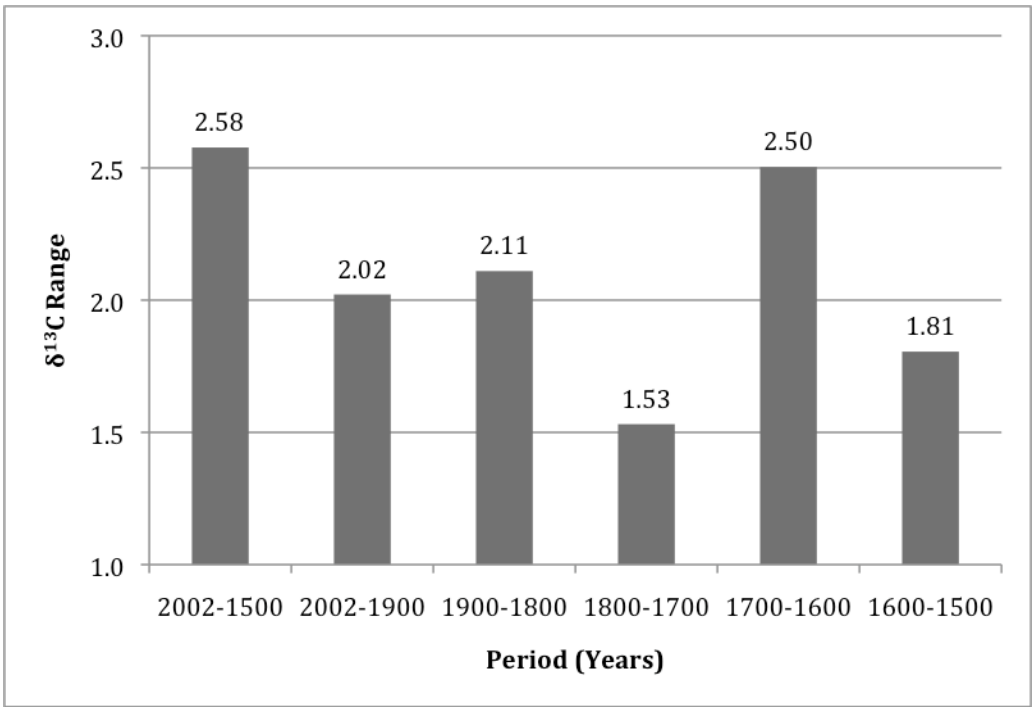

Figure 5.3: Isotopic variance among centuries. The range of normalized isotopic variations is above each bar.

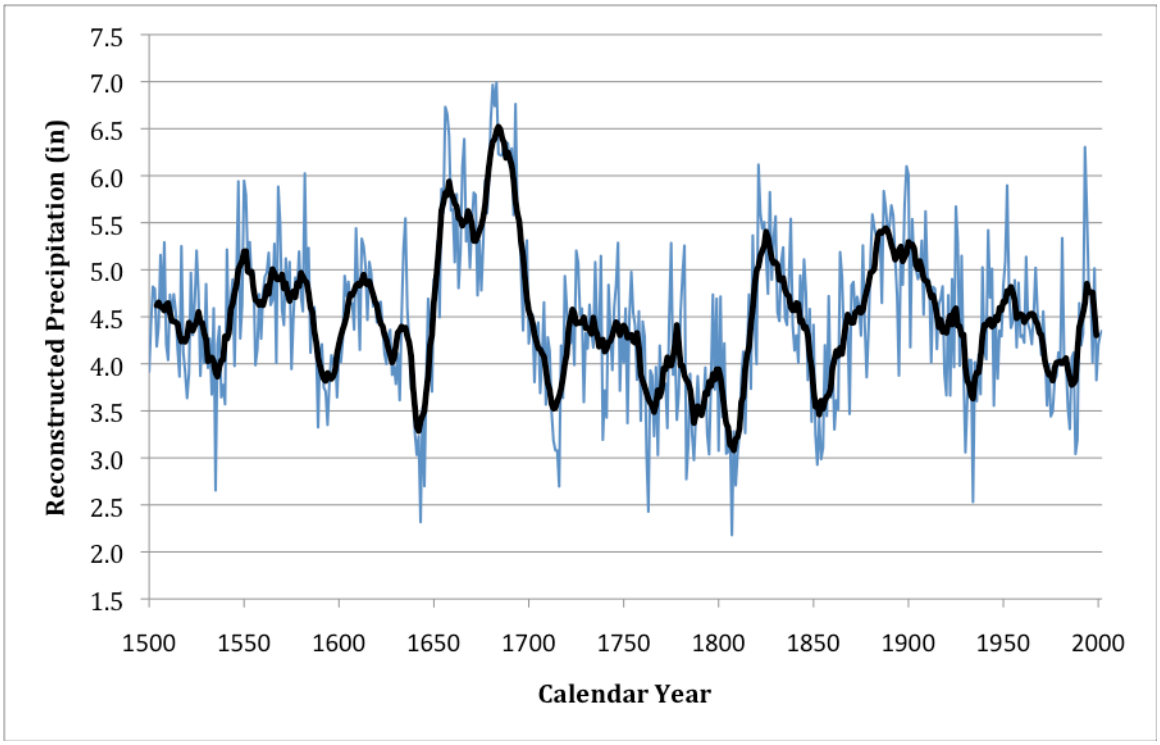

Figure 5.4: Reconstructed average summer (JJA) precipitation per month reconstructed from normalized $\delta^{13}C$ values. The darker line within the data is a 11-year moving average to show broader long-term trends.

Rank	Wettest Years	Precipitation (in)	Driest Years	Precipitation (in)
1	1683	6.99	1807	2.18
2	1681	6.97	1743	2.32
3	1693	6.76	1763	2.43
4	1682	6.74	1852	2.53
5	1656	6.73	1934	2.53
6	1657	6.66	1716	2.7
7	1680	6.60	1745	2.7
8	1658	6.43	1809	2.71
9	1666	6.39	1783	2.77
10	1687	6.37	1787	2.98
11	1688	6.36	1854	2.99
12	1689	6.34	1641	3.03
13	1993	6.30	1768	3.03
14	1691	6.29	1795	3.04
15	1684	6.23	1804	3.04
16	1685	6.22	1810	3.04
17	1686	6.22	1988	3.04
18	1821	6.12	1930	3.06
19	1899	6.10	1805	3.06
20	1690	6.10	1762	3.06

Table 5.1: Top 20 wettest and driest years from 1500-2002 according to reconstructed average summer precipitation values per month. The wettest 20th century event is ranked 13th while the driest 20th century event is ranked 5th.

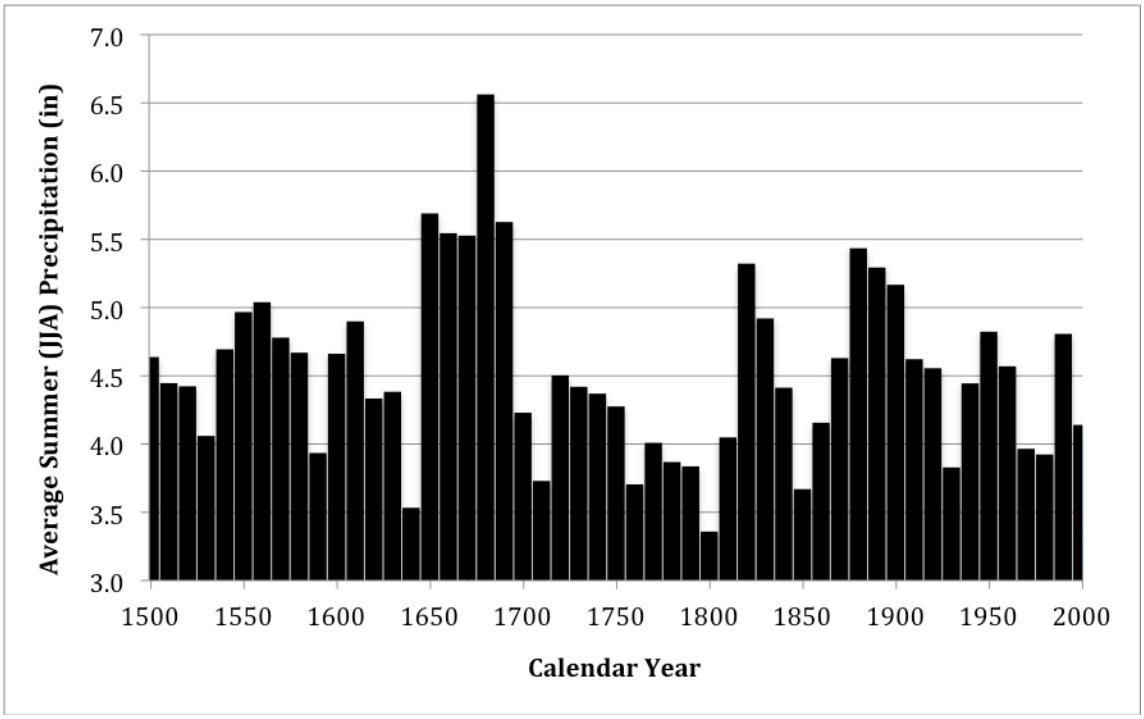

Figure 5.5: Predicted average summer (JJA) precipitation during each decade. Each bar represents one decade and is marked directly over its respective decade. When 10-year averages are calculated at different points between decades instead of within them, the general trends remain the same even though the absolute average values may slightly change.

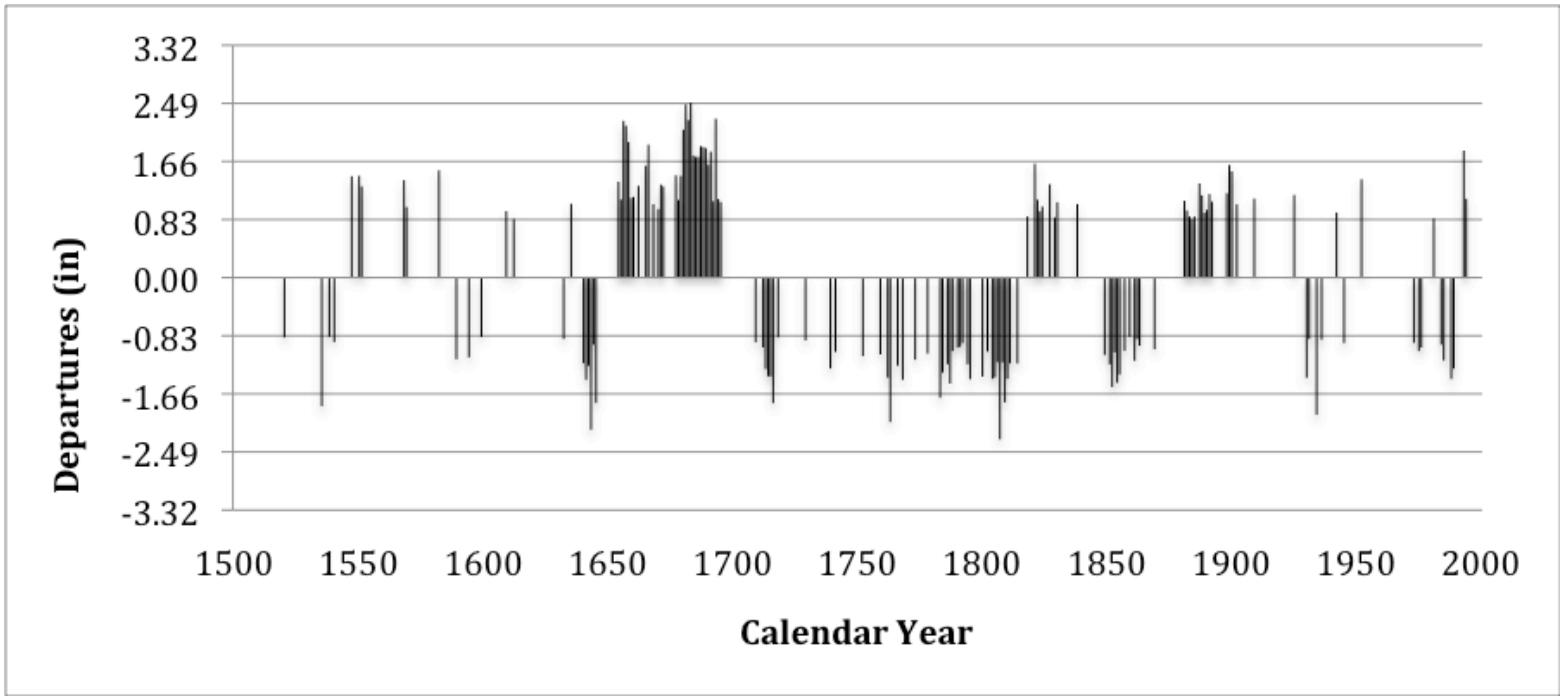

Figure 5.6: The departure of annual precipitation from its overall average. Only years that depart greater than 1σ (0.83) are plotted. 24 total events depart greater than 2σ (1.66).

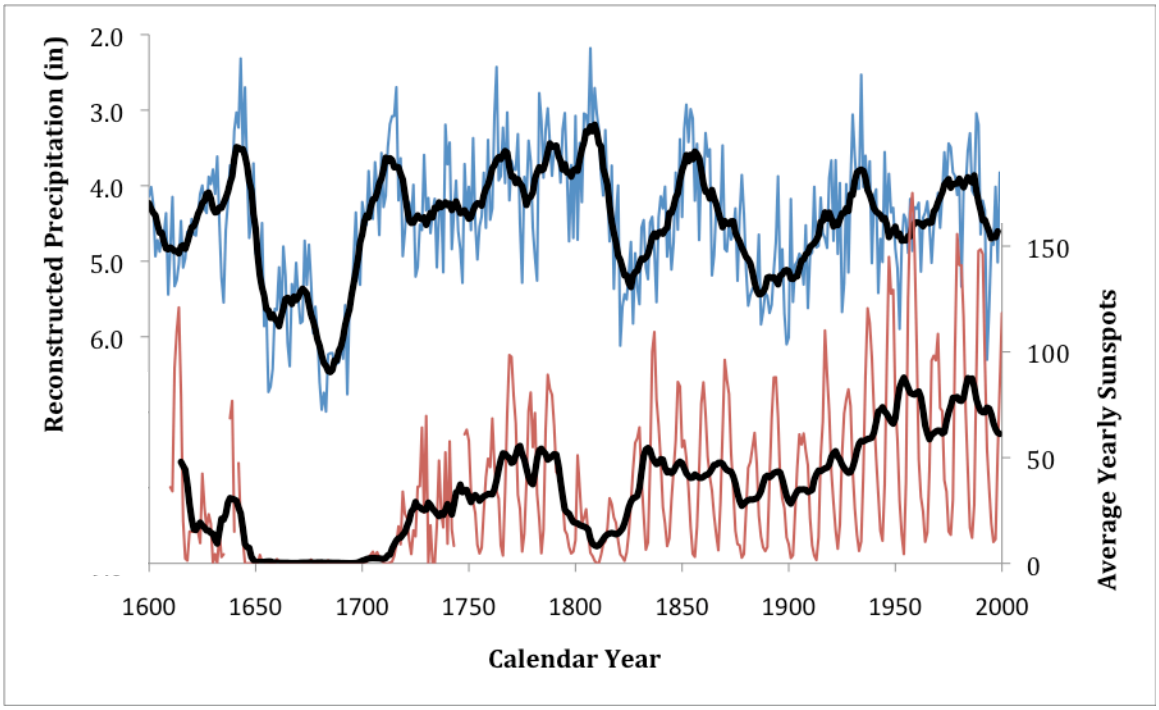

Figure 5.7: Reconstructed precipitation plotted against recorded sunspots.

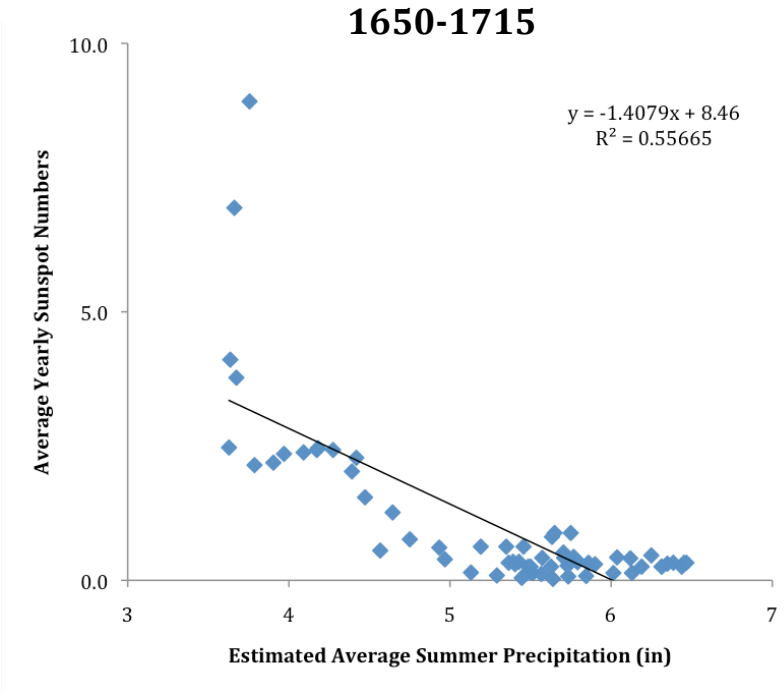

Figure 5.8: Scatter plots comparing 11-year moving averages of average yearly sunspot numbers and estimated average summer precipitation (in). The graph is data from 1650-1715 ($R = -0.75$, $p<10^{-12}$).

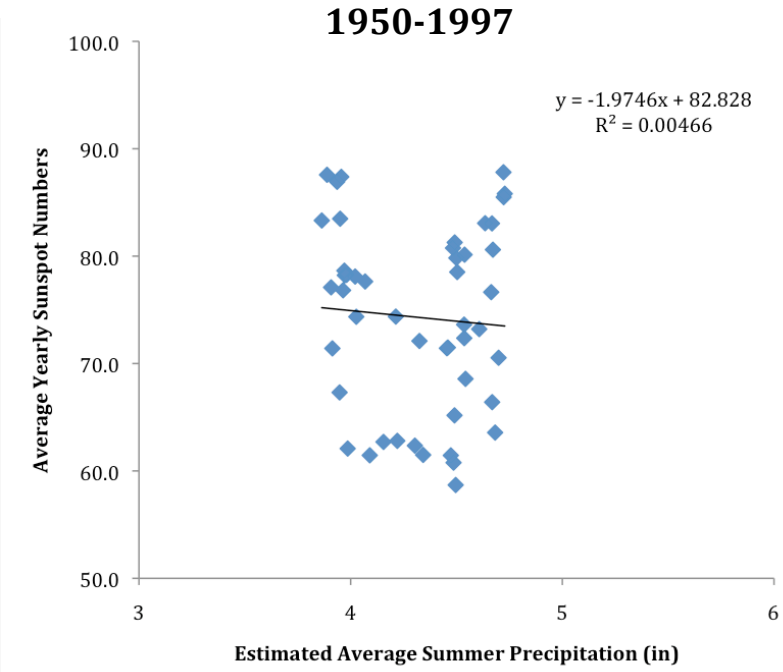

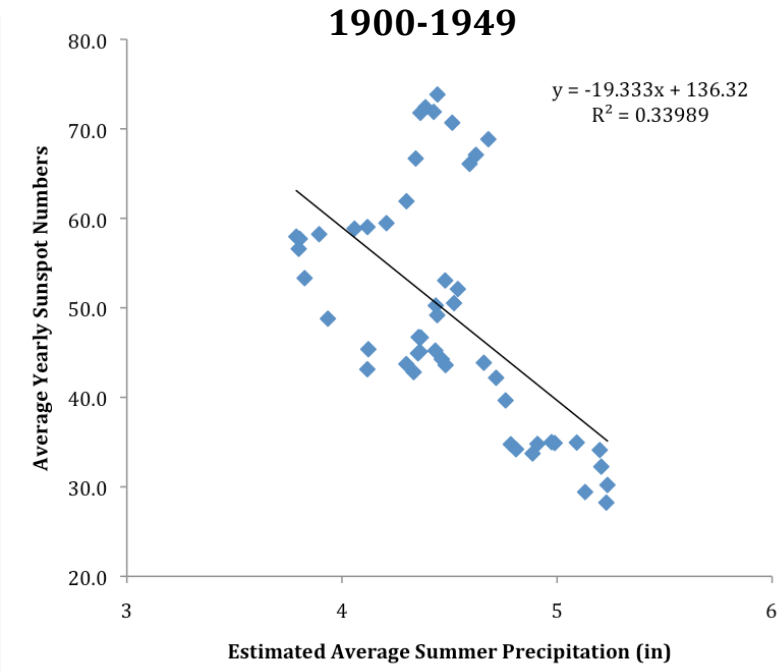

Figure 5.9: Scatter plots comparing 11-year moving averages calculated from average yearly sunspot numbers and estimated average summer precipitation (in). The top graph is data from 1950-1997 (R = -0.07, $p>0.6$) and the bottom graph is data from 1900-1949 (R = -0.58, $p<0.00001$).

Chapter 6

A TREE RING $\delta^{18}O$ PILOT STUDY

Abstract

A 28-year long (1975-2002) $\delta^{18}O$ time series was developed using alpha cellulose from three swamp white oak (*Quercus bicolor*) segments from the American Long Oak Chronology (ALOC) to test if tree ring oxygen isotopic variations can be utilized as a paleoclimate proxy in the central Midwest. Initial results demonstrate individual segments have high between-tree correlations ($R \geq 0.71$, $p \leq 10^{-9}$). Most importantly, this study finds that pooled $\delta^{18}O$ values are significantly correlated to summer (June-August) PDSI and precipitation ($R = -0.80$, $p<0.000001$ and $R = -0.63$, $p<0.001$ respectively), with no significant correlation between $\delta^{18}O$ values and summer temperature ($R = 0.30$, $p>0.1$). Between $\delta^{18}O$ and $\delta^{13}C$ there is also a significant correlation ($R = 0.73$, $p<0.00001$). However, $\delta^{18}O$ appears to more closely capture both moisture extremes whereas $\delta^{13}C$ may only capture wet periods. These results suggest that summer moisture is a central influence on tree ring $\delta^{18}O$ values on annual time scales.

6.1. Introduction

Paleoclimatic tree ring isotopic studies have been primarily focused on developing and understanding tree ring $\delta^{13}C$ time series (e.g., Weigl et al., 2007; Gagen et al., 2008; Leavitt, 2008; Saurer et al., 2008; McCarroll et al., 2009). These efforts have led to the generation of large $\delta^{13}C$ data sets, but oxygen isotopic records

are far less extensive. The development of $\delta^{18}O$ time series typically requires less common instrumentation as well as more expensive and time-consuming sample preparation techniques than for $\delta^{13}C$. To date, those $\delta^{18}O$ studies that do exist have largely focused on tropical trees because of the high correlation between precipitation and, through global climate teleconnections, such features as El Niño Southern Oscillation (e.g., Evans and Schrag, 2004; Poussart et al., 2004). This lack of comparable studies means developing long $\delta^{18}O$ time series for the Midwest requires that we must first characterize mid latitude tree ring $\delta^{18}O$ systematics and methodologies.

The motivation for such an effort is that, even though previous chapters have demonstrated a significant correlation between ALOC white oak tree ring $\delta^{13}C$ and climatic variables, carbon isotopes do not explain a majority of the variability. In addition, using $\delta^{18}O$ in parallel or combined with $\delta^{13}C$ could improve climate correlations and reveal additional climate information (e.g., McCarroll et al., 2003; Gagen et al., 2006; Loader et al., 2008). To investigate the potential of such an approach using ALOC, a pilot study was conducted to test the relationship between oxygen isotopes and records of temperature, precipitation, and PDSI in the central Midwest. In this study we've generated a preliminary tree ring $\delta^{18}O$ time series from 1975-2002 in order to demonstrate current sample preparation methodologies and establish potential $\delta^{18}O$ connections to climate.

6.2. Stable Isotope Background

Stable oxygen isotopes are expressed in standard δ-notation form defined as:

$$\delta^{18}O = ([^{18}O/^{16}O_{sample}]/[^{18}O/^{16}O_{standard}] - 1) * 1000$$

where $\delta^{18}O$ is expressed in parts per thousand (‰). The sample is the material being analyzed and the standard is a known isotopic reference (VSMOW) (Faure, 1986). Oxygen isotopic ratios in tree rings originate from the local isotopic signature of precipitation (McCarroll and Loader, 2004), although, numerous factors affect the final value. Average annual meteoric precipitation $\delta^{18}O$ values are -6.9‰ in southern Missouri, -7.2‰ in central Iowa and -8.1‰ in southeastern Nebraska but vary widely between storms and systematically through the year (Simpkins, 1995; Frederickson and Criss, 1999; Harvey, 2001). Oxygen isotope ratios can then be modified before precipitation reaches a tree's root system by evaporation at the surface or in the soil. $H_2{}^{16}O$ molecules preferentially enter the vapor phase increasing $\delta^{18}O$ values of remaining soil water (Buhay and Edwards, 1995). No apparent fractionation occurs as the roots remove water from the soil or during transport within the tree (Wershaw et al., 1966). However, in the leaves, transpiration through the stomata again leads to the relative internal leaf enrichment of ^{18}O due to the preferential loss of $H_2{}^{16}O$ molecules. Transpiration of water molecules is caused by a vapor pressure gradient between the inner leaf and the atmosphere. The fractionation in the leaf can be up to +20‰ (Saurer et al., 1998). Increased precipitation is usually associated with an increase in relative humidity that would decrease transpiration and lower leaf water enrichment

(decreasing the vapor pressure gradient which results in less transpiration) and result in lower $\delta^{18}O$ values (Edwards and Fritz, 1986; Roden and Ehleringer, 1999).

Leaf water is used to form sucrose during photosynthesis. Hence, the $\delta^{18}O$ of the sucrose reflects that of the leaf water. Tree ring cellulose is formed as leaf sugars are transported from the leaf to the trunk where some additional oxygen exchange with xylem water (relatively lower $\delta^{18}O$ values compared to sugars) may occur (Sternberg et al., 1986). Following cellulose synthesis, additional isotopic exchange may occur during lignin synthesis, that could partially overprint the environmental signal through addition of more $H_2{}^{18}O$ molecules (Barbour et al., 2001). The final isotopic $\delta^{18}O$ signature of tree rings can be described as

$$\delta^{18}O_{cx} = f_o*(\delta^{18}O_{wx} + \varepsilon_o) + (1 - f_o)(\delta^{18}O_{wl} + \varepsilon_o)$$

where $\delta^{18}O_{cx}$ is the isotopic composition of tree ring cellulose, $\delta^{18}O_{wx}$ is the $\delta^{18}O$ of tree xylem water, $\delta^{18}O_{wl}$ is the $\delta^{18}O$ of leaf water (following enrichment), f_o represents the fraction of the carbonyl oxygen that gets exchanged with medium water (~0.42) and ε_o is the biochemical fractionation factor (+27‰) (Roden et al., 2000).

Given that atmospheric moisture conditions (precipitation and relative humidity) effect tree ring $\delta^{18}O$ values, variations in these isotopic values should provide a yearly record of past atmospheric moisture conditions. During times of increased precipitation or humidity, decreased leaf transpiration results in lower $\delta^{18}O$ values. In contrast, when drier conditions exist, leaf transpiration of $H_2{}^{16}O$ increases and results in higher $\delta^{18}O$ values following photosynthesis. Hence,

fluctuations in the final isotopic signatures should be recorded through time with at least an annual resolution.

6.3. Methods and Materials

6.3.1. Sample Selection and Preparation

The three samples used in this pilot study were selected using the same criterion as for the $\delta^{13}C$ study in chapter three. In brief, samples were selected if their ring width pattern exhibits a high correlation to the overall ALOC ring width pattern from 1975-2002. Three samples were used to determine how variable the $\delta^{18}O$ signal is among trees.

Segments originate from slices of subfossil tree wedges and cores of living trees that were collected in the field and prepared for ring width analyses at the Missouri Tree Ring Laboratory. From each segment, latewood portions of each tree ring were removed using a razor blade. All visual ring components not of latewood material were avoided or carefully removed (i.e. earlywood, structural rays). Less than 1 mg of sample material was used for analyses and in most cases each individual ring could provide enough material for replicate analyses if needed. By conducting analytical measurements on yearly ring samples, we aimed to retain as much high-frequency variability as possible.

Whereas previous chapters utilized bulk latewood analyses of tree ring $\delta^{13}C$, only cellulose is typically used for $\delta^{18}O$ analyses. This difference is because, once cellulose is formed, the cellulose does not exchange or incorporate oxygen molecules with water or other ring materials (Farquhar et al., 1998; Barbour et al.,

2004). Thus, by isolating cellulose prior to isotopic analyses, we can increase our confidence that we are measuring values representative of a given year rather than an integrated signal that includes 'post-growth' oxygen molecules (i.e., from water sources such as river water, humidity in storage, etc.) (Gaudinski et al., 2005).

Alpha cellulose (Figure 6.1) was extracted using a modified Brendel procedure for small sample processing (Brendel et al., 2000; Evans and Schrag, 2004; Anchukaitis et al., 2008). This procedure allows for an increased amount of samples (or reduced sample size) to be prepared in significantly less time than older methods such as Loader et al. (1997) (Evans and Schrag, 2004; Anchukaitis et al., 2008). Replicates prepared using this procedure also yield $\delta^{18}O$ values with comparable precision to that seen in other extraction procedures used (e.g. Green, 1963; Leavitt and Danzer, 1993; Loader et al., 1997; Cullen and MacFarlane, 2005).

Cellulose is isolated by first removing less than 1mg of latewood from each ring with a razor blade. Samples were placed into labeled 1.5 mL microcentrifuge tubes. Then, 120 μL of 80% acetic acid and 12 μL of 69% nitric acid were pipetted into each tube and placed into an aluminum heating block that is heated to 120°C for 30 minutes. This step both delignifies the sample and removes non-cellulosic polysaccharides (Brendel et al., 2000). Samples are then removed and allowed to cool for five minutes before adding 400 μL of 100% ethanol. The tubes are capped, vortexed and then centrifuged for five minutes at 10,000 rpm to aid in the separation of non-cellulosic components. The supernatant was removed and the samples were washed in three steps (following each step samples were vortexed,

centrifuged at 10,000 rpm, and isolated from the supernatant): 1) 300 μL of deionized water was added into each vial to remove traces of nitric acid; 2) 150 μL of ethanol was added into each vial to remove any remaining non-cellulosic extraction components; and 3) 150 μL of acetone was added into each vial for a final wash and dehydration of the sample. All samples were placed in a drying oven at 50°C for 30 minutes and then placed into a vacuum desiccator overnight. A complete procedural description, modifications made, and equipment used is available in Appendix 2.

6.3.2. Analytical Procedure

Extracted alpha cellulose samples were weighed, loaded into silver boats, and analyzed by continuous flow isotope ratio mass spectrometry techniques (further details in Brenna et al., 1997; Ghosh and Brand, 2003). Prepared samples are loaded into a 50-port autosampler attached to a High Temperature Conversion Elemental Analyzer (TC/EA). An individual sample is dropped into a 'High Temperature Conversion Reactor' that is heated to ~1400°C where a high temperature decomposition occurs. Oxygen in the tree ring cellulose is quantitatively converted into CO that passes through a gas chromatographic column to separate CO from N_2. Gases then pass through a Finnigan Conflo III device into a Finnigan DeltaPlusXL Isotope Ratio Mass Spectrometer (IRMS) where the relative masses of CO are compared with a reference CO gas of known isotopic composition to determine a $\delta^{18}O$ value. To monitor accuracy and precision, an average of five

samples for every standard were used for each full run. In less than 10 hours, 48 analyses (samples plus standards) can be run with an analytical precision of ±0.3‰ (1σ standard deviation). Raw isotopic results are expressed as per mil (‰) deviations using the delta notation (δ) relative to the VSMOW standard.

6.3.3. Data Evaluation

Raw segment $\delta^{18}O$ values are normalized by each individual $\delta^{18}O$ mean to compare its relative isotopic change with $\delta^{13}C$ values. However, correlations reported are the same when raw $\delta^{18}O$ values are used. Correlation analyses assessed the individual (between-tree variations) and pooled $\delta^{18}O$ values from three trees against average JJA (June-August) records of temperature, precipitation and PDSI from nearby regional climate stations within northwest Missouri Climate Division 1 from 1975-2002 (NCDC, 2004). Additionally, correlation analyses were used to compare carbon and oxygen data sets.

6.4. Results

The total range of $\delta^{18}O$ values measured for the 1975-2002 interval is 26.7‰ to 32.3‰ with a pooled mean of 28.8‰. Individual segment means were 29.0‰, 28.7‰, and 28.9‰. The average standard deviation of the three measurements for each year is 0.4, close to analytical precision (Table 6.1). Individual segments (Table 6.2) are significantly correlated among each other (with a minimum correlation of $R \geq 0.71$, $p<0.0001$).

The pooled $\delta^{18}O$ values from three trees exhibit no significant correlation to average JJA temperature from 1975-2002 ($p>0.1$). However, segment Oak BBB does correlate with JJA temperature ($R = 0.44$, $p<0.05$) whereas segments Oak AAA and Oak CCC demonstrate no apparent correlation ($p>0.4$ and $p>0.15$ respectively). Conversely, both JJA PDSI and JJA precipitation are significantly correlated (Figure 6.2) to the pooled $\delta^{18}O$ time series ($R = -0.80$, $p<0.000001$ and $R = -0.63$, $p<0.0005$ respectively). Lastly, from 1975-2002, $\delta^{18}O$ and $\delta^{13}C$ time series are significantly correlated ($R = 0.73$, $p<0.00001$).

6.5. Discussion

6.5.1. Climatic Observations

Even though there is a 5.6‰ range in $\delta^{18}O$ values, similar segment mean values (and a low inter-segment differences) may reflect a common regional control on absolute isotopic values. Additionally, the high between-tree correlations ($R \geq 0.71$, $p<0.0001$) also suggest a regionally common influence on tree ring $\delta^{18}O$ values (Figure 6.3). This situation is different from $\delta^{13}C$ where patterns were similar among trees but values varied widely. Furthermore, pooled $\delta^{18}O$ values correlate better than any individual segment with PDSI and also correlate better than two of three individual segments with precipitation and temperature (Figure 6.4). Consequently, these observations suggest that as few as three white oak trees may be adequate to capture an average regional $\delta^{18}O$ signal.

The significant correlation to both PDSI and precipitation (and lack of correlation to temperature) suggests that moisture variations are the dominant

influence on tree ring $\delta^{18}O$ values. We also know from past chapters that both precipitation and PDSI play a significant role on influencing $\delta^{13}C$ values. Yet, $\delta^{18}O$ values (from three trees) show an improved correlation to the climate variables from 1975-2002 (Figure 6.5), which may imply that tree ring $\delta^{18}O$ values of cellulose more closely tracks moisture variations than bulk $\delta^{13}C$ values.

Initial $\delta^{18}O$ observations provide the foundation to investigate past moisture variations. By generating an oxygen isotope time series from 1931-2002 (similar to $\delta^{13}C$), a more complete assessment of 20th century moisture change is possible by correlations to instrumental climate data. This expansion of oxygen isotope data may also establish if there is added benefit in using a dual isotope approach to investigate past climate change.

6.5.2. Oxygen vs. Carbon Observations

Numerous studies indicate that an increase in moisture, precipitation totals, and intensity of precipitation events have occurred during the last half of the 20th century within the Midwest while other regions, such as the southwest US, have seen the opposite (Karl et al., 1995; Karl et el., 1996; Karl and Knight, 1998; Groisman et al., 1999; Easterling et al., 2000). When $\delta^{18}O$ and $\delta^{13}C$ are plotted against each other from 1975-2002 both exhibit a negative slope toward the present (Figure 6.5). This general decrease of isotopic values in both systems would imply a broad regional-scale shift to wetter summers during the last quarter of the 20th century and is consistent with climate studies mentioned above. Observation of this recognized trend demonstrates the individual strength of each isotope to capture

wet periods. Additionally, being that $\delta^{18}O$ appears to capture drier periods better than does $\delta^{13}C$, the combination of each isotope may prove beneficial to develop an isotopic record beyond instrumental data and should be a focus for future research.

When multiple proxies exhibit similar dominant forcing influences, the correlation may improve by combining them in order to remove potential noise within each signal (McCarroll et al., 2003; Gagen et al., 2006; Loader et al., 2008). To demonstrate the potential benefit of utilizing both carbon and oxygen isotopic systems together, $\delta^{18}O$ and $\delta^{13}C$ values were averaged and weighted by their respective percent of variance to obtain a weighted estimate (Gagen et al., 2006). For example, when compared to PDSI from 1975-2002, the $\delta^{18}O$ explained variance is $R^2 = 0.64$ and the $\delta^{13}C$ explained variance is $R^2 = 0.46$. Therefore, the respective weighted percent variance when combined is 58% for $\delta^{18}O$ and 42% for $\delta^{13}C$. Annual values for each normalized isotope can be calculated using the equation

$$\textit{Weighted Isotope Estimate} = (\delta^{18}O_t * 0.58) + (\delta^{13}C_t * 0.42)$$

where *t* is the specific year of interest. The results show the combined values correlation improves with PDSI to R = -0.81 and $p<0.000001$ (Figure 6.6) while correlation to precipitation improves similarly (R = -0.65). Interestingly, when weighted climate variables are used (as mentioned in chapter 3), the isotopic correlation to PDSI is reduced (R = -0.73) while the correlation to precipitation increases (R = -0.75). Using this method and data from 1975-2002, the results suggest $\delta^{18}O$ may be sufficient for climatic study. However, by extending the $\delta^{18}O$ data set back to 1931 (as was done with carbon) and exploring other combination methods (such as multiple linear regression) may reveal other important results.

6.6. Conclusions

A $\delta^{18}O$ time series (1975-2002) generated from tree ring alpha cellulose reveal significant correlations to both PDSI and precipitation (R = -0.80 and R = -0.63 respectively). In addition, individual segments exhibit high between-tree correlations that may indicate a common regional-scale controlling mechanism for determining $\delta^{18}O$ values during tree ring growth. Also, during this time period, both carbon and oxygen isotopes significantly covary suggesting a common isotopic influence during ring formation. As a result, utilizing tree ring $\delta^{18}O$ as a climate proxy from the central Midwest appears to be a viable isotopic system to determine past climate change.

References

Anchukatis, K.J., Evans, M.N., Lange, T., Smith, D.R., Leavitt, S.W., and Schrag, D.P., 2008. Consequences of a Rapid Cellulose Extraction Technique for Oxygen Isotope and Radiocarbon Analyses. *Analytical Chemistry* **80**: 2035-2041.

Barbour, M.M., Andrews, T.J., and Farquhar, G.D., 2001. Correlations between oxygen ratios of wood constituents of *Quercus* and *Pinus* samples from around the world. *Australian Journal of Plant Physiology* **28**: 335-348.

Barbour, M.M., Roden, J.R., Farquhar, G.D., and Ehleringer, J.R., 2004. Expressing leaf water and cellulose oxygen isotope ratios as enrichment above source water reveals evidence of a Péclet effect. *Ecosystem Geology* **138**: 426–435.

Brendel, O., Iannetta, P.P.M., and Stewart, D., 2000. A Rapid and Simple Method to Isolate Pure Alpha-Cellulose. *Phytochemical Analysis* **11**: 7-10.

Brenna, J.T., Corso, T.N., Tobias, H.J., and Caimi, R.J., 1997. High-precision continuous-flow isotope ratio mass spectrometry. *Mass Spectrometry Reviews* **16**: 227-258.

Buhay, W.M., and Edwards, T.W.D., 1995. Climate in southwestern Ontario, Canada, between AD 1610 and 1885 inferred from oxygen and hydrogen isotopic measurements of wood cellulose from trees in different hydrologic settings. *Quaternary Research* **44**: 438-446.

Cullen, L., and MacFarlane, C., 2005. Comparison of cellulose extraction methods for analysis of stable isotope ratios of carbon and oxygen in plant material. *Tree Physiology* **25**: 563-569.

Easterling, D.R., Evans, J.L., Groisman, P.Ya., Karl, T.R., Kunkel, K.E., and Ambenje, P., 2000. Observed Variability and Trends in Extreme Climate Events: A Brief Review. *Bulletin of the American Meteorological Society* **81-3**: 417-425.

Edwards, T.W.D., and Fritz, P., 1986. Assessing meteoric water composition and relative humidity from ^{18}O and ^{2}H in wood cellulose: Paleoclimatic implications for southern Ontario, Canada. *Applied Geochemistry* **1-6**: 715-723.

Evans, M. N. and Schrag, D. P., 2004. A stable isotope-based approach to tropical dendroclimatology. *Geochimica et Cosmochimica Acta* **68-16**: 3295-3305.

Farquhar, G.D., Barbour, M.M., and Henry, B.K., 1998. Interpretation of oxygen isotope composition of leaf material. In: Griffiths, H. (ed), *Stable Isotopes: integration of biological, ecological and geochemical processes*. BIOS Scientific Publishers, Oxford, pp 27-62.

Faure, G., 1986. *Principles of Isotope Geology*. John Wiley and Sons, New York, pp 589.

Frederickson, G.C., and Criss, R.E., 1999. Isotope hydrology and residence times of the unimpounded Meremac River Basin, Missouri. *Chemical Geology* **157-4**: 303-317.

Gagen, M., McCarroll, D., and Edouard, J.-L., 2006. Combining ring width, density and stable carbon isotope proxies to enhance the climate signal in tree-rings: an example from the southern French Alps. *Climatic Change* **78**: 363-379.

Gagen, M., McCarroll, D., Robertson, I., Loader, N.J., and Jalkanen, R., 2008. Do tree ring $\delta^{13}C$ series from *Pinus sylvestris* in northern Fennoscandia contain long-term non-climatic trends? *Chemical Geology* **252**: 42-51.

Gaudinski, J.B., Dawson, T.E., Quideau, S., Schuur, E.A.G., Roden, J.S., Trumbore, S.E., Sandquist, D.R., Oh, S.-E., and Wasylishen, R.E., 2005. Comparative Analysis of Cellulose Preparation Techniques for Use with ^{13}C, ^{14}C, and ^{18}O Isotopic Measurements. *Analytical Chemistry* **77**: 7212-7224.

Ghosh, P., and Brand, W., 2003. Stable isotope ratio mass spectrometry in global climate change research. *International Journal of Mass Spectrometry* **228**: 1-33.

Green, J.W., 1963. Wood Cellulose. In: Whistler, R.L., (ed.), *Methods of Carbohydrate Chemistry III*. Academic, New York. pp 9–21.

Groisman, P.Ya., Karl, T.R., Easterling, D.R., and Knight, R.W., 1999. Changes in the probability of heavy precipitation: Important indicators of climatic change. *Climatic Change* **42**: 243-283.

Harvey, F.E., 2001. Use of NADP Archive Samples to Determine the Isotopic Composition of Precipitation: Characterizing the Meteoric Input Function for Use in Ground Water Studies. *Ground Water* **39-3**: 380-390.

Karl, T.R., and Knight, R.W., 1998. Secular trends of precipitation amount, frequency, and intensity in the United States. *Bulletin of the American Meteorological Society* **79**: 1107-1119.

Karl, T.R., Knight, R.W., Easterling, D.R., and Quayle, R.G., 1995. Trends in U.S. Climate During the Twentieth Century. *Consequences* **1**: 3-12.

Karl, T.R., Knight, R.W., Easterling, D.R., and Quayle, R.G., 1996. Indices of climate change for the United States. *Bulletin of the American Meteorological Society* **77**: 279-291.

Leavitt, S.W., 2008. Tree-ring isotopic pooling without regard to mass: No difference from averaging $\delta^{13}C$ values of each tree. *Chemical Geology* **252**: 52-55.

Leavitt, S.W., and Danzer, S.R., 1993. Method for Batch Processing Small Wood Samples to Hollocellulose for Stable-Carbon Isotope Analysis. *Analytical Chemistry* **65**: 87-89.

Loader, N.J., Robertson, I., Barker, A.C., Switsur, V.R., and Waterhouse, J.S., 1997. An improved technique for the batch processing of small wholewood samples to α-cellulose. *Chemical Geology* **136**: 313-317.

Loader, N.J., Santillo, P.M., Woodman-Ralph, J.P., Rolfe, J.E., Hall, M.A., Gageb, M., Robertson, I., Wilson, R., Froyd, C.A., and McCarroll, D., 2008. Multiple stable isotopes from oak trees in southwestern Scotland and the potential for stable isotope Dendroclimatology in maritime climatic regions. *Chemical Geology* **252**: 62-71.

McCarroll D., and Loader N. J., 2004. Stable isotopes in tree rings. *Quaternary Science Reviews* **23**: 771–801.

McCarroll, D., Jalkanen, R., Hicks, S., Tuovinen, M., Gagen, M., Pawellek, F., Eckstein, D., Schmitt, U., Autio, J., and Heikkinen, O., 2003. Multiproxy dendroclimatology: a pilot study in northern Finland. *The Holocene* **13-6**: 831-841.

McCarroll, D.J., Gagen, M.H., Loader, N.J., Robertson, I., Anchukaitis, K.J., Los, S., Young, G.,H.F., Jalkanen, R., Kirchhefer, A., and Waterhouse, J.S., 2009. Correction of tree ring stable carbon isotope chronologies for changes in the carbon dioxide content of the atmosphere. *Geochimica et Cosmochimica Acta* **73**: 1539-1547.

National Climate Data Center (NCDC), 2004. Time bias corrected divisional temperature-precipitation-drought index. www.ncdc.noaa.gov/oa/climate/climatedata.html.

Poussart, P.F., Evans, M.N., and Schrag, D.P., 2004. Resolving seasonality in tropical trees: multi-decade, high-resolution oxygen and carbon isotope records from Indonesia and Thailand. *Earth and Planetary Science Letters* **218**: 301-316.

Roden, J.S., and Ehleringer, J.R., 1999. Observations of hydrogen and oxygen isotopes in leaf water confirm the Craig-Gordon model under wide-ranging environmental conditions. *Plant Physiology* **120-4**: 1165-1173.

Roden, J.S., Lin, G., and Ehleringer, J.R., 2000. A mechanistic model for interpretation of hydrogen and oxygen isotope ratios in tree-ring cellulose. *Geochimica et Cosmochimica Acta* **64**: 21-25.

Saurer, M., Siegwolf, R., Borella, S., and Schweingruber, F., 1998. Environmental information from stable isotopes in tree rings of *Fagus sylvatica*. In: Beniston, M., Innes, J.L. (eds.), *The Impacts of Climate Variability on Forests*. Springer, Berlin, pp. 241-253.

Saurer, M., Cherubini, P., Reynolds-Henne, C.E., Treydte, K.S., Anderson, W.T., and Siegwolf, R.T.W., 2008. An investigation of the common signal in tree ring stable isotope chronologies at temperate sites. *Journal of Geophysical Research* **113**: G04035.

Simpkins, W.W., 1995. Isotopic composition of precipitation in central Iowa. *Journal of Hydrology* **172**: 185-207.

Sternberg, L., De Niro, M., and Savidge, R., 1986. Oxygen isotope exchange between metabolites and water during biochemical reactions leading to cellulose synthesis. *Plant Physiology* **82**: 423-427.

Weigl, M., Grabner, M., Helle, G., Schleser, G.H., and Wimmer, R., 2007. Variability of latewood-widths and –stable isotope ratios in a sessile oak tree (*Quercus petraea* (Matt.) Liebl.). *Dendrochronologia* **24**: 117-122.

Wershaw, R.L., Friedman, I., and Heller, S.J., 1966. Hydrogen isotope fractionation in water passing through trees. In: Hobson, F., and Speers, M. (eds.), *Advances in Organic Geochemistry*. Pergamon, New York, 55-67.

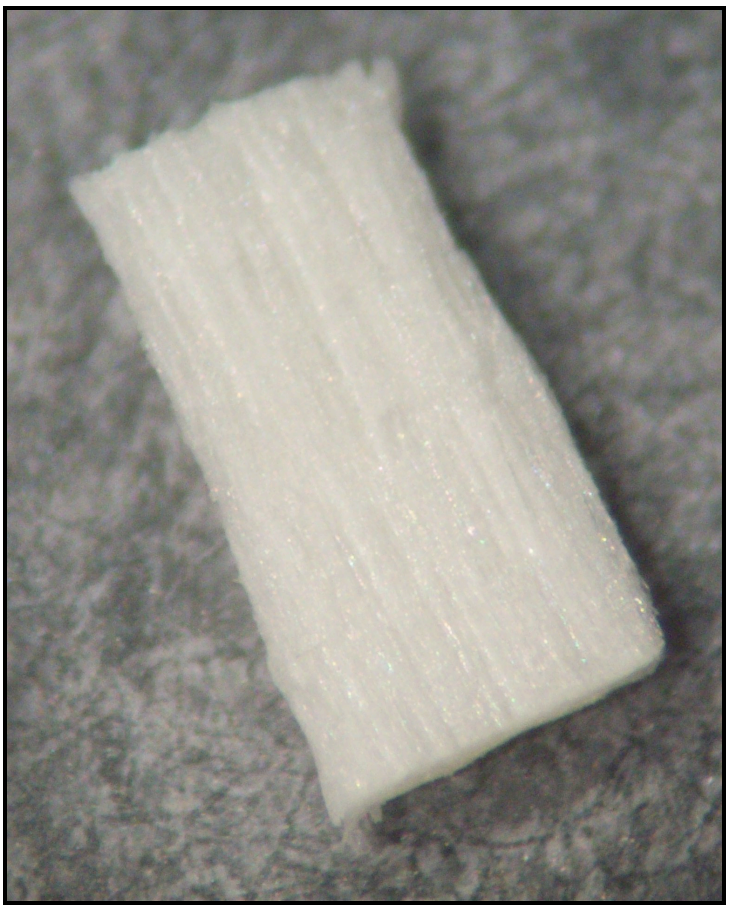

Figure 6.1: An example of tree ring alpha cellulose extracted by a modified Brendel procedure for small sample processing. The original sample color is tan whereas samples become white following the extraction procedure. The alpha cellulose sample above weighs approximately 0.4mg. Average mass yield for samples following the extraction procedure was ~40%.

YEAR	AVG $\delta^{18}O$	STD DEV	Oak AAA	Oak BBB	Oak CCC
2002	29.2	0.6	29.2	29.8	28.7
2001	28.5	0.3	28.7	28.6	28.1
2000	28.1	0.3	28.0	28.4	27.9
1999	27.7	0.7	27.3	28.6	27.3
1998	27.5	0.2	27.6	27.6	27.2
1997	28.6	0.5	29.3	28.2	28.4
1996	28.8	0.3	29.1	28.5	28.8
1995	28.0	0.0	28.1	28.0	28.0
1994	28.2	0.2	28.3	28.0	28.2
1993	27.5	0.1	27.6	27.3	27.4
1992	28.5	0.5	29.1	28.1	28.4
1991	29.6	0.2	29.7	29.3	29.8
1990	28.4	0.3	28.7	28.2	28.3
1989	29.6	0.4	29.8	29.1	29.9
1988	31.3	1.0	32.3	30.3	31.3
1987	28.6	0.6	28.9	27.9	29.0
1986	28.3	0.3	28.0	28.3	28.6
1985	29.7	0.6	30.2	29.0	29.9
1984	29.4	0.6	29.7	28.7	29.8
1983	29.5	0.3	29.2	29.6	29.7
1982	28.5	0.1	28.6	28.5	28.3
1981	27.3	0.6	27.9	26.7	27.2
1980	29.5	0.4	29.0	29.9	29.5
1979	28.3	0.5	28.7	27.8	28.5
1978	28.6	0.1	28.8	28.6	28.5
1977	30.0	0.3	30.0	29.7	30.2
1976	30.5	0.7	29.8	30.7	31.1
1975	29.8	0.4	29.5	29.8	30.3
Average	*28.8*	*0.4*	*29.0*	*28.7*	*28.9*

Table 6.1: Raw $\delta^{18}O$ values (‰) for each segment along with the average (AVG $\delta^{18}O$) and standard deviation (STD DEV) of all three segments combined.

	Oak AAA	Oak BBB	Oak CCC
Oak AAA	1.00	0.71	0.89
Oak BBB	0.71	1.00	0.85
Oak CCC	0.89	0.85	1.00

Table 6.2: Pearson correlation coefficients (R) for comparisons between individual segments.

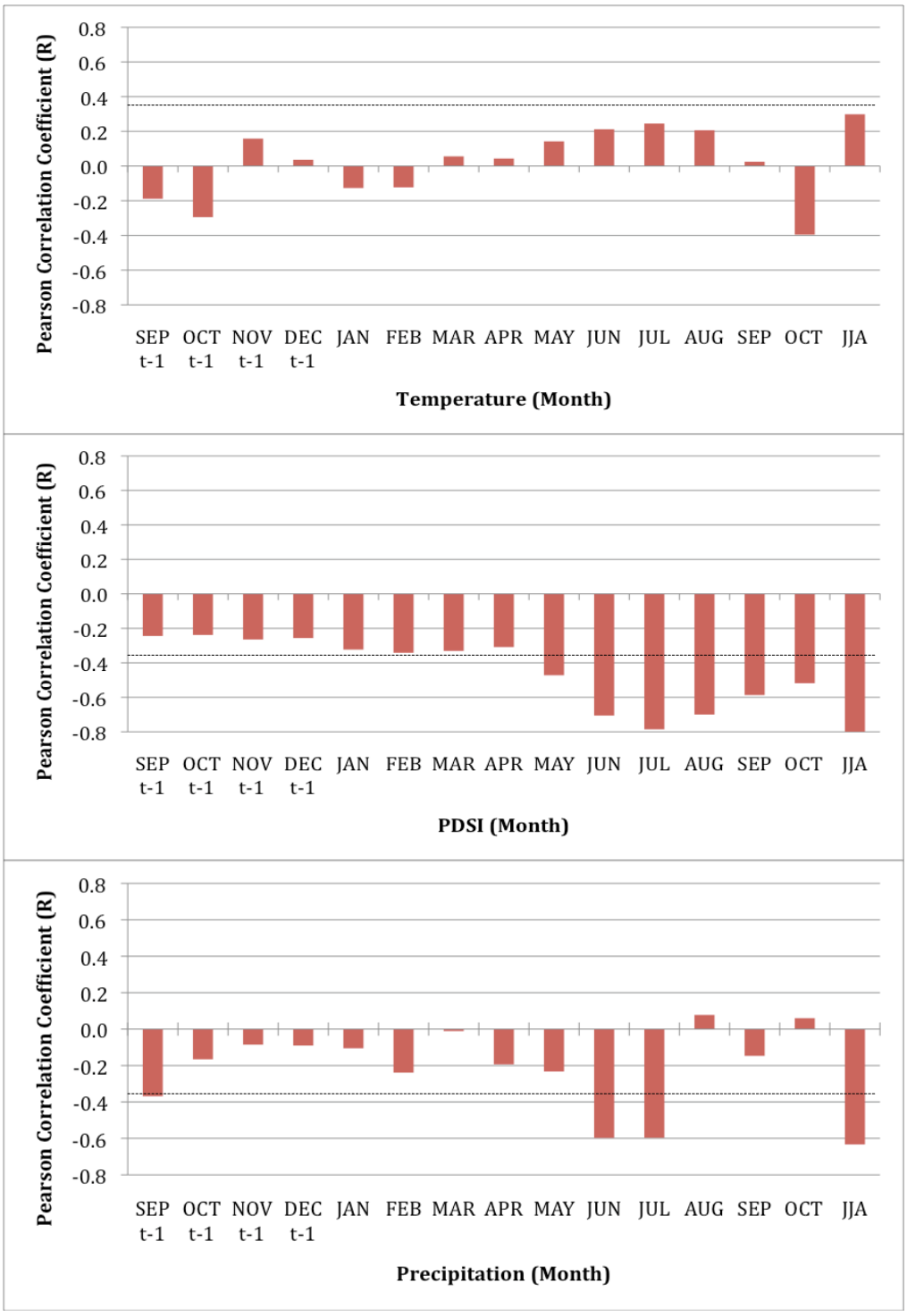

Figure 6.2: Composite correlation diagrams illustrating Pearson correlations (R) between normalized $\delta^{18}O$ values and temperature (top graph), PDSI (middle graph) and precipitation (lower graph). Only correlations above 0.374 are significant at the 95% confidence level (dashed lines). Previous year's months are denoted by t-1.

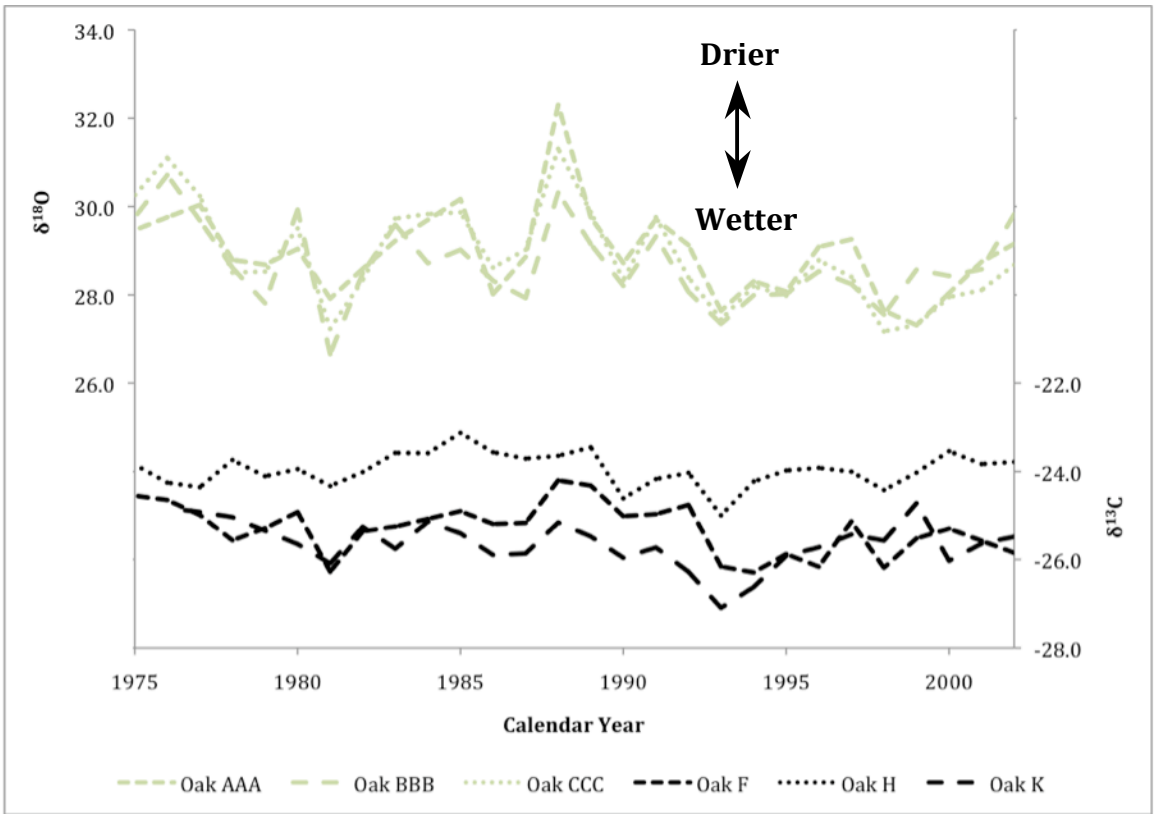

Figure 6.3: Individual segment $\delta^{18}O$ (gray lines - top) and corrected $\delta^{13}C$ (black lines - bottom) time series from 1975-2002. Less variability (low yearly standard deviation) between each segment is more apparent with $\delta^{18}O$ than with $\delta^{13}C$.

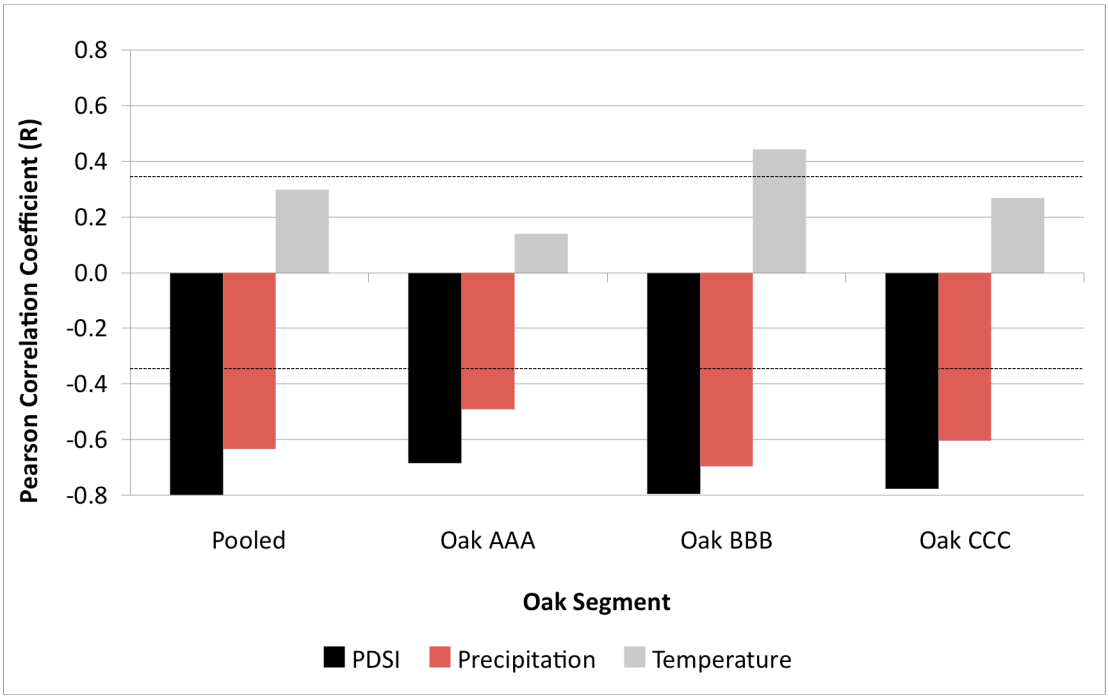

Figure 6.4: Composite correlation diagram illustrating Pearson correlations (R) between segment and pooled $\delta^{18}O$ values correlated to PDSI (black bar), precipitation (dark gray bar) and temperature (light gray bar) variables. Only correlations above 0.374 are significant at the 95% confidence level.

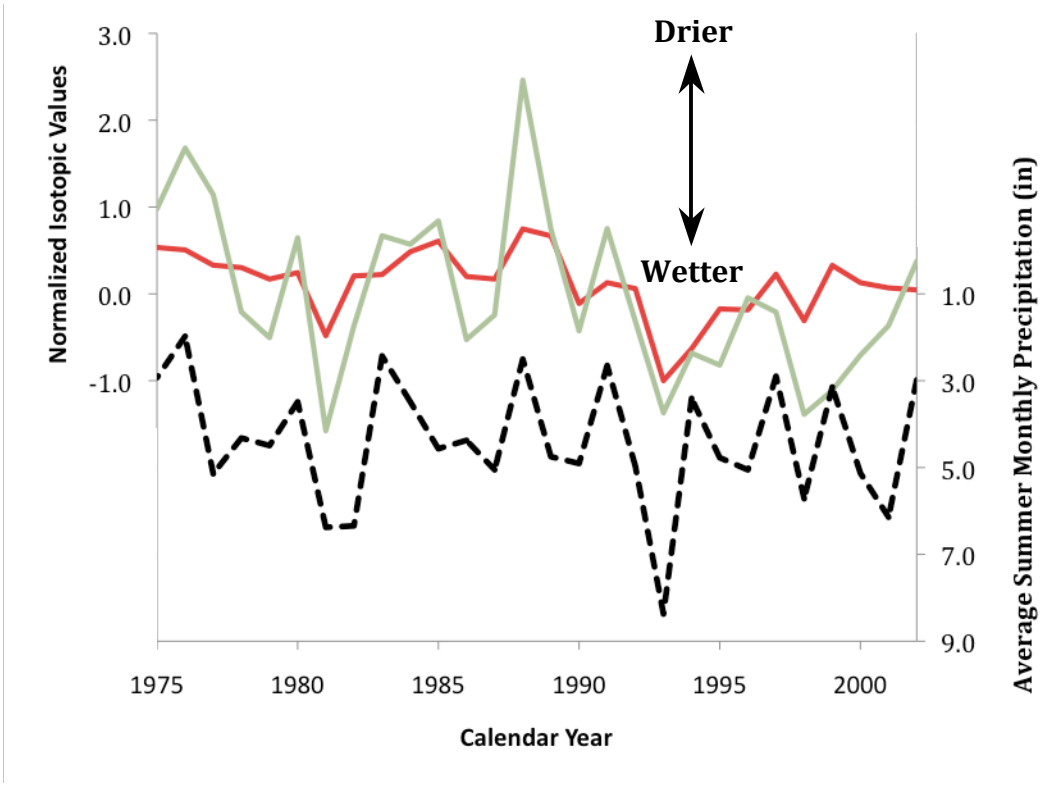

Figure 6.5: Normalized carbon (darker solid line) and oxygen (lightest solid line) isotopic time series compared to instrumental average summer monthly precipitation (black dashed line) from 1975-2002. Oxygen appears to capture a wider range of moisture stresses. In general, both records exhibit an overall isotopic decrease from 1975 toward the present.

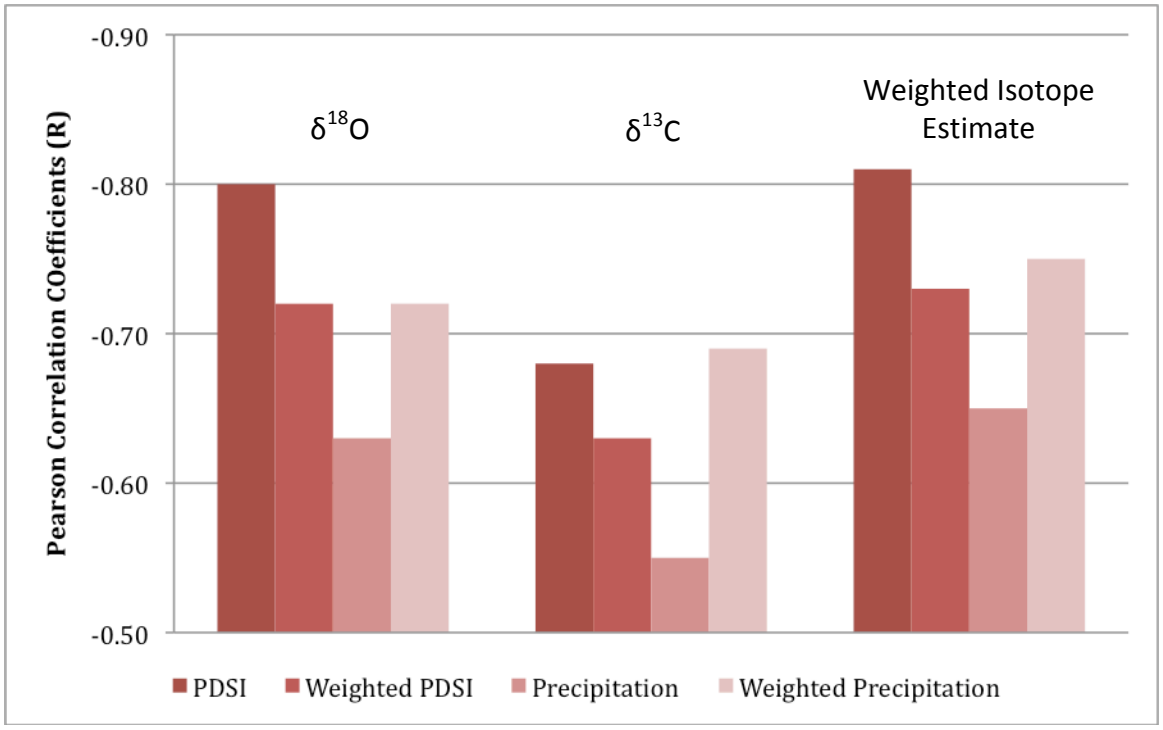

Figure 6.6: Pearson correlation coefficients from 1975-2002 of $\delta^{18}O$, $\delta^{13}C$, and the weighted isotope estimate. The vertical bars from left to right are PDSI, weighted PDSI (from chapter 3), precipitation, and weighted precipitation (from chapter 3). Each weighted isotope estimate increases from single isotope measurements. For all isotope configurations, correlations increase using weighted precipitation while correlations decrease using weighted PDSI.

Appendix 1

HC & LC Tree Names and Raw $\delta^{13}C$ Values

HC TREE	FORESTRY ID
OAK A-1	PTR109
OAK B-1	PTR106
OAK C-1	LCH001
OAK E-1	TMP165
OAK F-1	LMDC06
OAK G-1	LMDC21
OAK H-1	LMDC17
OAK J-1	MED12B
OAK K-1	LMDC12
OAK L-1	LMDC14
OAK M-1	MED16A
OAK N-1	TMP155B
OAK O-1	LMDC13
OAK P-1	Med18A
OAK Q-1	Med358
OAK R-1	tmp102A & B
OAK S-1	tmp156
OAK T-1	tmp176B
OAK U-1	Med393B
OAK V-1	lct077A
OAK W-1	Med386A
OAK X-1	lct071
OAK Y-1	med265B
OAK AA-1	med351B
OAK AB-1	lct68
OAK AC-1	Med406
OAK AD-1	wld421
OAK AE-1	lmd09b

LC TREE	FORESTRY ID
OAK AA-1	MED18A
OAK BB-1	CROC10
OAK CC-1	LCTC02
OAK DD-1	croc12
OAK EE-1	lctc06
OAK FF-1	croc01
OAK GG-1	med10a
OAK HH-1	med15a

YEAR	OAK A	OAK B	OAK C	OAK F	OAK G	OAK H	OAK J	OAK K	OAK L	OAK M	OAK N	OAK O	OAK P	OAK Q
2002				-27.5		-25.4		-27.1						
2001				-27.2		-25.5		-27.3						
2000				-26.9		-25.1		-27.6						
1999				-27.1		-25.6		-26.3						
1998				-27.7		-26.0		-27.1						
1997				-26.6		-25.5		-26.9						
1996				-27.6		-25.4		-27.2						
1995				-27.3		-25.4		-27.4						
1994				-27.7		-25.6		-28.0						
1993				-27.6		-26.4		-28.5						
1992				-26.1		-25.4		-27.6						
1991				-26.3		-25.5		-27.1						
1990				-26.3		-25.9		-27.3						
1989				-25.6		-24.7		-26.8						
1988				-25.5		-24.9		-26.4						
1987				-26.4		-24.9		-27.1						
1986				-26.4		-24.8		-27.1						
1985				-26.1		-24.3		-26.6						
1984				-26.2		-24.7		-26.3						
1983				-26.4		-24.7		-26.9						
1982				-26.4		-25.1		-26.3						
1981				-27.3		-25.4		-27.2						
1980				-26.0		-25.0		-26.7						
1979				-26.3		-25.1		-26.3						
1978				-26.5		-24.7		-26.0						
1977				-25.9		-25.3		-25.9						
1976				-25.6		-25.2		-25.8						
1975		-26.0		-25.4		-24.7								
1974		-25.8		-26.0		-25.2								
1973		-25.6		-25.8		-24.8								
1972		-26.1		-25.9		-24.9								
1971		-25.9		-26.4		-25.3								
1970		-25.6		-26.3		-24.8								
1969		-25.3		-26.6		-25.2								
1968		-25.6		-26.6		-25.1								
1967		-25.8		-27.3		-25.0								
1966		-25.8		-26.4		-24.9								
1965		-25.7		-26.2		-24.6								
1964		-25.6		-26.8		-24.3								
1963		-25.8		-26.2		-24.7								
1962		-26.1		-26.5		-25.2								
1961		-25.8		-26.6		-23.9								
1960		-26.0		-26.4		-24.0								
1959		-25.8		-26.6		-24.0								

YEAR	OAK A	OAK B	OAK C	OAK F	OAK G	OAK H	OAK J	OAK K	OAK L	OAK M	OAK N	OAK O	OAK P	OAK Q
1958		-25.9		-27.1		-24.2								
1957		-25.2		-26.6		-24.4								
1956		-25.2		-27.0		-25.1								
1955		-25.1		-26.4		-25.0								
1954		-25.2		-26.3		-24.9								
1953		-25.7		-26.4		-24.9								
1952		-26.2		-27.2		-25.4								
1951		-26.0		-26.6		-24.8								
1950		-25.8		-26.8		-24.4								
1949		-25.3			-26.6				-24.6					
1948		-25.5			-26.7				-24.4					
1947		-25.1			-26.4				-24.2					
1946		-25.8			-26.9				-24.0					
1945		-25.3			-26.0				-23.9					
1944		-26.3			-26.7				-24.7					
1943		-25.5			-26.9				-24.6					
1942		-25.9			-26.9				-25.4					
1941		-25.1			-26.8				-24.0					
1940		-25.3			-26.3				-24.6					
1939		-25.5			-27.1				-25.0					
1938		-25.1			-26.4				-23.8					
1937		-25.4			-26.7				-24.0					
1936		-25.0			-25.9				-24.3					
1935		-24.8			-26.6				-24.4					
1934		-24.3			-25.4				-23.8					
1933		-25.5			-26.1				-24.3					
1932		-25.4			-25.8				-24.7					
1931		-25.0			-26.2				-23.9					
1930		-25.0			-25.5				-23.8					
1929		-25.8			-25.6				-24.3					
1928		-26.6			-26.4				-24.6					
1927		-26.0			-25.5				-24.2					
1926		-26.3			-26.4				-25.1					
1925		-26.9			-26.2				-25.3					
1924	-25.6	-26.2	-24.5											
1923	-26.2	-27.0	-24.6											
1922	-25.8	-25.9	-24.1											
1921	-25.3	-26.6	-25.5											
1920	-25.4	-25.9	-24.4											
1919	-25.3	-26.3	-24.5											
1918	-25.5	-27.1	-25.0											
1917	-25.3	-26.9	-25.2											
1916	-25.3	-26.6	-25.3											
1915	-25.1	-26.4	-25.0											

YEAR	OAK A	OAK B	OAK C	OAK F	OAK G	OAK H	OAK J	OAK K	OAK L	OAK M	OAK N	OAK O	OAK P	OAK Q
1914	-25.6	-26.4	-25.6											
1913	-25.5	-26.6	-25.4											
1912	-24.7	-26.5	-25.0											
1911	-25.5	-26.5	-25.6											
1910	-25.7	-26.2	-25.7											
1909	-26.2	-26.5	-26.1											
1908	-25.6	-26.3	-25.0											
1907	-25.9	-27.0	-25.3											
1906	-26.0	-26.5	-25.2											
1905	-26.3	-26.7	-24.6											
1904	-26.0	-26.4	-25.3											
1903	-26.3	-26.5	-24.9											
1902	-26.4	-26.4	-25.8											
1901	-26.5	-25.2	-24.7											
1900	-27.5	-26.1	-25.6											
1899	-27.9		-25.5				-26.3							
1898	-27.7		-25.7				-25.6							
1897	-26.4		-25.7				-25.5							
1896	-26.6		-25.7				-25.9							
1895	-26.2		-24.1				-25.7							
1894	-26.5		-24.8				-26.1							
1893	-26.3		-25.3				-26.4							
1892	-27.0		-25.5				-26.2							
1891	-26.8		-25.5				-26.6							
1890	-26.8		-25.1				-26.5							
1889	-26.8		-25.3				-26.3							
1888	-26.9		-25.2				-26.6							
1887	-26.9		-25.2				-27.0							
1886	-26.1		-24.7				-26.3							
1885	-26.7		-25.3				-26.3							
1884	-27.5		-24.9				-25.7							
1883	-26.8		-25.5				-26.0							
1882	-26.3		-25.6				-26.4							
1881	-26.5		-26.0				-26.1							
1880	-26.6		-25.1				-26.0							
1879	-25.6						-25.6					-25.0		
1878	-25.2						-25.6					-24.7		
1877	-25.3						-26.6					-24.3		
1876	-25.7						-27.2					-24.7		
1875	-24.7						-26.6					-24.7		
1874	-25.4						-26.4					-24.8		
1873	-24.8						-27.1					-24.8		
1872	-24.7						-26.6					-25.0		
1871	-24.8						-27.5					-24.6		

YEAR	OAK A	OAK B	OAK C	OAK F	OAK G	OAK H	OAK J	OAK K	OAK L	OAK M	OAK N	OAK O	OAK P	OAK Q
1870	-25.5						-26.7					-24.6		
1869	-24.3						-26.0						-26.2	
1868	-25.6						-25.5						-26.8	
1867	-24.5						-26.7						-26.5	
1866	-24.7						-26.2						-26.8	
1865	-25.2						-26.3						-27.2	
1864	-25.8						-25.9						-27.4	
1863	-24.6						-25.3						-26.5	
1862	-24.5						-25.2						-26.8	
1861	-24.2						-25.3						-26.6	
1860	-25.3						-25.4						-26.5	
1859	-25.5						-25.4						-26.2	
1858	-24.9						-26.1						-26.7	
1857							-25.3			-25.9			-26.4	
1856							-26.1			-25.9			-26.8	
1855							-25.3			-25.7			-26.0	
1854							-25.1			-25.5			-26.1	
1853							-25.4			-25.9			-26.1	
1852							-25.1			-25.6			-25.9	
1851							-25.5			-25.8			-25.7	
1850							-25.9			-26.4			-26.5	
1849							-24.9			-26.1			-25.4	
1848							-25.4			-26.5			-26.4	
1847							-25.0			-26.2			-25.9	
1846							-25.7			-26.6			-26.3	
1845							-25.6			-27.1			-26.4	
1844							-25.0			-26.9			-26.2	
1843							-25.5			-26.7			-26.7	
1842							-24.9			-26.2			-26.3	
1841							-25.3			-26.3			-26.2	
1840							-25.2			-26.1			-26.3	
1839							-25.4			-26.6			-26.1	
1838							-26.3			-27.3			-26.3	
1837							-25.9			-26.1	-25.6			
1836							-25.2			-26.7	-24.9			
1835							-24.9			-27.2	-24.8			
1834							-26.0			-27.2	-25.0			
1833							-25.9			-27.0	-25.0			
1832							-24.8			-27.4	-24.7			
1831							-25.4			-26.8	-24.8			
1830							-26.0			-27.1	-25.6			
1829							-26.1			-26.9	-25.4			
1828							-26.1			-26.4	-25.1			
1827							-26.2			-27.1	-25.8			

YEAR	OAK A	OAK B	OAK C	OAK F	OAK G	OAK H	OAK J	OAK K	OAK L	OAK M	OAK N	OAK O	OAK P	OAK Q
1826							-26.0			-26.4	-25.0			
1825							-26.5			-26.2	-25.4			
1824							-26.4			-26.3	-25.8			
1823							-26.2			-26.6	-25.6			
1822							-26.1			-26.7	-25.9			
1821							-26.6			-27.0	-26.0			
1820										-25.8				
1819										-26.4	-24.7			
1818							-26.2			-26.9	-25.3			
1817							-26.0			-25.9	-23.8			
1816							-26.0			-26.4	-24.9			
1815							-25.4			-26.0	-24.9			
1814							-25.2			-25.1	-24.7			
1813							-25.8			-25.5	-25.0			
1812							-25.5			-25.6	-24.9			
1811							-24.6			-25.7	-24.7			
1810							-24.7			-25.3	-24.6			
1809							-24.8			-25.0	-24.3			
1808							-24.7			-24.8	-25.5			
1807							-24.2			-24.2	-24.9			
1806							-24.4			-25.3	-25.3			
1805							-24.2			-25.0	-25.5			
1804							-24.6			-25.1	-25.0			
1803							-25.1			-25.8	-25.6			
1802							-24.4			-25.4	-25.4			
1801							-24.9			-26.4	-26.0			
1800										-25.2				-24.9
1799														-25.5
1798														-24.8
1797														-25.2
1796														-24.7
1795														-24.1
1794														-24.7
1793														-24.9
1792														-24.8
1791														-24.8
1790														-24.3
1789														-24.6
1788														-24.4
1787														-24.0
1786														-23.9
1785														-24.7
1784														-24.1
1783														-24.0

YEAR	OAK A	OAK B	OAK C	OAK F	OAK G	OAK H	OAK J	OAK K	OAK L	OAK M	OAK N	OAK O	OAK P	OAK Q
1782														-25.3
1781														-25.3
1780														-24.7
1779														-25.1
1778														-24.9
1777														-25.1
1776														-25.2
1775														-25.8
1774														-25.7
1773														-25.4
1772														-25.3
1771														-25.0
1770														-25.5
1769														-25.4
1768														-24.8
1767														-25.3
1766														-25.0
1765														-25.3
1764														-24.9
1763														-24.5
1762														-24.7
1761														-25.3
1760														-25.6
1759														-25.4
1758														-25.9
1757														-25.3
1756														-25.5
1755														-25.0
1754														-24.9
1753														-24.9
1752														-24.4
1751														-24.8
1750														-24.8
1749														-25.1
1748														-24.7
1747														-25.3
1746														-25.3
1745														-25.1
1744														-25.0
1743														-25.1
1742														-25.5
1741														-24.8
1740														-25.3
1739														-24.8

YEAR	OAK A	OAK B	OAK C	OAK F	OAK G	OAK H	OAK J	OAK K	OAK L	OAK M	OAK N	OAK O	OAK P	OAK Q
1738														-25.6
1737														-25.3
1736														-25.1
1735														-25.2
1734														-25.0
1733														-25.3
1732														-25.7
1731														-25.5
1730														-25.6
1729														-25.6
1728														-26.5
1727														-26.2
1726														-26.3
1725														-26.7
1724														-25.8
1723														-26.7
1722														-25.8
1721														-25.9
1720														-25.9
1719														-26.5
1718														-25.0
1717														-25.5
1716														-24.8
1715														-25.3
1714														-24.6
1713														-25.0
1712														-25.0
1711														-25.4
1710														-25.3
1709														-25.1
1708														-25.7
1707														-25.1
1706														-25.0
1705														-25.2
1704														-25.3
1703														-24.7
1702														-25.6
1701														-25.6
1700														-25.4
1699														
1698														
1697														
1696														
1695														

YEAR	OAK R	OAK S	OAK T	OAK U	OAK V	OAK W	OAK X	OAK Y	OAK E	OAK AA	OAK AB	OAK AC	OAK AD	OAK AE
1826														
1825														
1824														
1823														
1822														
1821														
1820														
1819														
1818														
1817														
1816														
1815														
1814														
1813														
1812														
1811														
1810														
1809														
1808														
1807														
1806														
1805														
1804														
1803														
1802														
1801														
1800	-23.5													
1799	-24.3	-25.2												
1798	-24.0	-24.6												
1797	-24.8	-25.0												
1796	-24.0	-24.8												
1795	-24.1	-24.2												
1794	-23.9	-24.0												
1793	-24.1	-24.8												
1792	-24.0	-24.3												
1791	-23.2	-25.0												
1790	-24.3	-24.5												
1789	-24.3	-24.7												
1788	-24.0	-24.6												
1787	-23.9	-24.3												
1786	-24.0	-24.7												
1785	-23.9	-25.1												
1784	-23.8	-24.5												
1783	-23.4	-24.5												

YEAR	OAK R	OAK S	OAK T	OAK U	OAK V	OAK W	OAK X	OAK Y	OAK E	OAK AA	OAK AB	OAK AC	OAK AD	OAK AE
1782	-24.8	-25.8												
1781	-24.8	-25.3												
1780	-24.7	-25.3												
1779	-24.7		-25.5											
1778	-24.7		-25.2											
1777	-25.0		-26.1											
1776	-24.7		-25.6											
1775	-25.2		-26.9											
1774	-24.4		-26.6											
1773	-23.7		-25.7											
1772	-24.0		-26.2											
1771	-24.4		-26.1											
1770	-24.2		-25.6											
1769	-24.1		-26.6											
1768	-23.6		-25.9											
1767	-24.6		-25.9											
1766	-23.7		-25.9											
1765	-23.9		-26.4											
1764	-24.2		-26.6											
1763	-23.4		-25.4											
1762	-23.7		-26.0											
1761	-23.8		-27.2											
1760	-23.9		-27.0											
1759	-23.8		-25.6											
1758	-24.3		-26.5											
1757	-24.0		-26.3											
1756	-23.8		-27.2											
1755	-24.2		-27.4											
1754	-24.8		-27.7											
1753	-23.9		-27.8											
1752	-23.6		-26.8											
1751	-24.0		-28.0											
1750	-23.6		-27.4											
1749	-23.6		-27.8											
1748	-23.6		-27.1											
1747	-24.4		-28.2											
1746	-24.2		-27.7											
1745	-24.4		-27.3											
1744	-23.5		-27.3											
1743	-24.1		-27.2											
1742	-23.8		-27.9											
1741	-23.6		-26.5											
1740	-23.0		-27.1											
1739	-23.2		-26.5											

YEAR	OAK R	OAK S	OAK T	OAK U	OAK V	OAK W	OAK X	OAK Y	OAK E	OAK AA	OAK AB	OAK AC	OAK AD	OAK AE
1738	-24.8		-27.3											
1737	-24.4		-26.5											
1736	-24.5		-26.8											
1735	-24.7		-27.7											
1734	-23.8		-27.3											
1733	-23.9		-27.1											
1732	-24.1		-27.0											
1731	-23.9		-26.7											
1730	-24.2			-24.7										
1729	-23.9			-23.8										
1728	-24.2			-24.2										
1727	-24.3			-24.3										
1726	-25.0			-24.5										
1725	-25.1			-24.1										
1724	-24.4			-23.8										
1723	-24.0			-24.0										
1722	-24.2			-24.4										
1721	-24.4			-24.0										
1720	-24.6			-24.5										
1719	-24.7			-24.3										
1718	-24.8			-23.7										
1717	-25.4			-23.4										
1716	-23.8			-23.4										
1715	-23.8			-23.5										
1714	-23.8			-24.1										
1713	-24.2			-23.5										
1712	-24.5			-23.7										
1711	-25.1			-23.8										
1710	-24.9			-24.2										
1709	-24.2			-24.0										
1708	-25.2			-24.1										
1707	-24.9			-24.1										
1706	-24.3			-24.2										
1705	-25.0			-24.5										
1704	-25.1			-24.1										
1703	-25.3			-23.7										
1702	-25.3			-24.0										
1701	-24.8			-24.2										
1700	-24.8			-24.1										
1699	-24.7			-25.3	-25.8									
1698	-25.4			-24.8	-25.2									
1697	-25.5			-24.3	-24.5									
1696	-25.6			-24.9	-24.6									
1695	-26.2			-25.2	-24.7									

YEAR	OAK R	OAK S	OAK T	OAK U	OAK V	OAK W	OAK X	OAK Y	OAK E	OAK AA	OAK AB	OAK AC	OAK AD	OAK AE
1694	-26.3			-24.8	-25.0									
1693	-26.9			-25.6	-25.5									
1692	-26.0			-25.1	-25.0									
1691	-26.8			-25.5	-25.0									
1690	-26.3			-25.8	-24.9									
1689	-26.7			-25.5	-25.2									
1688	-26.9			-25.8	-24.6									
1687	-26.7			-25.9	-24.8									
1686	-26.6			-25.8	-24.8									
1685	-26.9			-25.7	-24.6									
1684	-26.4			-26.1	-24.7									
1683	-27.5			-26.2	-24.7									
1682	-27.2			-26.2	-24.5									
1681	-27.0			-26.7	-24.7									
1680	-26.5			-26.3	-25.0									
1679	-25.9			-26.0	-24.8									
1678	-25.7			-26.0	-24.5									
1677	-26.3			-25.6	-24.8									
1676	-25.7			-25.5	-24.5									
1675	-25.2			-25.3	-24.3									
1674	-25.7			-25.5	-24.5									
1673	-25.4			-25.0	-24.3									
1672	-26.7			-25.3	-24.5									
1671	-26.7			-25.2	-24.6									
1670	-26.6			-25.0	-24.4									
1669	-26.3			-24.4	-24.5									
1668	-26.4			-25.3	-24.3									
1667	-25.6			-25.7	-24.3									
1666	-26.5			-26.6	-24.3									
1665	-26.4			-26.2	-24.3									
1664	-25.5			-25.8	-24.2									
1663	-26.3			-24.7	-23.9									
1662	-26.6			-25.7	-24.2									
1661	-25.8			-25.3	-24.2									
1660	-26.3			-25.2	-24.7									
1659	-25.9			-25.6	-24.7									
1658	-26.4			-25.7	-25.4									
1657	-26.4			-25.7	-25.8									
1656	-26.3			-25.8	-26.0									
1655	-25.9			-24.9	-25.4									
1654	-25.9			-25.6	-25.1									
1653	-24.9			-24.6	-24.9									
1652	-25.2			-25.3	-25.2									
1651	-24.9			-25.0	-24.8									

YEAR	OAK R	OAK S	OAK T	OAK U	OAK V	OAK W	OAK X	OAK Y	OAK E	OAK AA	OAK AB	OAK AC	OAK AD	OAK AE
1650	-25.3			-25.3	-24.5									
1649						-24.7	-26.0	-26.3						
1648						-25.4	-26.4	-26.4						
1647						-25.5	-27.1	-26.0						
1646						-25.4	-26.4	-25.4						
1645						-25.0	-25.6	-24.8						
1644						-24.8	-26.7	-25.2						
1643						-24.3	-26.0	-24.6						
1642						-24.6	-27.2	-24.5						
1641						-24.2	-26.5	-25.2						
1640						-23.9	-27.0	-25.4						
1639						-24.6	-27.4	-25.5						
1638						-24.4	-27.1	-25.5						
1637						-24.3	-27.0	-26.6						
1636						-24.7	-26.9	-26.9						
1635						-25.6	-27.2	-27.2						
1634						-25.2	-27.1	-27.1						
1633						-24.9	-26.8	-26.7						
1632						-24.3	-26.5	-26.0						
1631						-24.7	-27.1	-25.9						
1630						-24.7	-26.9	-25.5						
1629						-24.9	-26.6	-25.9						
1628						-24.8	-26.7	-25.9						
1627						-24.9	-26.9	-26.3						
1626						-24.6	-26.8	-26.6						
1625						-24.5	-26.9	-26.8			-23.9			
1624							-26.5	-27.3			-24.0			
1623							-26.3	-27.7			-24.2			
1622							-26.3	-28.1			-24.3			
1621							-26.4	-27.8			-24.5			
1620							-26.4	-27.6			-24.4			
1619							-26.4	-27.4			-25.0			
1618							-26.0	-27.5			-25.1			
1617							-26.3	-27.8			-25.0			
1616							-26.9	-27.9			-24.6			
1615							-26.6	-27.4			-24.3			
1614							-26.9	-27.8			-24.5			
1613							-27.0	-27.7			-24.9			
1612							-27.2	-28.0			-24.5			
1611							-26.2	-27.4			-24.3			
1610							-26.7	-27.5			-24.7			
1609							-26.8	-27.6			-25.5			
1608							-26.6	-26.9			-24.6			
1607							-26.6	-27.6			-24.5			

YEAR	OAK R	OAK S	OAK T	OAK U	OAK V	OAK W	OAK X	OAK Y	OAK E	OAK AA	OAK AB	OAK AC	OAK AD	OAK AE
1606							-26.9	-27.4			-24.3			
1605							-27.1	-27.5			-24.4			
1604							-26.9	-27.7			-24.1			
1603							-27.5	-27.4			-24.3			
1602							-26.0	-27.8				-24.3		
1601							-26.5	-27.9			-23.2			
1600							-26.3	-27.4			-24.1			
1599									-24.4	-26.0	-24.3			
1598									-24.2	-26.2	-24.9			
1597									-24.5	-26.3	-24.3			
1596									-24.5	-26.5	-24.4			
1595									-24.2	-26.2	-24.5			
1594									-23.9	-26.0	-24.3			
1593									-24.3	-26.1	-24.3			
1592									-24.7	-25.2	-24.9			
1591									-24.5	-25.7	-25.3			
1590									-24.6	-26.6	-24.3			
1589									-24.7	-25.1	-24.4			
1588									-25.0	-25.5	-25.1			
1587									-25.0	-25.9	-25.2			
1586									-25.0	-26.0	-25.1			
1585									-25.5	-25.4	-24.5			
1584									-25.7	-25.7	-25.7			
1583									-25.2	-26.1	-25.2			
1582									-26.2	-26.5	-25.8			
1581									-25.7	-25.5	-25.0			
1580										-25.6	-25.7	-25.1		
1579										-26.3	-25.5	-25.5		
1578										-26.1	-25.6	-24.9		
1577										-26.5	-25.0	-25.3		
1576										-26.4	-24.9	-24.8		
1575									-24.7	-25.3	-25.1			
1574									-25.4	-26.3	-25.2			
1573									-25.0	-26.4	-24.9			
1572									-25.6	-26.0	-25.5			
1571									-24.4	-26.1	-25.4			
1570									-24.9	-26.3	-25.0			
1569									-25.3	-26.7	-25.6			
1568									-25.5	-27.4	-25.3			
1567									-24.7	-25.8	-24.6			
1566									-25.3	-26.4	-25.5			
1565									-25.0	-26.2	-25.1			
1564									-24.4	-26.8	-25.0			
1563									-25.1	-26.5	-25.5			

YEAR	OAK R	OAK S	OAK T	OAK U	OAK V	OAK W	OAK X	OAK Y	OAK E	OAK AA	OAK AB	OAK AC	OAK AD	OAK AE
1562									-24.8	-26.2	-25.7			
1561									-24.9	-26.2	-25.6			
1560									-25.3	-26.4	-24.7			
1559									-25.2	-26.3	-24.2			
1558									-24.9	-26.5	-25.0			
1557									-24.8	-25.7	-24.9			
1556									-23.9	-26.3	-25.0			
1555									-25.2	-26.2	-25.3			
1554									-24.5	-27.0	-25.1			
1553									-24.8	-27.5	-25.0			
1552									-25.2	-27.1	-24.7			
1551									-25.1	-27.7	-25.3			
1550									-25.0		-27.0		-25.9	
1549									-24.7	-26.9			-25.4	
1548									-24.2	-26.7			-25.5	
1547									-24.8	-27.7			-26.6	
1546									-24.5	-27.3			-25.7	
1545									-24.5	-26.5			-24.9	
1544									-24.9	-27.0			-25.5	
1543									-24.6	-26.8			-25.7	
1542									-24.4	-26.6			-25.4	
1541									-24.7	-27.1			-26.1	
1540									-24.3	-25.7			-25.3	
1539									-24.6	-25.1			-26.0	
1538									-24.7	-25.2			-25.5	
1537									-25.3	-25.1			-26.2	
1536									-24.9	-25.7			-25.7	
1535									-23.9	-24.6			-25.3	
1534									-25.5	-25.3			-26.2	
1533									-24.6	-25.5			-25.3	
1532									-24.7	-26.1			-25.6	
1531									-25.6	-25.1			-25.2	
1530									-25.8	-25.9			-25.7	
1529									-24.5				-25.2	-25.0
1528									-24.6				-25.6	-25.1
1527									-24.7				-25.2	-24.6
1526									-25.3				-25.8	-24.8
1525									-25.3				-26.3	-25.0
1524									-25.2				-25.9	-24.6
1523									-24.6				-25.5	-25.0
1522									-25.4				-26.4	-24.5
1521									-25.0				-25.2	-24.3
1520									-24.6				-25.1	-24.4
1519									-25.1				-25.3	-24.1

YEAR	OAK R	OAK S	OAK T	OAK U	OAK V	OAK W	OAK X	OAK Y	OAK E	OAK AA	OAK AB	OAK AC	OAK AD	OAK AE
1518									-24.9				-25.4	-24.5
1517									-25.7				-25.7	-25.3
1516									-24.8				-24.9	-24.8
1515									-24.8				-24.9	-25.3
1514									-25.2				-24.9	-25.4
1513									-25.0				-25.4	-25.5
1512									-24.8				-25.5	-25.2
1511									-25.4				-25.3	-25.2
1510									-24.8				-25.4	-24.5
1509									-24.8				-25.4	-24.8
1508									-25.3				-26.1	-25.3
1507									-24.9				-25.9	-24.8
1506									-25.0				-26.4	-25.1
1505									-24.8				-25.5	-25.0
1504									-24.3				-26.0	-24.6
1503									-24.3				-26.5	-25.1
1502									-24.5				-26.9	-24.6
1501									-24.2				-26.5	-24.6
1500									-24.4				-26.1	-24.1

YEAR	OAK AA	OAK BB	OAK CC	OAK DD	OAK EE	OAK FF	OAK GG	OAK HH
2002				-26.7	-27.6	-27.2		
2001				-26.7	-27.2	-28.6		
2000				-27.9	-27.5	-28.7		
1999				-28.1	-27.7	-28.1		
1998				-27.3	-27.6	-28.2		
1997				-26.5	-27.5	-26.5		
1996				-27.0	-27.7	-27.5		
1995				-27.4	-27.0	-26.9		
1994				-27.5	-27.9	-26.0		
1993				-27.5	-28.4	-25.6		
1992				-26.8	-27.5	-24.9		
1991				-27.0	-27.7	-25.1		
1990				-27.0	-28.1	-25.0		
1989				-26.5	-27.1	-26.9		
1988				-26.2	-27.1	-25.7		
1987				-27.2	-26.8	-27.0		
1986				-27.2	-26.7	-26.9		
1985				-26.9	-26.0	-26.2		
1984				-26.5	-25.9	-25.1		
1983				-25.9	-25.7	-23.7		
1982				-26.7	-25.6	-25.0		
1981				-27.1	-26.8	-25.5		
1980				-26.7	-27.2	-24.9		
1979				-25.7	-26.2	-24.9		
1978				-25.3	-26.7	-25.6		
1977				-25.9	-27.0	-26.0		
1976				-25.2	-27.2	-24.0		
1975				-27.8	-28.0	-24.8		
1974		-28.1			-27.7	-24.5		
1973		-28.2			-27.0	-24.9		
1972		-27.8			-26.4	-25.0		
1971		-28.3			-26.8	-25.1		
1970		-27.4			-26.5	-24.5		
1969		-27.5			-26.6	-25.1		
1968		-27.5			-27.3	-24.8		
1967		-27.2			-27.1	-25.5		
1966		-26.9			-27.1	-24.2		
1965		-26.6			-26.2	-24.6		
1964		-26.5			-26.3	-24.3		
1963		-26.3			-27.0	-23.7		
1962		-27.9			-26.7	-23.8		
1961		-26.7			-25.8	-23.6		
1960		-27.2			-25.9	-23.9		
1959		-26.6			-26.0	-23.3		

YEAR	OAK AA	OAK BB	OAK CC	OAK DD	OAK EE	OAK FF	OAK GG	OAK HH
1958		-26.3			-26.5	-24.2		
1957		-25.7			-26.3	-24.1		
1956		-25.9			-27.0	-23.8		
1955		-26.0			-26.3	-23.5		
1954		-26.2			-26.7	-23.6		
1953		-27.6			-26.6	-23.6		
1952		-28.2			-26.9	-24.5		
1951		-27.9			-26.6	-25.1		
1950		-27.3			-26.7	-25.1		
1949	-27.1	-27.4	-29.3					
1948	-26.7	-27.2	-29.3					
1947	-26.8	-27.0	-28.4					
1946	-27.0	-27.4	-29.7					
1945	-26.2	-27.0	-29.5					
1944	-27.1	-27.7	-29.3					
1943	-27.4	-27.2	-29.9					
1942	-26.9	-27.0	-29.9					
1941	-27.8	-26.3	-28.1					
1940	-27.0	-26.1	-28.5					
1939	-27.8	-26.2	-28.7					
1938	-27.5	-25.8	-28.1					
1937	-26.8	-26.4	-27.5					
1936	-27.2	-25.8	-27.9					
1935	-25.8	-25.8	-27.6					
1934	-25.8	-24.5	-27.0					
1933	-26.0	-25.8	-27.8					
1932	-26.5	-25.5	-28.0					
1931	-26.6	-25.8	-27.6					
1930	-26.8	-25.4	-27.3					
1929	-26.9	-25.8	-27.3					
1928	-27.2	-26.1	-27.1					
1927	-26.9	-25.3	-26.5					
1926	-27.0	-25.4	-27.3					
1925	-26.6	-25.4	-27.3					
1924		-25.4	-27.1				-28.2	
1923		-25.5	-27.4				-28.2	
1922		-25.3	-27.3				-28.2	
1921		-25.2	-27.4				-28.7	
1920		-24.8	-25.9				-28.5	
1919		-25.2	-27.0				-28.3	
1918		-25.2	-26.8				-28.4	
1917		-25.0	-26.9				-28.0	
1916		-24.8	-26.4				-27.6	
1915		-26.3	-27.5				-27.3	

YEAR	OAK AA	OAK BB	OAK CC	OAK DD	OAK EE	OAK FF	OAK GG	OAK HH
1914		-25.9	-26.8				-27.6	
1913		-26.0	-26.5				-27.5	
1912		-25.1	-25.9				-26.8	
1911		-25.9	-26.3				-27.0	
1910		-24.9	-26.5				-26.7	
1909			-27.5				-26.3	-27.0
1908			-27.5				-26.4	-26.2
1907			-27.1				-28.5	-26.3
1906			-26.9				-28.5	-25.9
1905			-27.2				-28.7	-26.5
1904			-26.5				-29.4	-25.0
1903			-25.9				-28.7	-25.4
1902			-26.3				-28.4	-26.1
1901			-25.7				-27.4	-26.1
1900			-26.4				-27.9	-26.9

Appendix 2

Alpha Cellulose Extraction from Wood

Comments

***Modified from Brendel et al. (2000) & Evans and Schrag (2004)*
***Additional descriptions by Kevin Anchukaitis, July 2007*
***Final adjustments-descriptions (for Lab 301) from Scott Lepley, April 2009*

Materials

1. Wood samples
    a. Amount: 200-1500μg
2. Microcentrifuge tubes
    a. Size: 1.5 mL
    b. Polypropylene, low retension
    c. Located in labeled drawers in outer lab
3. Microcentrifuge tube holders
    a. As many as desired depending on sample prep amounts
    b. Located in labeled drawers in outer lab
4. Acetic acid
    a. 80% reagent grade
    b. Can be made from glacial acetic acid (4 parts glacial, 1 part DDW)
    c. Located in Room 4 flammable cabinet
5. Nitric acid
    a. 69% reagent grade
    b. Can be bought directly at this grade
    c. Located in Room 4 underneath fume hood
6. Ethanol 100%
    a. Located in Room 4 flammable cabinet
7. Acetone 100%
    a. Located in Room 4 flammable cabinet
8. Distilled Deionized Water (DDW)
    a. Located in bottles in Lab 301, or in large 20 Liter Jug by Sink
    b. DI machine is across the hall in Room 318
9. Pipetters
    a. Capable of 20, 200, 1000μL
    b. Located on counter in outer lab, only for these experiments
10. Disposable Pipette tips
    a. Match appropriately with pipetters
    b. Located in labeled drawers in outer lab

11. Centrifuge
    a. Has approximately 10,000 rpm speeds
    b. Located in outer lab on counter next to ovens
    c. Holds 16 microcentrifuge tubes
12. Hot Plate
    a. Capable of holding accurate temperatures ± 2°C
    b. VWR, Located in outer lab on counter next to ovens
13. Aluminum Heating Blocks
    a. Capable of holding microcentrifuge tubes
    b. Cannot be bigger than hot plate
14. Drying Oven
    a. Capable to holding temperatures around 50°C
    b. Use right oven to dry samples
15. Vacuum Evaporator System
    a. Vacuum Desiccator (Labconco) with slow release valve
    b. Basic dry pump (Welch)
    c. Vacuum tubing with clamps
    d. Located in outer lab on counter by ovens
16. Small bottles for reagent "working solutions" in hood
    a. Can be of glass, pyrex, etc
    b. Label properly and place under hood
    c. Four glass bottles with orange caps are labeled and contain working solutions of Acetic Acid, Nitric Acid, Acetone, and Ethanol
17. Safety Equipment
    a. Goggles/glasses
    b. Latex gloves & hot gloves
    c. Lab coat

Safety Considerations

1. Use all safety equipment during procedure
    a. Must use lab coat, goggles and gloves during chemical transfers
2. Know where sinks, fire extinguishers, exits, telephones & emergency numbers, emergency lab procedures are before beginning chemistry
    a. Fire extinguisher is hanging by lab entrance
    b. Any emergency, dial 911 (telephone is by outer lab computer)
3. Perform all chemical transfers under fume hood with splash shield lowered
4. Pipette slowly against microcentrifuge tube walls to prevent splashing
5. Do not eat or drink while performing protocols

Procedural Notes

1. Wood Samples should be finely chopped or in small solid form (very thin is desired) to improve acid extraction.
    a. When samples are finely shaved and under 0.7 mg, clean white cellulose is produced. No need to ground samples.

2. Depending on time available, ability to organize and label properly, as well as size of equipment, batches of 20 – 60 can be processed at a time.
    a. Each heating block can handle 20 samples
    b. Each tube holder can handle 72 samples
3. Heating blocks require nearly 1 hour to reach desired temperature.
    a. Begin heating blocks, then prepare samples (with steps 1-4 in pre-procedure) and by then blocks should be heated to desired temperature.
4. Avoid sucking up sample in the pipette by pipetting supernatant very slowly
5. You should use a working stock solution of reagents instead of using large quantities to prevent large spills or problems
    a. Four glass bottles with orange caps are labeled and contain working solutions for experiments of Acetic Acid, Nitric Acid, Acetone, and Ethanol
6. Final product should appear white-ish and fine, papery or cottony
    a. This usually occurs after the heating reaction steps
7. Amount of desired product is nearly 1/3 of the weight of original product. Practice beforehand with procedure to determine how much sample is needed based on IRMS requirements of laboratory.
8. Time allotments for all procedures (~2 days)
    a. Sample preparation (25 samples) – minimum of 4 hours
    b. Chemical procedures – minimum of 3 hours
    c. Drying and vacuum desiccation – overnight (>8 hours)
    d. IRMS preparation time (standards + machine) – minimum of 4 hours
    e. IRMS run time (36 total samples) – 7.2 hours

Pre-Procedure

1. Prepare individual wood samples from tree rings
    a. Ideal weights are less than 1.5 mg
    b. Dremel drill and bits are located in drawer below Nikon Microscope
    c. Razor blades are located in labeled drawer beneath ovens
2. Weigh each sample as accurately as possible
    a. Use flat balance (Sartorious) in outer lab next to extraction lines
3. Place individual wood samples in microcentrifuge tubes and cap tightly
    a. Label accordingly on tubes and on sample sheets
4. Place labeled tubes in a microcentrifuge tube holder in a safe area
    a. Preferably a low RH area (desiccator)

Procedure

1. Turn on hot plate to approximately 120°C and place heating blocks on top of plate and allow at least 30 minutes for blocks to heat to desired temperature.
    a. Optimal temperature range is between 119 and 125°C, do not allow temperature to exceed 130°C
2. Only begin pipetting as many samples as can fit in heating blocks
3. Using a 200 μL pipette, slowly add 120 μL acetic acid into sample tubes

4. Using a 50 μL pipette, slowly add 12 μL nitric acid into sample tubes
    a. Cap all samples securely!
5. Insert tubes into heating blocks and leave for 30 minutes
    a. Occasionally tap tube caps (every 5-10 minutes) improve the reaction (7 hard taps on each) and mixes the acids with the sample in the tubes
6. After 30 minutes, remove all tubes from heat and allow to cool (3-5 minutes)
    a. Remove tubes with curved pliers as tubes and heating block are hot
    b. Place tubes back into microcentrifuge tube holder
    c. If no more samples are waiting, turn off hot plate and set aside
    d. If more samples are waiting, leave hot plate on, but be careful of heat from blocks and plate
7. Under the hood, uncap tubes as slowly as possible in case of overpressure
    a. Steps 9-12 are done under the hood as well
8. Using a 1000μL pipette, slowly add 400 μL ethanol to each tube
    a. Cap all samples tightly and use vortex genie to mix
    b. Place tubes (16 at a time) in centrifuge for 5 minutes at 10,000 rpm
    c. Using same pipetter and tip, carefully remove as much supernatant as possible from tubes into waste beaker
    d. Discard pipette tip
9. Using a 1000μL pipette, slowly add 300 μL DDW to each tube
    a. Cap all samples tightly and use vortex genie to mix
    b. Place tubes (16 at a time) in centrifuge for 5 minutes at 10,000 rpm
    c. Using same pipetter and tip, carefully remove as much supernatant as possible from tubes into waste beaker
    d. Discard pipette tip
10. Using a 200μL pipette, slowly add 150μL ethanol to each tube
    a. Cap all samples tightly and tap tops firmly 2-3 times
    b. Place tubes (16 at a time) in centrifuge for 5 minutes at 10,000 rpm
    c. Using same pipetter and tip, carefully remove as much supernatant as possible from tubes into waste beaker
    d. Discard pipette tip
11. Using a 200μL pipette, slowly add 150μL acetone to each tube
    a. Cap all samples tightly and DO NOT SHAKE
    b. Place tubes (16 at a time) in centrifuge for 2 minutes at 10,000 rpm
    c. Using same pipetter and tip, carefully remove as much supernatant as possible from tubes into waste beaker
    d. Discard pipette tip
12. Place samples in oven (50°C) for approximately 30-60 minutes or until dry
13. Place samples in vacuum evaporation setup
    a. Cover samples with aluminum foil
    b. Make sure all vacuum lines are sealed well
    c. Make sure desiccator vent valve is closed upon startup (pointing up)
    d. Turn left valve on pump all the way to left (open)
    e. Turn on pump and let it pump down to a stable pressure (in lines)
        i. Close (turn all the way to right) the left valve on the pump

1. Pressure will rise ~25 in Hg

f. SLOWLY open (toward tube) vacuum line valve and watch to make sure samples do not move from containers
g. Leave inside vacuum for ~8 hours or overnight
h. Following time period, close valve, then shut off pump and slowly release pressure in vacuum lines and then vacuum evaporator
i. Samples are now ready for analysis

Post-Procedure

1. Remove samples from tubes and place into silver capsules
    a. Weigh each sample at weight station in outer lab using flat balance
    b. Cube sample, mark on sheet, and place into sample tray
2. Discarded microcentrifuge tubes
    a. Rinse 3X in H_2O water over sink
    b. Rinse 1X in ethanol over sink
    c. Place back into tube holder and place into oven to dry overnight
    d. Discard into designated box to discard later
3. Cleanup
    a. Make sure hot plates are turned off and unplugged
    b. Place all acid and reagent bottles into cabinets when finished
    c. Wipe up and acid or reagent spills/splashes in hood with methanol
    d. Place empty waste from beakers down sink drain with running water
    e. Rinse waste beakers with detergent and water and let sit in DI water for ~10 minutes
    f. Refill all working reagent jars if necessary
    g. Place all materials used back into original location in lab

Analytical Measurements

1. Keep samples in sample tray in desiccator until analyses are ready
    a. Good idea to not have samples sitting around for months
2. Prepare standards for run on the day of analysis.
    a. Usually in a full run, up to 20 standards are needed.
3. Follow procedures outlined for oxygen analysis using the TC/EA

References

Brendel, O., Iannetta, P.P.M., and Stewart, D., 2000. A Rapid and Simple Method to Isolate Pure Alpha-Cellulose. *Phytochemical Analysis* **11**: 7-10.

Evans, M. N. and Schrag, D. P., 2004. A stable isotope-based approach to tropical dendroclimatology. *Geochimica et Cosmochimica Acta* **68-16**: 3295-3305.

Lepley, S.W., 2009. Midwestern Climate Records from Tree Ring $\delta^{18}O$ and $\delta^{18}O$ Values. *PhD Dissertation*, University of Missouri. 164 pp.

Appendix 3

Missouri Climate Division 1 Climate Data

- Average of June-August climate variables from 1931-2002
- P = Precipitation (in), T = Temperature (°C), PDSI (no units)

YEAR	P	T	PDSI	YEAR	P	T	PDSI
2002	3.0	76.7	-1.1	**1966**	4.0	73.9	-1.4
2001	6.1	75.0	3.4	**1965**	6.0	73.7	1.3
2000	5.1	74.8	0.9	**1964**	4.3	74.4	0.6
1999	3.1	74.9	0.8	**1963**	3.6	76.2	-1.9
1998	5.7	74.7	2.5	**1962**	3.5	74.3	-1.1
1997	2.9	73.9	1.7	**1961**	5.1	73.3	2.3
1996	5.1	73.3	2.2	**1960**	4.8	74.0	1.9
1995	4.8	75.6	3.7	**1959**	3.4	75.4	-0.2
1994	3.4	73.6	2.5	**1958**	6.1	73.3	1.2
1993	8.4	74.2	6.0	**1957**	3.4	76.6	-4.2
1992	5.0	70.4	0.7	**1956**	4.3	76.6	-4.8
1991	2.7	75.9	-0.9	**1955**	3.7	76.1	-2.0
1990	4.9	74.7	3.0	**1954**	4.2	79.1	-4.4
1989	4.8	73.1	-1.1	**1953**	2.0	78.0	-2.0
1988	2.5	76.8	-3.4	**1952**	4.7	76.7	-0.1
1987	5.1	75.6	1.1	**1951**	7.8	73.6	3.3
1986	4.4	74.8	1.4	**1950**	5.3	70.6	0.7
1985	4.6	71.9	1.1	**1949**	5.1	75.1	0.8
1984	3.5	75.3	0.4	**1948**	4.4	74.7	0.3
1983	2.4	77.7	-1.0	**1947**	6.3	75.7	1.1
1982	6.3	72.4	3.9	**1946**	3.6	74.4	-0.4
1981	6.4	74.5	2.5	**1945**	4.0	72.3	3.3
1980	3.5	79.0	-2.7	**1944**	4.9	74.7	2.0
1979	4.5	73.8	0.2	**1943**	5.6	76.6	1.7
1978	4.3	75.1	2.5	**1942**	5.6	74.5	2.9
1977	5.1	75.6	-1.8	**1941**	3.5	76.1	-2.4
1976	2.0	74.5	-1.6	**1940**	4.0	74.9	-2.7
1975	2.9	76.0	-1.0	**1939**	5.3	75.9	-1.6
1974	3.4	74.0	2.3	**1938**	4.2	76.9	-1.5
1973	3.9	75.4	3.8	**1937**	4.0	76.6	-1.6
1972	3.3	74.4	-0.6	**1936**	1.1	81.6	-3.6
1971	2.9	74.7	-1.8	**1935**	3.8	75.4	0.6
1970	3.7	75.0	-0.3	**1934**	2.3	82.2	-6.6
1969	6.0	74.3	2.3	**1933**	3.4	76.9	-1.3
1968	3.8	74.9	0.0	**1932**	4.8	76.0	-0.7
1967	4.3	71.9	1.7	**1931**	3.5	76.8	-1.8

Appendix 4

Figure 5.1: Average HC-type $\delta^{13}C$ Values from 1500-2002

Normalized and Raw (corrected for the industrial effect) $\delta^{13}C$ values

YEAR	$\delta^{13}C$ Normalized	$\delta^{13}C$ Raw Corrected	YEAR	$\delta^{13}C$ Normalized	$\delta^{13}C$ Raw Corrected
2002	0.0	-25.0	**1966**	-0.1	-25.1
2001	0.1	-25.0	**1965**	0.1	-24.9
2000	0.1	-25.0	**1964**	0.0	-25.0
1999	0.3	-24.8	**1963**	0.0	-25.0
1998	-0.3	-25.4	**1962**	-0.4	-25.4
1997	0.2	-24.9	**1961**	0.1	-24.9
1996	-0.2	-25.3	**1960**	0.1	-25.0
1995	-0.2	-25.3	**1959**	0.1	-25.0
1994	-0.6	-25.7	**1958**	-0.2	-25.3
1993	-1.0	-26.1	**1957**	0.1	-24.9
1992	0.1	-25.0	**1956**	-0.2	-25.3
1991	0.1	-25.0	**1955**	0.0	-25.0
1990	-0.1	-25.2	**1954**	0.0	-25.0
1989	0.7	-24.4	**1953**	-0.2	-25.2
1988	0.7	-24.3	**1952**	-0.8	-25.8
1987	0.2	-24.9	**1951**	-0.3	-25.4
1986	0.2	-24.9	**1950**	-0.2	-25.2
1985	0.6	-24.5	**1949**	0.1	-25.0
1984	0.5	-24.6	**1948**	0.0	-25.1
1983	0.2	-24.9	**1947**	0.3	-24.8
1982	0.2	-24.9	**1946**	0.0	-25.2
1981	-0.5	-25.6	**1945**	0.5	-24.6
1980	0.2	-24.8	**1944**	-0.3	-25.4
1979	0.2	-24.9	**1943**	-0.1	-25.3
1978	0.3	-24.8	**1942**	-0.5	-25.6
1977	0.3	-24.8	**1941**	0.2	-24.9
1976	0.5	-24.6	**1940**	0.2	-25.0
1975	0.5	-24.5	**1939**	-0.3	-25.4
1974	0.2	-24.8	**1938**	0.4	-24.7
1973	0.5	-24.6	**1937**	0.2	-24.9
1972	0.2	-24.9	**1936**	0.4	-24.7
1971	-0.1	-25.1	**1935**	0.2	-24.9
1970	0.2	-24.8	**1934**	1.0	-24.1
1969	0.0	-25.0	**1933**	0.2	-24.9
1968	-0.1	-25.1	**1932**	0.2	-24.9
1967	-0.3	-25.3	**1931**	0.4	-24.7

YEAR	δ13C Normalized	δ13C Raw Corrected	YEAR	δ13C Normalized	δ13C Raw Corrected
1930	0.7	-24.4	**1894**	-0.2	-25.6
1929	0.3	-24.9	**1893**	-0.4	-25.8
1928	-0.4	-25.5	**1892**	-0.6	-26.0
1927	0.2	-24.9	**1891**	-0.7	-26.1
1926	-0.5	-25.6	**1890**	-0.5	-26.0
1925	-0.7	-25.8	**1889**	-0.5	-25.9
1924	0.3	-25.1	**1888**	-0.7	-26.1
1923	-0.2	-25.6	**1887**	-0.7	-26.2
1922	0.4	-24.9	**1886**	-0.1	-25.5
1921	-0.2	-25.5	**1885**	-0.5	-25.9
1920	0.4	-24.9	**1884**	-0.5	-25.9
1919	0.3	-25.1	**1883**	-0.5	-25.9
1918	-0.2	-25.6	**1882**	-0.5	-26.0
1917	-0.1	-25.5	**1881**	-0.6	-26.0
1916	-0.1	-25.5	**1880**	-0.4	-25.8
1915	0.2	-25.2	**1879**	0.0	-25.3
1914	-0.2	-25.5	**1878**	0.3	-25.0
1913	-0.2	-25.6	**1877**	0.0	-25.3
1912	0.2	-25.1	**1876**	-0.4	-25.7
1911	-0.2	-25.6	**1875**	0.1	-25.2
1910	-0.3	-25.6	**1874**	-0.1	-25.4
1909	-0.6	-26.0	**1873**	-0.1	-25.5
1908	0.0	-25.4	**1872**	0.0	-25.3
1907	-0.5	-25.8	**1871**	-0.2	-25.5
1906	-0.3	-25.6	**1870**	-0.2	-25.5
1905	-0.2	-25.6	**1869**	0.5	-25.4
1904	-0.3	-25.7	**1868**	0.0	-25.9
1903	-0.3	-25.7	**1867**	0.1	-25.8
1902	-0.6	-25.9	**1866**	0.1	-25.8
1901	0.1	-25.2	**1865**	-0.3	-26.1
1900	-0.8	-26.2	**1864**	-0.4	-26.3
1899	-0.9	-26.3	**1863**	0.5	-25.4
1898	-0.7	-26.1	**1862**	0.4	-25.4
1897	-0.2	-25.6	**1861**	0.6	-25.3
1896	-0.4	-25.9	**1860**	0.2	-25.7
1895	0.3	-25.1	**1859**	0.4	-25.5

YEAR	$\delta^{13}C$ Normalized	$\delta^{13}C$ Raw Corrected	YEAR	$\delta^{13}C$ Normalized	$\delta^{13}C$ Raw Corrected
1858	-0.2	-26.0	**1822**	-0.6	-26.2
1857	0.5	-25.5	**1821**	-0.9	-26.5
1856	0.1	-25.9	**1820**	0.2	-25.8
1855	0.7	-25.3	**1819**	0.0	-25.6
1854	0.8	-25.2	**1818**	-0.5	-26.1
1853	0.5	-25.5	**1817**	0.4	-25.2
1852	0.8	-25.2	**1816**	-0.2	-25.8
1851	0.6	-25.4	**1815**	0.2	-25.4
1850	0.0	-26.0	**1814**	0.6	-25.0
1849	0.6	-25.5	**1813**	0.2	-25.5
1848	-0.1	-26.1	**1812**	0.3	-25.3
1847	0.3	-25.7	**1811**	0.6	-25.0
1846	-0.2	-26.2	**1810**	0.7	-24.9
1845	-0.4	-26.4	**1809**	0.9	-24.7
1844	0.0	-26.0	**1808**	0.6	-25.0
1843	-0.3	-26.3	**1807**	1.2	-24.4
1842	0.2	-25.8	**1806**	0.6	-25.0
1841	0.1	-25.9	**1805**	0.7	-24.9
1840	0.2	-25.9	**1804**	0.7	-24.9
1839	0.0	-26.0	**1803**	0.1	-25.5
1838	-0.6	-26.6	**1802**	0.5	-25.1
1837	-0.2	-25.8	**1801**	-0.1	-25.8
1836	0.0	-25.6	**1800**	0.7	-24.5
1835	0.0	-25.6	**1799**	-0.1	-25.0
1834	-0.4	-26.0	**1798**	0.4	-24.5
1833	-0.3	-26.0	**1797**	-0.2	-25.0
1832	0.0	-25.6	**1796**	0.3	-24.5
1831	-0.1	-25.7	**1795**	0.7	-24.1
1830	-0.6	-26.2	**1794**	0.6	-24.2
1829	-0.5	-26.1	**1793**	0.3	-24.6
1828	-0.2	-25.9	**1792**	0.5	-24.4
1827	-0.7	-26.4	**1791**	0.5	-24.3
1826	-0.2	-25.8	**1790**	0.5	-24.3
1825	-0.4	-26.0	**1789**	0.3	-24.5
1824	-0.6	-26.2	**1788**	0.5	-24.3
1823	-0.5	-26.2	**1787**	0.8	-24.1

YEAR	$\delta^{13}C$ Normalized	$\delta^{13}C$ Raw Corrected	YEAR	$\delta^{13}C$ Normalized	$\delta^{13}C$ Raw Corrected
1786	0.6	-24.2	**1750**	0.2	-25.3
1785	0.3	-24.6	**1749**	0.0	-25.5
1784	0.7	-24.2	**1748**	0.4	-25.1
1783	0.9	-24.0	**1747**	-0.5	-26.0
1782	-0.4	-25.3	**1746**	-0.2	-25.7
1781	-0.3	-25.1	**1745**	-0.1	-25.6
1780	-0.1	-24.9	**1744**	0.3	-25.2
1779	0.4	-25.1	**1743**	0.0	-25.5
1778	0.6	-25.0	**1742**	-0.2	-25.7
1777	0.1	-25.4	**1741**	0.5	-25.0
1776	0.3	-25.2	**1740**	0.4	-25.1
1775	-0.5	-26.0	**1739**	0.7	-24.8
1774	0.0	-25.5	**1738**	-0.4	-25.9
1773	0.6	-24.9	**1737**	0.1	-25.4
1772	0.3	-25.2	**1736**	0.1	-25.5
1771	0.4	-25.2	**1735**	-0.3	-25.9
1770	0.4	-25.1	**1734**	0.1	-25.4
1769	0.1	-25.4	**1733**	0.0	-25.5
1768	0.8	-24.8	**1732**	-0.1	-25.6
1767	0.3	-25.3	**1731**	0.1	-25.4
1766	0.6	-24.9	**1730**	0.1	-24.8
1765	0.3	-25.2	**1729**	0.5	-24.5
1764	0.3	-25.2	**1728**	-0.1	-25.0
1763	1.1	-24.4	**1727**	0.0	-24.9
1762	0.7	-24.8	**1726**	-0.3	-25.2
1761	0.1	-25.4	**1725**	-0.4	-25.3
1760	0.0	-25.5	**1724**	0.2	-24.7
1759	0.6	-24.9	**1723**	0.0	-24.9
1758	-0.1	-25.6	**1722**	0.1	-24.8
1757	0.3	-25.2	**1721**	0.1	-24.8
1756	0.0	-25.5	**1720**	-0.1	-25.0
1755	-0.1	-25.6	**1719**	-0.3	-25.2
1754	-0.3	-25.8	**1718**	0.4	-24.5
1753	0.0	-25.5	**1717**	0.1	-24.8
1752	0.6	-24.9	**1716**	0.9	-24.0
1751	-0.1	-25.6	**1715**	0.7	-24.2

YEAR	$\delta^{13}C$ Normalized	$\delta^{13}C$ Raw Corrected	YEAR	$\delta^{13}C$ Normalized	$\delta^{13}C$ Raw Corrected
1714	0.7	-24.2	**1678**	-0.6	-25.4
1713	0.7	-24.2	**1677**	-0.8	-25.6
1712	0.5	-24.4	**1676**	-0.5	-25.2
1711	0.2	-24.7	**1675**	-0.2	-24.9
1710	0.1	-24.8	**1674**	-0.5	-25.2
1709	0.5	-24.4	**1673**	-0.2	-24.9
1708	-0.1	-25.0	**1672**	-0.7	-25.5
1707	0.2	-24.7	**1671**	-0.7	-25.5
1706	0.4	-24.5	**1670**	-0.6	-25.3
1705	0.0	-24.9	**1669**	-0.3	-25.1
1704	0.0	-24.9	**1668**	-0.6	-25.4
1703	0.3	-24.6	**1667**	-0.5	-25.2
1702	0.0	-24.9	**1666**	-1.0	-25.8
1701	0.0	-24.9	**1665**	-0.9	-25.6
1700	0.1	-24.8	**1664**	-0.4	-25.2
1699	-0.5	-25.2	**1663**	-0.2	-25.0
1698	-0.4	-25.1	**1662**	-0.7	-25.5
1697	0.0	-24.7	**1661**	-0.3	-25.1
1696	-0.3	-25.0	**1660**	-0.6	-25.4
1695	-0.6	-25.4	**1659**	-0.6	-25.4
1694	-0.6	-25.4	**1658**	-1.1	-25.8
1693	-1.2	-26.0	**1657**	-1.2	-26.0
1692	-0.6	-25.4	**1656**	-1.2	-26.0
1691	-1.0	-25.8	**1655**	-0.6	-25.4
1690	-0.9	-25.7	**1654**	-0.8	-25.5
1689	-1.0	-25.8	**1653**	0.0	-24.8
1688	-1.0	-25.8	**1652**	-0.5	-25.2
1687	-1.0	-25.8	**1651**	-0.1	-24.9
1686	-1.0	-25.7	**1650**	-0.2	-25.0
1685	-1.0	-25.7	**1649**	0.4	-25.7
1684	-1.0	-25.7	**1648**	0.0	-26.1
1683	-1.4	-26.1	**1647**	-0.1	-26.2
1682	-1.2	-26.0	**1646**	0.3	-25.7
1681	-1.4	-26.1	**1645**	0.9	-25.1
1680	-1.2	-25.9	**1644**	0.5	-25.6
1679	-0.8	-25.6	**1643**	1.1	-24.9

YEAR	$\delta^{13}C$ Normalized	$\delta^{13}C$ Raw Corrected	YEAR	$\delta^{13}C$ Normalized	$\delta^{13}C$ Raw Corrected
1642	0.6	-25.4	**1606**	-0.1	-26.2
1641	0.8	-25.3	**1605**	-0.2	-26.3
1640	0.6	-25.4	**1604**	-0.2	-26.3
1639	0.3	-25.8	**1603**	-0.3	-26.4
1638	0.4	-25.7	**1602**	0.1	-26.0
1637	0.1	-26.0	**1601**	0.2	-25.9
1636	-0.1	-26.1	**1600**	0.2	-25.9
1635	-0.6	-26.7	**1599**	0.4	-24.9
1634	-0.4	-26.5	**1598**	0.2	-25.1
1633	0.0	-26.1	**1597**	0.2	-25.1
1632	0.4	-25.6	**1596**	0.2	-25.1
1631	0.2	-25.9	**1595**	0.3	-25.0
1630	0.3	-25.7	**1594**	0.6	-24.7
1629	0.2	-25.8	**1593**	0.4	-24.9
1628	0.3	-25.8	**1592**	0.4	-24.9
1627	0.0	-26.0	**1591**	0.1	-25.2
1626	0.1	-26.0	**1590**	0.2	-25.1
1625	0.2	-25.5	**1589**	0.6	-24.7
1624	0.2	-25.9	**1588**	0.1	-25.2
1623	0.0	-26.1	**1587**	-0.1	-25.4
1622	-0.1	-26.2	**1586**	-0.1	-25.4
1621	-0.1	-26.2	**1585**	0.2	-25.1
1620	0.0	-26.1	**1584**	-0.4	-25.7
1619	-0.1	-26.2	**1583**	-0.2	-25.5
1618	-0.1	-26.2	**1582**	-0.8	-26.1
1617	-0.3	-26.4	**1581**	-0.1	-25.4
1616	-0.3	-26.4	**1580**	-0.1	-25.5
1615	0.0	-26.1	**1579**	-0.4	-25.7
1614	-0.3	-26.4	**1578**	-0.2	-25.5
1613	-0.4	-26.5	**1577**	-0.3	-25.6
1612	-0.5	-26.6	**1576**	0.0	-25.4
1611	0.2	-25.9	**1575**	0.3	-25.0
1610	-0.2	-26.3	**1574**	-0.3	-25.6
1609	-0.5	-26.6	**1573**	-0.1	-25.4
1608	0.0	-26.1	**1572**	-0.4	-25.7
1607	-0.1	-26.2	**1571**	0.0	-25.3

YEAR	$\delta^{13}C$ Normalized	$\delta^{13}C$ Raw Corrected	YEAR	$\delta^{13}C$ Normalized	$\delta^{13}C$ Raw Corrected
1570	-0.1	-25.4	**1534**	-0.1	-25.6
1569	-0.6	-25.9	**1533**	0.4	-25.2
1568	-0.8	-26.1	**1532**	0.1	-25.5
1567	0.2	-25.1	**1531**	0.3	-25.3
1566	-0.4	-25.7	**1530**	-0.2	-25.8
1565	-0.1	-25.4	**1529**	0.2	-24.9
1564	-0.1	-25.4	**1528**	0.0	-25.1
1563	-0.4	-25.7	**1527**	0.3	-24.8
1562	-0.3	-25.6	**1526**	-0.2	-25.3
1561	-0.3	-25.6	**1525**	-0.4	-25.5
1560	-0.2	-25.5	**1524**	-0.1	-25.2
1559	0.1	-25.2	**1523**	0.1	-25.1
1558	-0.2	-25.5	**1522**	-0.3	-25.4
1557	0.2	-25.1	**1521**	0.3	-24.8
1556	0.2	-25.1	**1520**	0.4	-24.7
1555	-0.3	-25.6	**1519**	0.3	-24.8
1554	-0.2	-25.5	**1518**	0.2	-25.0
1553	-0.5	-25.8	**1517**	-0.4	-25.6
1552	-0.3	-25.6	**1516**	0.3	-24.8
1551	-0.7	-26.0	**1515**	0.2	-25.0
1550	-0.8	-25.9	**1514**	-0.1	-25.2
1549	-0.1	-25.7	**1513**	-0.2	-25.3
1548	0.1	-25.5	**1512**	0.0	-25.2
1547	-0.8	-26.4	**1511**	-0.2	-25.3
1546	-0.3	-25.8	**1510**	0.2	-24.9
1545	0.2	-25.3	**1509**	0.1	-25.0
1544	-0.2	-25.8	**1508**	-0.5	-25.6
1543	-0.1	-25.7	**1507**	-0.1	-25.2
1542	0.1	-25.5	**1506**	-0.4	-25.5
1541	-0.4	-26.0	**1505**	0.0	-25.1
1540	0.5	-25.1	**1504**	0.1	-25.0
1539	0.4	-25.2	**1503**	-0.2	-25.3
1538	0.4	-25.1	**1502**	-0.2	-25.3
1537	0.0	-25.5	**1501**	0.0	-25.1
1536	0.1	-25.4	**1500**	0.3	-24.8
1535	1.0	-24.6			

VITA

Ph.D. in Geology, 2009, University of Missouri

Advisor: Dr. Kenneth MacLeod

Dissertation Topic: Midwest climate change from tree ring $\delta^{13}C$ and $\delta^{18}O$ values

M.S. in Geology, 2004, University of Missouri

Advisor: Dr. Jeffrey Dorale

Thesis Title: A high-resolution record of Holocene El Niño cyclicity from Crevice Cave, MO

B.S. in Geology, 2002, University of Illinois at Urbana-Champaign

Advisor: Dr. Bruce Fouke

Senior Thesis Title: Cathodoluminescence petrography of travertine encrusting crystallization blocks from Angel Terrace, Mammoth Hot Springs, Yellowstone National Park, Wyoming, U.S.A.

Upon receiving his PhD in Geology during the summer of 2009, Scott plans to begin work as an Exploration Geologist at British Petroleum (BP) in Houston, Texas. He will also be getting married in late 2010 to Dr. Carolina Isaza Londoño.